Store-operated calcium channels and the development of liver steatosis

A thesis submitted in fulfillment of the
requirements for the
degree of:

Doctor of Philosophy

by

M. Eunus Ali
B.Sc.(Hons.), M.Sc.

Department of Medical Biochemistry
School of Medicine, Faculty of Medicine, Nursing and Health Sciences
Flinders University
December 2014

TABLE OF CONTENTS

LIST OF FIGURES

SUMMARY

Obesity, the development of a fatty liver growth, and insulin resistance in hepatocytes are some of the critical hallmarks of type 2 diabetes. Lipid accumulation (steatosis) in hepatocytes may lead to non-alcoholic fatty liver disease (NAFLD), which can progress to non-alcoholic steatohepatitis and type 2 diabetes. The mechanisms by which steatosis leads to NAFLD and insulin resistance are not well understood. Moreover, intracellular Ca^{2+} signalling and endoplasmic reticulum function are known to be altered in steatotic hepatocytes. Therefore the aims of this thesis were to determine if store-operated Ca^{2+} entry (SOCE) is altered in steatotic liver cells, to evaluate the mechanisms involved, and to evaluate the effects of impaired SOCE on glucose and lipid metabolism in steatotic liver cells.

Lipid accumulation *in vitro* was induced in cultured liver cells by amiodarone or palmitate, and *in vivo* in hepatocytes isolated from obese Zucker rats. Intracellular lipid accumulation was determined by Nile red fluorescent stain and Ca^{2+} entry through store-operated Ca^{2+} channels (SOCs) was measured using fura-2 fluorescence imaging.

It was found that the rates of store-operated Ca^{2+} entry and Ca^{2+} release from intracellular stores were substantially reduced in lipid loaded cells. Inhibition of protein kinase C reversed the impairment of Ca^{2+} entry in lipid-loaded cells. The lipid-induced inhibition of SOCE was substantially reversed by exendin-4, a member of the glucagon like peptide-1 (GLP-1) analogue family of anti-diabetic drugs in frequent use for the treatment of insulin resistance. Inhibition of Ca^{2+} entry was associated with

reduced hormone-initiated intracellular Ca^{2+} signalling, enhanced lipid accumulation and altered glucose metabolism.

It is concluded that these results provide evidence that steatosis leads to substantial inhibition of store-operated Ca^{2+} entry through a mechanism involving the activation of one or more isoforms of protein kinase C. The inhibition of SOCE enhances the accumulation of intracellular lipids and may contribute to the development of non-alcoholic steatohepatitis and insulin resistance. In addition, the finding that the lipid-induced inhibition of SOCE is reversed by antidiabetic drug exendin-4 may indicate to a novel site of action for this drug.

DECLARATION

I certify that this thesis does not incorporate without acknowledgment any material previously submitted for a degree or diploma in any university; and that to the best of my knowledge and belief it does not contain any material previously published or written by another person except where due reference is made in the text.

Eunus Ali

Signed:

ACKNOWLEDGEMENTS

My sincere thanks goes to my chief supervisor Prof. Greg Barritt, for the opportunity of undertaking my doctoral work in his laboratory and for the continuing support, scientific guidance and dedication he has given me throughout this scientific work. Greg, your suggestions on scientific writing is so amazing; your suggestions on writing will act as a 'positive feedback loop' from where my scientific writing skills will be sharpening over time to come, I believe. I am also grateful to my co-supervisors Assoc. Prof. Grigori Rychkov and Dr. Roland Gregory for their helpful comments and guidance during my doctoral research. I also appreciate the interest shown by Prof. Neil Sims as well as his suggestions relating to my research.

Thanks to all of the lab members (Brian, Farhana, Alyce and many others) for their unwavering support and solid scientific discussion. I would like to acknowledge Jin Hua for performing the qPCR and glucose assay in result chapter six, and isolation of hepatocytes. I thank Ehsan Kheradpezhouh for sharing hepatocytes.

The financial assistance from the Australian Government, Flinders University and professor's research grant is grately and sincerely acknowledged.

Lastly, I would like to acknowledge the support of my family and friends. I would like to dedicate this work to some of my former teachers who taught me fundamentals of lipid biology and protein chemistry- Göran Widmalm, Gunnar von Heijne, Peter Brzezinski, Mokaddez Sarder (protein chemistry); T. H. Nutan, Firoj Ahmed (biological and physical chemistry); Björn Åkermark (peptide synthesis); the late Åke Wieslander (lipid biology).

ABBREVIATIONS

BTP-2	3,5-bis(trifluoromethyl)pyrazole (BTP) anlogue
Ca^{2+}	Cytoplasmic free Ca^{2+}
$[Ca^{2+}]_{cyt}$	Cytoplasmic free Ca^{2+} concentration
$(Ca^{2+})_{er}$	Endoplasmic reticulum Ca^{2+} levels
(Ca^{2+}_{ext})	Extracellular Ca^{2+}
CRAC	Ca^{2+} Release-Activated Ca^{2+} Channel
DBHQ	Di-*tert*-butylhydroquinone
DMEM	Dulbecco's Modified Eagles Medium
DMSO	Dimethylsulfoside
EDTA	Ethylenediaminetetraacetic acid
EGTA	Ethylene Glycol-bis(b-aminoethyl ether)-*N*,*N*,*N´N´*-Tetraacetic Acid
ER	Endoplasmic reticulum
FBS	Fetal bovine serum
Gd^{3+}	Gadolinium
GFP	Green Fluorescent Protein
GFX	GF109203X
I_{crac}	Ca^{2+} Release-Activated Ca^{2+} Current
IP_3	Inositol 1,4,5-trisphosphate
IP_3R	Inositol 1,4,5-trisphosphate receptor
KRH	Krebs-Ringer-HEPES buffer
La^{3+}	Lanthanum
NAFLD	Non-alcoholic fatty liver disease
NASH	Non-alcoholic steatohepatitis
PBS	Phosphate Buffered Saline
PKC	Protein Kinase C

PM	Plasma membrane
PMA	Phorbol 12-myristate 13-acetate
PMCA	Plasma Membrane (Ca^{2+} + Mg^{2+}) ATP-ases pump
ROI	Regions of interest
SERCA	Endoplasmic Reticulum (Ca^{2+} + Mg^{2+}) ATP-ase pump
SOCs	Store-operated Ca^{2+} channels
SOCE	Store-operated Ca^{2+} entry
STIM1	Stromal Interaction Molecule 1
STIM2	Stromal Interaction Molecule 2
T2D	Type 2 diabetes
Tg	Thapsigargin
TRPM2	Transient Receptor Potential Melastatin channel 2
YM 58483	3,5-bis(trifluoromethyl)pyrazole (BTP) analogue
2-APB	2-aminoethoxydiphenylborane

CHAPTER I: INTRODUCTION AND LITERATURE REVIEW

This thesis reports investigation of the role of store-operated Ca^{2+} channels in the steatotic liver and the effects of steatosis on intracellular Ca^{2+} homeostasis and lipid synthesis. In this chapter, the literature related with these themes will be included. Therefore this literature review will describe: (i) the physiology and the normal functions of the liver; (ii) the role of Ca^{2+} as an intracellular messenger in hepatocytes; (iii) the properties of store-operated Ca^{2+} channels; (iv) the biochemistry and pathology of the steatotic liver.

1.1 Liver physiology, hormonal regulation of liver metabolism

1.1.1 Liver structure, physiology and biochemistry

The liver, consisting of approximately 2% to 3% of the average body weight (Abdel-Misih and Bloomston, 2010), is organized into lobules (Ganong, 1995). The classical anatomy differentiates it into two main (right and left) and two accessory (quadrate and caudate) lobes (Desmet, 1994). In each lobe, the tissue, liver parenchyma, is organized into hexagonal shaped lobules. A central vein surrounded by six portal triads is arranged in each hexagonal shaped lobule (Mohammed and Khokha, 2005) (Fig.1.1A). Figure 1.1B shows one portal triad, which is composed of hepatic artery, hepatic vein and bile duct.

The liver can be divided into five tissue systems: (i) vascular system (ii) hepatocytes and hepatic lobule (iii) hepatic sinusoidal tissue system (iv) biliary system and (v) stroma (Ishibashi et al., 2009). Liver activity, in general, depends on its unique tissue architecture consisting of several different cell types which can be divided into parenchymal cells (hepatocytes) and non-parenchymal cells (Ishibashi et al., 2009). The major cell type in the liver is the hepatocyte and the hepatocytes are equivalent to 90% of the liver volume. The non-parenchymal cells consist of biliary epithelial cells, Kupffer cells, endothelial cells, hepatic stellate cells and oval cells (Blouin et al., 1977).

Hepatocytes are one type of specialized epithelial cells and are organized in single-cell plates. The hepatocyte plates are perfused by blood from the gastrointestinal tract (hepatic portal vein) and heart (hepatic artery), which drains into the central vein (Fig.1.1). The cells are highly differentiated exhibiting spatial polarisation and a distinctive intracellular organization (Barritt et al., 2008).

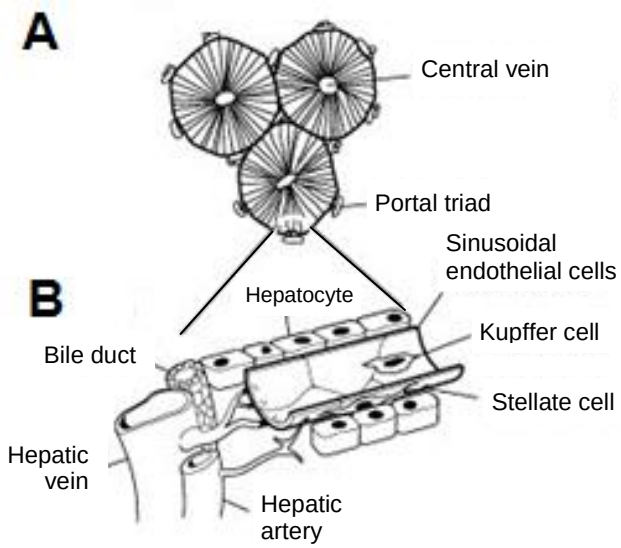

Fig. 1.1. Schematic representation of organization of hepatocytes in the liver. (A) Diagram displaying the relationship between the central vein and portal triads, (B) The schematic general architecture of the hepatic vein, hepatic artery, hepatocyte plate, sinusoidal space and bile duct (Figure adapted from Barritt et al. (2008)).

1.1.2 Roles of liver in whole body homeostasis

The liver has a major role in the uptake of carbohydrates, amino acids, lipids, vitamins and their storage, metabolism, release into blood and bile. It performs many vital functions such as, the synthesis of bile, detoxification of drugs, alcohol, and other potentially harmful chemicals (Ramadori et al., 2008). It continuously processes nutrients absorbed by the intestine and stores glycogen, vitamins and minerals. In addition, the liver chemically processes bilirubin so it can be dissolved in water and be excreted (Barritt et al., 2008; Ramadori et al., 2008).

The activities of hepatocytes, the essential unit of the liver, are regulated by the hormones and growth factors. These use changes in Ca^{2+} concentrations as an intracellular signal and many other intracellular messengers (Amaya and Nathanson, 2013; Gaspers and Thomas, 2005).

1.1.3 Hormonal regulation of liver metabolism

1.1.3.1. Main hormones and messengers involved in regulation of liver metabolism

The regulation of liver metabolism involves many metabolic hormones among which insulin and glucagon play a significant role in hepatic signalling pathway (Basseri and Austin, 2012). The hormones, epinephrine, vasopressin and norepinephrine also play an important role in the regulation of liver metabolism (Barritt et al., 2008). Hormonal regulation of hepatic metabolism involves various intracellular messengers, including cyclic adenosine monophosphate (cAMP), cyclic guanosine monophosphate (cGMP), Ca^{2+} and protein kinase C (PKC) (Amaya and Nathanson, 2013; Barritt et al., 2008).

1.1.3.2. Insulin regulated liver metabolism

Insulin is a polypeptide hormone synthesized in, and secreted by, the β cells of the pancreas. Insulin secretion depends on blood glucose concentrations, so that concentrations above 4.5-5.5 mM (80-100 mg/100 ml) stimulate the secretion of insulin (Nelson, 2008). Insulin, in response to high blood glucose levels, stimulates the liver to convert more glucose into glycogen for storage (glycogenesis) (Bailey, 2007). It decreases high blood glucose by acting through insulin receptors on the plasma membrane (Bailey, 2007). The binding of insulin to the insulin receptor results in the phosphorylation of insulin receptor substrate-1, which carries the

message from the insulin receptor to the cytoplasmic space, the nucleus or other organelles through intermediary proteins (Patti and Kahn, 1998). This insulin-signalling pathway finally stimulates glycogen synthesis via glycogen synthase activation, thus increasing the synthesis of glycogen in the liver, and has various effects on different kinases and enzyme synthesis (Bailey, 2007).

Excess acetyl-CoA, a product resulting from high dietary glucose ingestion, is used in the building blocks of fatty acid synthesis and production of triacylglycerols (TAGs) (Ganguly, 1960), which are then delivered to adipose tissue and stored as fat. The overall effect of insulin, therefore, on the liver is to regulate or convert excess (not immediately required by the tissues) blood glucose to glycogen, stored in the liver, and TAGs, which are stored in adipose tissue (Bailey, 2007; Ganguly, 1960).

1.1.3.3. Glucagon regulated liver metabolism

Glucagon, produced by the α cells of the pancreas, inhibits glycolysis and stimulates gluconeogenesis within the liver (Pilkis and Granner, 1992). When the concentration of glucose in the blood falls too low, the pancreas releases glucagon. Glucagon causes the liver to convert stored glycogen into glucose, which is released into the blood. Glucagon and insulin work in a concerted way to keep blood glucose concentration at an optimal level (Nelson, 2008; Pilkis and Granner, 1992). Glucagon also activates the breakdown of TAGs in adipose tissue to form free fatty acids. These fatty acids are then exported to the liver and other tissues to use as an important energy source. Thus, it can be said that the net effect of glucagon is the stimulation of glucose synthesis and release by the liver, along with the mobilization

of fatty acids from adipose tissue for use in a low glucose environment (Nelson, 2008).

1.1.3.4. Epinephrine regulated liver metabolism

Epinephrine binds to receptors on the hepatocyte plasma membrane and can regulate the breakdown of glycogen (Barritt et al., 2008). Epinephrine may act by binding to a variety of adrenergic receptors α1, α2, β1, β2, and β3. Binding to α-adrenergic receptors, epinephrine increases the cytoplasmic Ca^{2+} level which can activate glycogenolysis in the hepatocytes (Barritt et al., 2008; Exton, 1987; Exton et al., 1981; Schofl et al., 1999). Phenylephrine, as an agonist of α-adrenergic receptors and analogue of epinephrine, mimics the actions of epinephrine (Kleineke and Soling, 1987).

1.2 Role of calcium in hormone-regulated hepatic metabolism

Insulin, glucagon, epinephrine and other hormones regulate metabolic responses in the liver in response to the changes in the cytoplasmic Ca^{2+} concentration. In single hepatocyte, hormone-initiated increases in cytoplasmic Ca^{2+} are encoded as the frequency of Ca^{2+} oscillations or waves (Rooney et al., 1989). This plays an important role in the regulation of the metabolism of carbohydrates and lipids in the liver (Barritt et al., 2008). Evidence indicates that Ca^{2+}-calmodulin-dependent kinase II plays an important role in the regulation of glycogen and glucose synthesis (Ozcan et al., 2012). In hepatocytes, while the citric acid cycle and ATP synthesis are regulated by the concentration of Ca^{2+} in the mitochondrial matrix (Robb-Gaspers et al., 1998), the concentration of Ca^{2+} in the ER regulates the metabolism of xenobiotic compounds, as well as protein and lipid synthesis (Berridge, 2002).

1.3 Regulation of intracellular calcium concentration in hepatocytes

1.3.1. General features

In hepatocytes, cytoplasmic Ca^{2+} is an important regulator of glucose and lipids metabolism, bile secretion, mitochondrial activity, cell motion, cell volume, cell growth and apoptosis (Leite and Nathanson, 2001; Amaya and Nathanson, 2013). In normal cells, several components and organelles of cells are dedicated to maintaining the optimal cytoplasmic Ca^{2+} concentration. The major elements of a cell regulating the distribution and mobilization of intracellular Ca^{2+} are schematically shown in the Fig. 1.2.

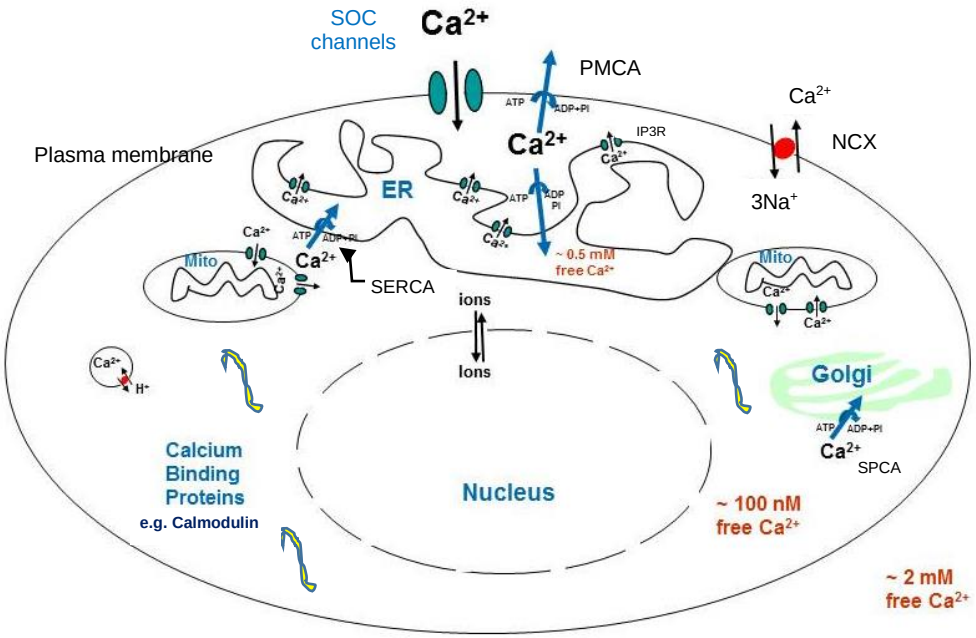

Fig. 1.2. Schematic representation of cellular calcium homeostasis. The Ca^{2+} entry channels (e.g., store-operated Ca^{2+} channels, SOCs) are located on the plasma membrane**.** The plasma membrane (Ca^{2+} + Mg^{2+})ATP-ases (PMCA) and the Na^{+}-Ca^{2+} exchanger (NCX) mediates Ca^{2+} extrusion across the plasma membrane. The ER can take up cytosolic Ca^{2+} via ER (Ca^{2+} + Mg^{2+})ATP-ase (SERCA) and release ER luminal Ca^{2+} through IP_3 and ryanodine receptors (RyR). The Golgi apparatus contains (Ca^{2+} + Mg^{2+})ATP-ase (SPCA). In mitochondria, Ca^{2+} uni-porters are responsible for Ca^{2+} uptake, and Na^{+}/Ca^{2+} and H^{+}/Ca^{2+} anti-porters mediate Ca^{2+} outflow from mitochondria to the cytosol. The cytoplasm and some intracellular organelles have different types of Ca^{2+} binding proteins (adapted and modified from Castro, 2008).

1.3.2. Mechanisms of intracellular Ca^{2+} signalling in hepatocytes

In cells, Ca^{2+} operates over minutes to hours for driving different types of events such as gene transcription and cell proliferation as well as many other cellular processes (Berridge et al., 2003). The increase in the concentration of Ca^{2+} in the cytoplasmic space ($[Ca^{2+}]_{cyt}$) induced by the hormones (mentioned above in subsection 1.2.) is due to the activation of phospholipase C (Litjens et al., 2007a; Putney, 2005), generation of inositol 1,4,5-trisphophate (IP_3), and the release of Ca^{2+} from the ER. The depleted ER Ca^{2+} is subsequently replenished with Ca^{2+} inflow through the activation of store-operated Ca^{2+} entry pathways (Putney, 2005). In appropriate range of concentration (from 0.1 to about 2 µM), Ca^{2+} is a vital messenger and regulator of different cellular pathways. Conversely, excess intracellular Ca^{2+} is toxic to the cells and may cause different cellular pathological conditions and metabolic syndromes (Barritt et al., 2008). As hepatic Ca^{2+} homoestasis is important for liver lipid and carbohydrate metabolism, its dyshomeostasis may be linked with hepatocytes lipid accumulation, obesity and fatty liver disease or associated disorders.

1.3.3. Ca^{2+} entry across the plasma membrane

1.3.3.1 Normal gradient of Ca^{2+} across the plasma membrane

It has been known that the concentration gradient for Ca^{2+} across the plasma membrane in different types of cells including hepatocytes shows a difference in concentrations of around 20,000 fold, as shown in Figs. 1.2 and 1.3. Normal extracellular concentrations of calcium are in the range of 1 to 3 mM and intracellular concentrations are in the micromolar range (from 0.1 to 0.2 µM) (Ivannikov and Macleod, 2013). This gradient of concentration is maintained through various plasma membrane calcium pumps that use ATP for energy. As a

consequence, in resting conditions, cells usually have very low membrane permeability to free Ca^{2+}.

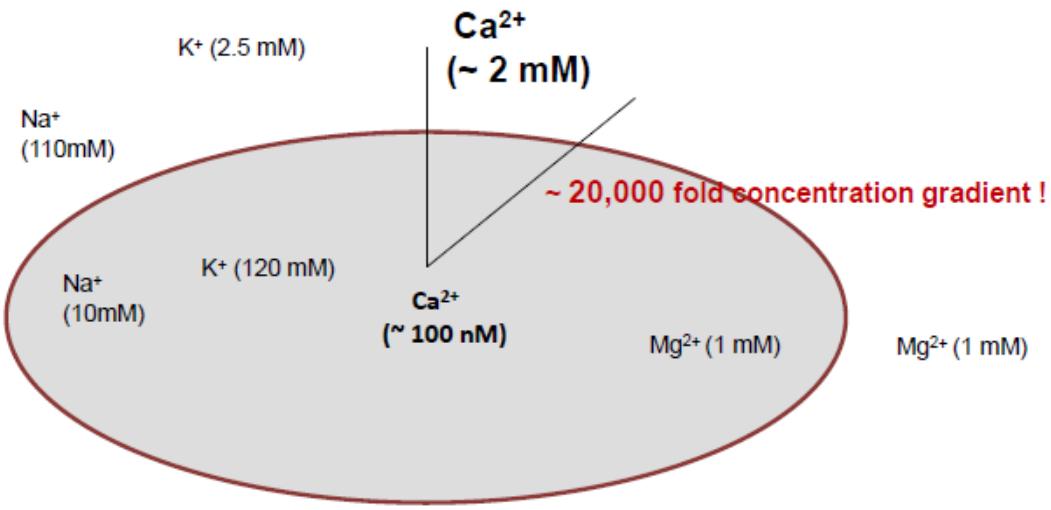

Fig. 1.3. Schematic representation of ion concentration across the cell plasma membrane. The concentration gradient for Ca^{2+} across the plasma membrane in hepatocytes shows a difference in concentration of around 20,000 fold (Adapted from: Toyoshima, 2009).

1.3.3.2 Ca^{2+}-permeable channels in the plasma membrane of liver cells

In hepatocyte and liver cell lines, a number of Ca^{2+} permeable channels have been identified, such as,

1) Receptor-operated calcium channels (reviewed in Barritt et al. (2008));

2) Mechanically-gate calcium channels such as: Stretch activated, non-selective calcium channels (Bear, 1990; Bear and Li, 1991);

3) Ligand-gated channels activated by external ligands such as: local hormone-activated channels and ATP activated P_{2X} purinergic Ca^{2+} permeable channels (Barritt et al., 2008; Capiod, 1998; Spassova et al., 2004).

4) Store-operated Ca^{2+} channels (Castro et al., 2009; Rychkov et al., 2001): When Ca^{2+} is depleted from the endoplasmic reticulum (a major store of Ca^{2+}) of liver cells, the store-operated Ca^{2+} channel, a plasma membrane Ca^{2+} channel, is activated to slowly compensate the level of calcium in the endoplasmic reticulum.

1.4 Store-operated Ca^{2+} channels (SOCs) in hepatocytes

Store-operated Ca^{2+} channels (SOCs) in hepatocytes, being highly selective for Ca^{2+}, maintain the replenishment of the normal amount Ca^{2+} in the ER (Barritt et al., 2008; Castro et al., 2009). Intracellular Ca^{2+} is mainly stored in the ER of cells (Castro et al., 2009). The entry of Ca^{2+} into the cell is termed store-operated Ca^{2+} entry (SOCE), and the current produced from these channels is described as the Ca^{2+}-release activated Ca^{2+} (CRAC) current (Litjens et al., 2007b; Parekh and Putney, 2005). SOCs are defined by the fact that they are activated by the decrease in Ca^{2+} in the ER. Different approaches can be employed to activate SOCs or SOCE. In the physiological situation, increased levels of IP_3 may induce the release of ER Ca^{2+} which subsequently leads to the activation of the store-operated Ca^{2+} channels (reviewed in (Parekh and Putney, 2005)). Experimentally, in liver cells and many other cell types, there are several ways to reduce ER Ca^{2+} content which ultimately activates SOCs: i) Addition of SERCA inhibitors such as di-tert-butylhydroquinone (DBHQ) or thapsigargin (Hoth and Penner, 1992, 1993; Lewis, 1999); ii) Increasing the level of cytoplasmic IP_3 (Parekh and Penner, 1997; Rychkov et al., 2001); iii)

Addition of the Ca^{2+} ionophore, ionomycin, that permeabilises the ER membrane and causes the reduction of ER Ca^{2+} content (Morgan and Jacob, 1994).

1.4.1. Physiological functions of Ca^{2+} entry through SOCs

In the majority of cell types, including hepatocytes, probably the main function of SOCs is to replenish endoplasmic reticulum Ca^{2+} stores (Parekh and Putney, 2005). It has been also reported that to maintain sustained cytoplasmic Ca^{2+} oscillations or waves, SOCs play a significant role (Robb-Gaspers et al., 1998). As suggested for other cells types, SOCs in hepatocytes may be responsible for delivering Ca^{2+} to specific regions of the cytoplasmic space adjacent to the plasma membrane (Liou et al., 2007; Smith et al., 2002). SOCs may also be involved in transcellular Ca^{2+} movement (Hamada et al., 1995) and the maintenance of bile flow in rat liver (Gregory et al., 2004). A pharmacological approach demonstrated that SOCs play a significant role in the proliferation of human hepatoma cells (Enfissi et al., 2004).

SOCE is also involved in the regulatory mechanisms of some enzymes such as adenylate cyclase in other cell types providing an increase in Ca^{2+}_{cyt} near the plasma membrane region (Gu and Cooper, 2000). For hepatocytes, however, no such type of evidence has been reported yet.

1.4.2. Structure of store-operated Ca^{2+} channels (SOCs)

Store-operated Ca^{2+} channels have two essential components, Orai and STIM proteins, as shown by Soboloff et al. (2006). In the case of liver cells, it has been shown that hepatic SOCs principally consists of STIM1 and Orai1 polypeptides (Litjens et al., 2007a). The knockdown of either STIMl or Orail by siRNA

substantially reduced the native Ca^{2+} current in cells (Litjens et al., 2007a), suggesting the importance of both of these proteins to the function of SOCs.

1.4.2.1 Orai1 polypeptide

Orai proteins are a family of Ca^{2+}-permeable channels resident on the plasma membrane, which permit the movement of Ca^{2+} from the extracellular space into the cytoplasm of the cell. There are three known subtypes of Orai proteins: Orail, Orai2 and Orai3 (DeHaven et al., 2007). Orail is the pore-forming subunit of the SOCs that is, probably, central to SOCs function (Park et al., 2009). The important characteristics of the Orail channel is that they open in response to a reduction of Ca^{2+} concentration in the ER lumen, and are highly selective for Ca^{2+} under physiological environments (Parekh and Putney, 2005; Park et al., 2009). In Fig 1.4, the organization of the components of SOCs, STIM1 and orai1, is schematically illustrated.

It has been shown that Orai1 can be assembled as a tetramer, or a higher oligomer upon activation by STIM1 (Lewis, 2007; Zhou et al., 2010), and the intracellular N- and C-termini have been shown to be required for CRAC channel activation (Kawasaki et al., 2010; Lewis, 2007). A single glutamine residue, on a centrally located transmembrane helix is critically involved for the Ca^{2+} selectivity and influx through the Orail channel and absence or mutation of this residue may result in the inability of the protein to function as a store-operated Ca^{2+} channel (Zhou et al., 2010).

1.4.2.2 Stromal Interaction Molecule 1 (STIM1)

STIM1, having one transmembrane domain, is one of the isoforms (STIM1, STIM2) of the Stromal Interaction Molecule (STIM) proteins. The primary function of STIM1 is to act as a sensory protein to detect changes in the concentration of Ca^{2+} within the ER stores (Zhang et al., 2005). STIM1 protein resides within the ER membrane, the N-terminal end of the protein projects into the ER lumen, and it is this component that acts as the luminal Ca^{2+} sensor (Lewis, 2007; Zhang et al., 2005). On the cytosolic side of the ER, the C-terminus of activated STIM interacts with Orail (Figure 1.4). Although STIM1 and STIM2 isoforms are present in hepatocytes, the STIM1 isoform is the most abundant and has the higher affinity for luminal Ca^{2+} (Stathopulos et al., 2006). Since, STIM1 is the most abundant isoform found in hepatocytes and liver cell lines (Barritt et al., 2008; Stathopulos et al., 2006), it could be said that STIM1 is responsible for major Ca^{2+} signalling events within the liver cell.

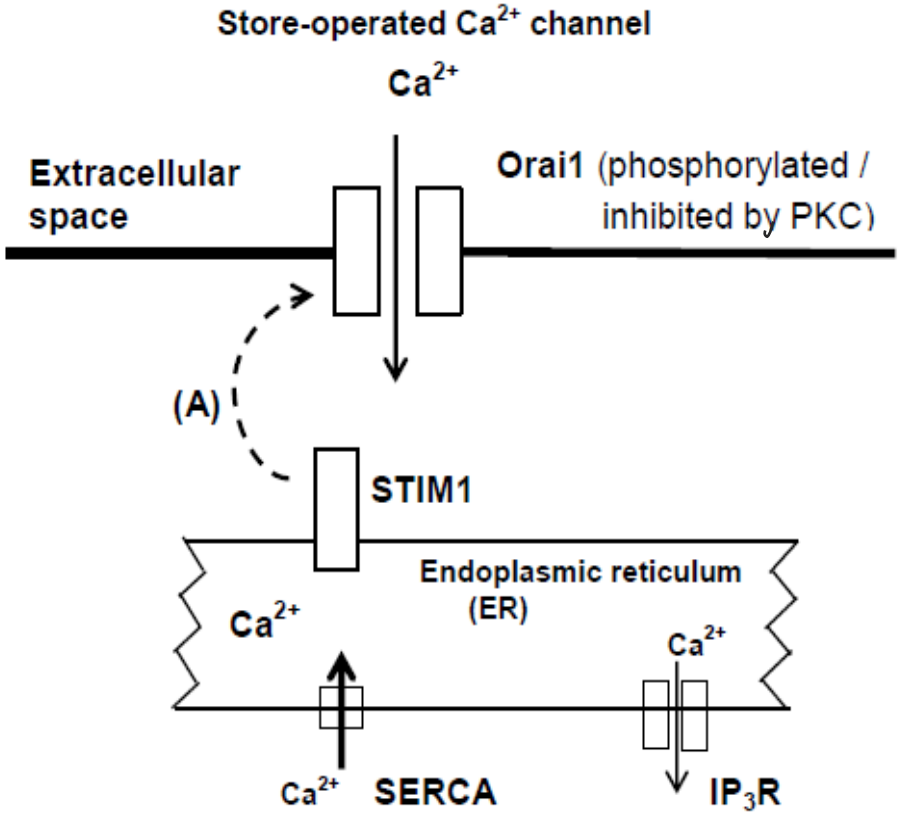

Fig. 1.4. Schematic representation of SOCs channels. Orai1 is located at the plasma membrane. It has intracellular N and C terminal and four trans-membrane sequences. STIM1, consisting of one transmembrane domain, is, located on the ER membrane (Adapted from Barritt et al. (2008)). (A) denotes Activation. SERCA, ER (Ca^{2+} + Mg^{2+})ATP-ase; IP_3R, inositol 1,4,5-triphosphate receptor.

1.4.3. Mechanism of activation of SOCs

The mechanism of activation of SOCs consists of a sequence of events. It has been suggested that STIM proteins, acting as Ca^{2+} sensors, are located in the ER membrane during the resting condition of the cells. STIM can sense a decrease in the concentration of ER Ca^{2+} and move towards the plasma membrane where it binds to the Orai polypeptide and subsequently the Orai pore is activated (Castro et al., 2009; Putney, 2010).

In the case of SOCs activation in liver cells, while STIM1 and Orai1 are the main components, some other proteins, including $G_{i2\alpha}$, PLCγ1 and F-actin may be involved to maintain the integrity of the hepatocyte ER-plasma junctions and ER (Barritt et al., 2008).

1.4.4. Measurement of Ca^{2+} entry through SOCs

1.4.4.1 Fluorescent Ca^{2+} dyes to measure Ca^{2+} entry through SOCs or $[Ca^{2+}]_{cyt}$

The measurement of cytoplasmic Ca^{2+} concentration with fluorescent dyes has been shown to be an important tool for the investigation of SOCs. Using the 'Ca^{2+} add-back protocol', Ca^{2+} entry through SOCs across the plasma membrane can be measured with a cytoplasm-located fluorescent dye coupled with fluorescence microscopy. In the 'Ca^{2+} add-back protocol', cells are loaded with a fluorescent Ca^{2+} dye (e.g., fura-2) and incubated in the absence of extracellular Ca^{2+}, before being exposed to the SERCA inhibitor to release ER Ca^{2+}. Subsequently, extracellular Ca^{2+} is added to allow Ca^{2+} entry through SOCs, and the increase in cytoplasmic Ca^{2+} is measured (Castro et al., 2009). It is also possible to determine the content of Ca^{2+} released from ER lumen with this technique (Castro et al., 2009).

1.4.4.2 Electrophysiology to measure Ca^{2+} entry through SOCs

The patch clamp technique, a highly valuable tool in electrophysiology (Hoth and Penner, 1992), can indicate the characteristics of the current of the ion channel, and permeation and gating properties of the channel (Mak et al., 2013). For plasma membrane channels, the electrode used in this technique detects the movement of ions in or out of the ion channels located in the plasma membrane, and transmits the signal to the amplifier (Castro, 2008). In the case of store-operated Ca^{2+} channels, the patch clamp technique allows the monitoring of the SOCs current generated by SOCs channels located in the plasma membrane (Barritt et al., 2008; Scrimgeour et al., 2009). Using patch clamp recording in the whole cell mode, it is possible to measure ATP- or IP_3-activated Ca^{2+} entry through SOCs in the liver cells (Barritt et al., 2008).

In this thesis, fura-2 fluorescent calcium dye was used to measure the Ca^{2+} entry through SOCs using fluorescence microscopy.

1.4.5. Pharmacological inhibition of SOCs

In much experimental work, Ca^{2+} entry through SOCs can be pharmacologically inhibited by the addition of SOCs inhibitors such as 2-aminoethoxydiphenyl borate (2-APB) (Bootman et al., 2002; Ma et al., 2000), YM-58483/BTP2 (Ishikawa et al., 2003), Lanthanum (La^{3+}) (Hoth and Penner, 1993), or Gadolinium (Gd^{3+}) (Hoth and Penner, 1993) into the incubation medium. BTP2 may be more specific than other SOCs inhibitors because it does not show any blocking activity on K^+ channels (Zitt et al., 2004); although, BTP2 may block some TRPC cation channel activity (He et al., 2005).

1.5 Liver steatosis

1.5.1. Non-alcoholic fatty liver disease and non-alcoholic steatohepatitis (NASH)

Non-alcoholic fatty liver disease (NAFLD) is one of the common chronic liver diseases (Angulo, 2002) which is linked with obesity and metabolic syndrome (Anstee et al., 2013; Musso et al., 2010). It is associated with the accumulation of lipid droplets, diacyl-glycerol (DAGs) in hepatocytes. If untreated, NAFLD can further develop NAFLD-induced NASH (liver inflammation caused by fat accumulation in the liver) and insulin resistance. Hepatocellular carcinoma can result from NASH induced oxidative stress (deterioration of cells) within the hepatocytes (Michelotti et al., 2013).

Smith et al. (2011) suggests that insulin resistance and excess adiposity can be allied with increased lipid influx into the liver and augmented liver lipogenesis, stimulating hepatic triglyceride accumulation. It has been also suggested that in livers of obese subjects, the rate of synthesis of free fatty acids from carbohydrates is increased. This results in an increased intracellular concentration of free fatty acids and the storage of di- and tri-glyceride in hepatocytes (Brookheart et al., 2009). In addition, the faulty fatty acid metabolism via mitochondrial oxidation and lipid export can contribute to hepatic lipid droplets formation (Angulo, 2002; Smith and Adams, 2011).

Hepatic insulin resistance and T2D are the downstream pathological conditions of NAFLD. In normal physiological conditions, liver plays a pivotal role in glucose and lipid metabolism which is predominantly regulated by insulin. Therefore, when insulin resistance develops, the liver shows impaired hepatic glucose production and other major unwanted effects in the body (Matsumoto et al., 2007).

1.5.2. Mechanisms by which steatosis leads to liver injury and insulin resistance

1.5.2.1. Generation of reactive oxygen species (ROS)

There is growing evidence to indicate that lipid accumulation in hepatocytes is associated with mitochondrial dysfunction and the generation of reactive oxygen species in mitochondria (Begriche et al., 2006; Cardoso et al., 2013; Fromenty et al., 2004; Rolo et al., 2012). The generated ROS, in turn, oxidize fat droplets to release lipid peroxidation products which have toxic effects on the liver cells (Fromenty et al., 2004). The resulting oxidative stress stimulates the generation of inflammatory cytokines, which ultimately results in liver injury (Rolo et al., 2012). It has been further reported that mitochondrial oxidation of the excess fatty acids may produce reactive oxygen species which, in turn, may cause endoplasmic reticulum stress, unfolded protein response and impaired lipid, protein and cholesterol synthesis (Bailey, 2007) (Fig. 1.5.).

1.5.2.2. Endoplasmic reticulum stress response

ER stress response can be caused by the perturbation of any of the homeostatic functions (e.g., intracellular Ca^{2+} storage, lipid synthesis, protein folding) of the ER (Schroder, 2008). It has been reported that decreased ER luminal Ca^{2+} concentration in steatotic liver cells of obese mice can lead to ER stress response (Fu et al., 2011; Park et al., 2010). Prolonged activation of ER stress response has been shown to have an important role in the development of insulin resistance and diabetes in animal models of obesity and obese human patients (Hotamisligil, 2010). The ER has a particularly vital role in sustaining cellular homeostasis, but may not have the ability to afford the required support with increased and continuous stress (Fu et al., 2012). With continuous exposure to excess nutrients, such as fatty acids and glucose,

there may be an extra load placed on the adaptive stress responses produced by the ER. When these fail, the ER may create continuous inflammatory and stress responses in the cell, leading to chronic metabolic diseases such as obesity, insulin resistance and T2D (Fu et al., 2012).

1.5.2.3. Activation of protein kinase C (PKC)

The activation of protein kinase C, induced by lipid accumulation (Fig.1.5), is thought to have a link in the development of hepatic insulin resistance (Greene et al., 2010b; Samuel et al., 2007). There is evidence that liver PKCβ, PKCδ and PKCε are activated in steatotic liver (Greene et al., 2010b; Huang et al., 2009; Jornayvaz et al., 2011; Jornayvaz and Shulman, 2012; Puljak et al., 2005). The role of PKCε in hepatic insulin resistance has been validated by knocking down PKCε expression in the livers of rats (Samuel et al., 2007). The presence of DAGs can result from the glycerol 3-phosphate pathway, which represents the lipogenesis route in the synthesis of triacyl-glycerols (TAGs) and phospholipids. It has also been found that DAGs in the cytosolic compartment of the hepatocytes best correlate with the activation of PKCs and insulin resistance in contrast to DAGs in other cellular compartments (Jornayvaz et al., 2011). Moreover, it has been reported that activation of protein kinase C may be linked to reduced intracellular and ER Ca^{2+} storage capacity in HEK cells (Ribeiro et al., 2000). It is also known that activation of PKC is associated with the development of ER stress in human vascular smooth muscle cells (Larroque-Cardoso et al., 2013). While suggested for other cell types, these are the likely pathways that may be present in steatotic hepatocytes.

1.5.2.4. Development of insulin resistance

In the case of regular insulin function, the reduction in blood glucose is associated with the reduction of hepatic glucose production (Kahn and Flier, 2000). The progress of visceral adiposity in obesity may cause free fatty acids to flux into the liver via the portal vein. This leads to the build-up of lipid droplets within the liver, resulting in the development of NAFLD and subsequent hepatic insulin resistance (Nakamura et al., 2009). While insulin resistance may occur at a number of target tissues, the condition is predominantly seen in the liver (Boden and Shulman, 2002). In the case of liver cells, in an insulin resistant state, insulin action on the liver cells is greatly reduced (Kahn and Flier, 2000; Nakamura et al., 2009), probably, due to the reduced insulin-stimulated IRS-2 tyrosine phosphorylation by the insulin receptor kinase (Samuel et al., 2004). Additionally, in the steatotic condition, lipid droplets can alter PKC function which may, in turn, alter insulin receptor kinase function. Altered insulin receptor kinase function further impairs tyrosine phosphorylation of IRS-1, which may lead to altered gluconeogenesis via the MEK pathway (Bhattacharya et al., 2007; Jornayvaz and Shulman, 2012). Lipid droplets may further alter insulin-stimulated glucose transport and impair the effects of insulin-like growth factors-I (IGF-I) (Bhattacharya et al., 2007) – which, ultimately, can be associated with the development of insulin resistance.

In summary, during the development of NAFLD, the oxidation of excess free fatty acids produces reactive oxygen species (ROS) which cause damage to lipids and protein in the ER (Houstis et al., 2006). Impairment to the ER leads to ER stress, which is characterized by a decreased concentration of Ca^{2+} in the ER, impaired protein folding (the unfolded protein response) and impaired lipid and cholesterol

synthesis (Ozcan et al., 2004; Schroder, 2008). To compensate for impaired protein folding, the synthesis of chaperone proteins can be increased. In addition to ER stress, the activation of several isoforms of PKC may reduce ER Ca^{2+} content (Ribeiro et al., 2000) which, in turn, may play an important role in the mechanisms by which steatosis leads to insulin resistance (Greene et al., 2010a; Huang et al., 2009). Fig. 1.5. shows schematically, the stepwise development of insulin resistance in steatotic hepatocytes.

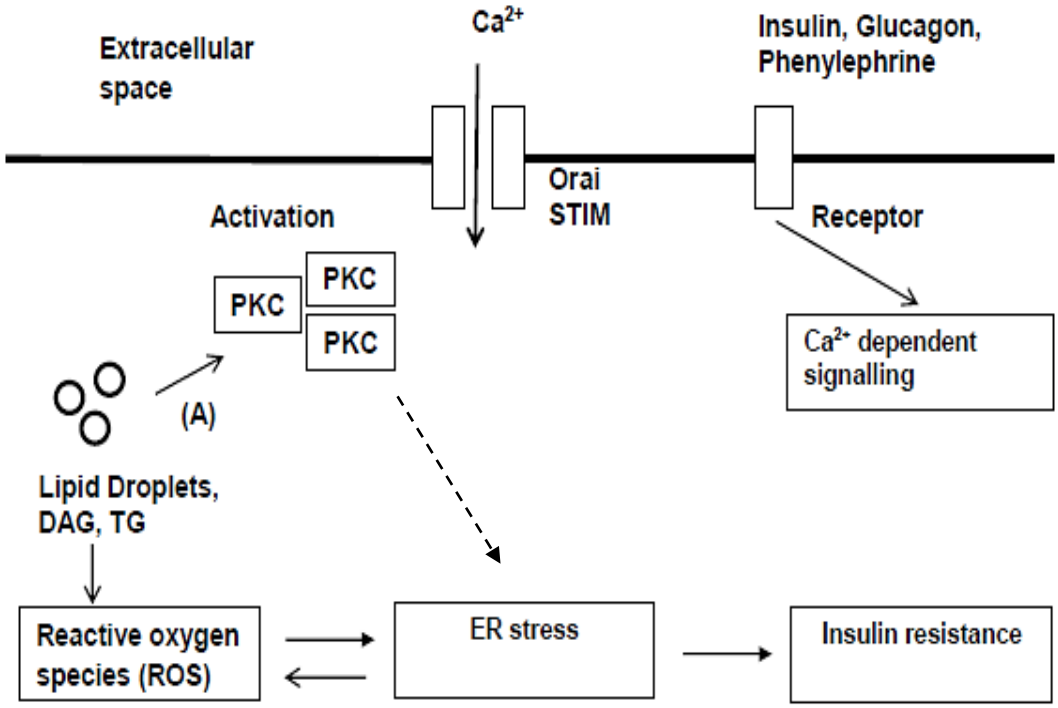

Fig. 1.5. Steatosis induces formation of reactive oxygen species (ROS), activation of PKC, and ER stress response in hepatocytes. Accumulation of lipid droplets, DAGs in hepatocytes may be associated with the generation of ROS which, in turn, may cause ER stress response that ultimately leads to the development of insulin resistance (Samuel et al., 2004). Lipid accumulation in hepatocytes is also responsible for the activation of different PKC isoforms (Samuel et al., 2004; Shulman, 2000). (A) denotes Activation. The single broken arrow denotes that the pathway is not clearly known (in case of hepatocytes).

1.6 Altered Ca^{2+} signalling in steatotic hepatocytes

1.6.1. Altered SERCA expression and activity

The high concentration of Ca^{2+} within the ER is maintained by the sarco(endo)plasmic reticulum (Ca^{2+} + Mg^{2+})ATPase (SERCA) protein. In the liver, SERCA2b is the main isoform and is considered to be the housekeeping isoform (Vangheluwe et al., 2005). Park and colleagues have shown that there was a significant reduction in SERCA2b protein, and mRNA levels in the liver ER microsomal fractions of obese mice, in relation to lean control mice (Park et al., 2010). There is also evidence that steatosis can be associated with impaired activity of SERCA2b of the ER membrane (Fu et al., 2011). Additionally, the activity of SERCA2 proteins is strongly influenced by the nature and composition of the hydrophobic lipid membrane of the ER. The ideal environment for this transporter protein is a highly fluid membrane lacking in cholesterol (Lee, 2002). The accumulation of cholesterol, during the steatotic condition, can be associated with marked Ca^{2+} depletion from ER stores, along with induction of unfolded protein responses and apoptosis (Li et al., 2004).

1.6.2. Altered Ca^{2+} signalling

It has recently been documented, as mentioned above, that decreased activity or expression of SERCA2b in the ER in hepatocytes from obese mice can be linked to a reduction in ER luminal Ca^{2+} concentration (Fu et al., 2011; Park et al., 2010). Thus the consequence of altered SERCA protein may be associated with altered Ca^{2+} signalling in the ER and cytoplasmic space (Fig. 1.6). Some recent studies further support the idea that hepatic lipid accumulation might be linked to impaired

hormonal signalling, and Ca^{2+} dependent metabolic response e.g., gluconeogenesis (Bhattacharya et al., 2007; Jornayvaz and Shulman, 2012).

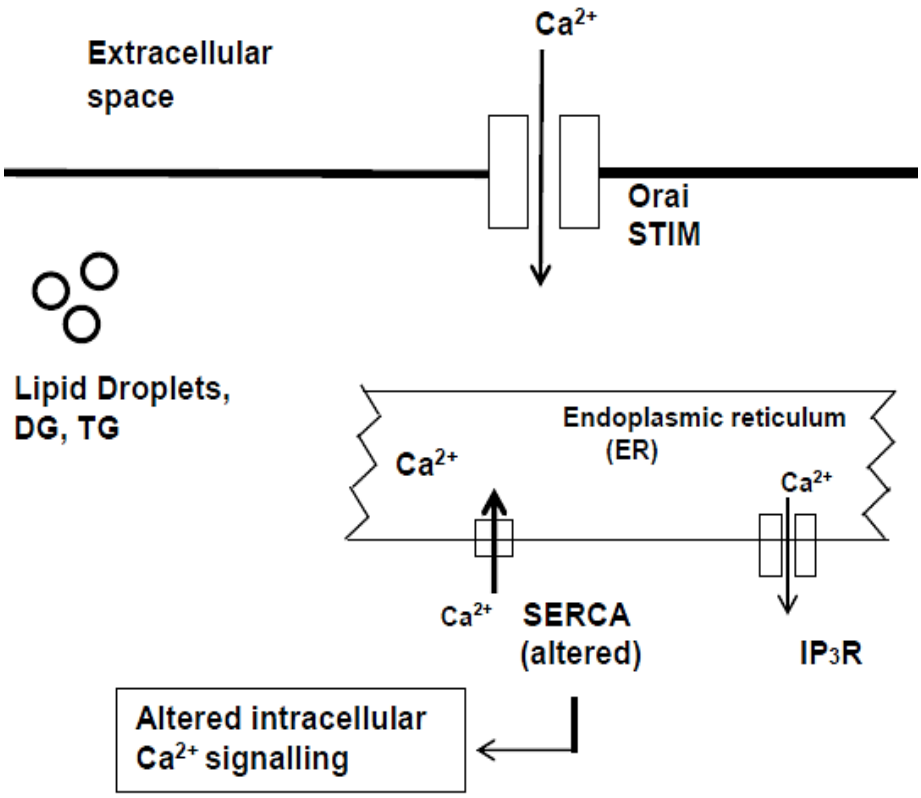

Fig. 1.6. The expression of SERCA2b protein can be altered in the steatotic condition – which may, in turn, cause altered Ca^{2+} signalling. In the steatotic condition, inhibited SERCA2b activity/expression may lead to a reduced Ca^{2+} amount in the ER (Fu et al., 2012; Fu et al., 2011; Park et al., 2010). DG, di-acylglycerol; TG, tri-acyl glycerol, SERCA, Endoplasmic reticulum (Ca^{2+} + Mg^{2+})ATP-ase; IP_3R, inositol 1,4,5-triphosphate receptor; STIM, Stromal Interaction Molecule.

1.7 Pharmacological treatments for steatosis and lipid-induced insulin resistance

1.7.1. Molecular targets for the treatment of insulin resistance and T2D

Insulin receptor, glucagon receptor, glucose transporters, Akt phosphorylation, peroxisome proliferator-activated receptor γ (PPARγ), and glucagon-like-peptide-1 receptor (GLP-1R) have been identified as the molecular targets for the treatment of insulin resistance and T2D (Gallwitz, 2011; Hundal et al., 1992; Nyenwe, 2012; Nyenwe et al., 2011). Additionally, AMP-activated protein kinase, cyclic adenosine monophosphate (cAMP), protein kinase A (PKA), and mitochondrial glycerophosphate dehydrogenase have recently been reported as molecular targets for the treatment of insulin resistance (Burcelin, 2014; Madiraju et al., 2014; Rena et al., 2013).

1.7.2. Drugs currently employed to reduce steatosis

It has been reported that some drugs can be used to prevent the unwanted lipid accumulation in the body. Orlistat can work by blocking the enzyme lipase that breaks down fats in the diet; therefore, some of the unbroken fats are not absorbed by the body but pass to the excretion pathway (Peirson et al., 2014; Tara, 2007). Acting on the serotonin receptors in the brain, lorcaserin can help individuals eat less and feel full after taking smaller amounts of food (Smith et al., 2014). Exendin-4 is a glucagon-like peptide 1 (GLP-1) mimetic which can reduce steatosis or lipid accumulation in diabetic patients by increasing insulin secretion and possibly enhancing insulin sensitivity (Rotella et al., 2005).

1.7.3. Drugs currently employed to treat insulin resistance and T2D

Therapeutic agents currently employed in the treatment of insulin resistance and type 2 diabetes are the glucagon-like-peptide-1 analogues, which bind to the glucagon-

like peptide-1 receptor, the thiazolidinediones, which are peroxisome proliferator-activated receptor γ (PPARγ) agonists, and the biguanides (Gallwitz, 2011; Nyenwe et al., 2011). The biguanides have the tendency to reduce gluconeogenesis in the liver, and, thereby, can reduce the level of glucose in the blood (Kirpichnikov et al., 2002).

However, many hyperglycaemic patients treated with a drug (mentioned in the list above) do not achieve the expected blood glucose level and some treatments, including insulin, can have undesirable weight gains (Gallwitz, 2011). There is, therefore, need for more effective therapeutic strategies for the treatment of the obesity and insulin-resistance (Gallwitz, 2011).

1.7.4. Glucagon like peptide-1 (GLP-1) analogue

GLP-1 analogues are the mimetics of gastro-intestinally derived incretin, glucagon-like peptide-1 (GLP-1). GLP-1 analogues, which have been shown to stimulate weight loss (Rotella et al., 2005), are used as anti-diabetic agents. There is evidence to suggest that GLP-1 analogues such as exendin-4 may lead to increased division of lipid droplets, and may up-regulate phosphorylation of perilipin and hormone sensitive lipase – those are all hallmarks of lipolysis (Gupta et al., 2012).

GLP-1 receptor can activate kinases and/or factors involved in glycogen synthesis and glucose uptake (Dardevet et al., 2004). In this mechanism, a GLP-1 agonist may expedite the uptake of excess glucose from the blood in diabetic conditions. It has been also reported that GLP-1 analogues may be able to reduce the fat contents in *ob/ob* mice (Campbell and Drucker, 2013; Ding et al., 2006) and regulate insulin secretion in β-cells through a Ca^{2+}-dependent pathway (Meloni et al., 2013).

As GLP-1 analogue has the capability to reduce steatosis and interacts with Ca^{2+} signaling (Meloni et al., 2013), we investigated whether GLP-1 analogue, exendin-4 can modulate SOCE in steatotic liver cells.

1.7.5. Evidence that several antidiabetic drugs interact with components of intracellular Ca^{2+} signaling pathways

There is very limited evidence available to demonstrate whether the intracellular Ca^{2+} or Ca^{2+} channels play a role (or not) in the action of anti-diabetic drugs. One recent study suggested that rosiglitazone, a PPARγ agonist, can modulate Ca^{2+} entry through TRP Ca^{2+} channels (Majeed et al., 2011) and can modulate intracellular Ca^{2+} in smooth muscle cells (Rizzo et al., 2009). GLP-1 analogue, through a Ca^{2+}-dependent pathway, has been shown to regulate insulin secretion in β-cells (Meloni et al., 2013). There is some evidence to suggest that metformin can modulate mitochondrial Ca^{2+} transport and intracellular Ca^{2+} signaling (Hwang and Jeong, 2010; Lablanche et al., 2011). In addition, several biguanides have been shown to inhibit hormone induced intracellular Ca^{2+} oscillications (Ubl et al., 1994).

While Ca^{2+} signalling or Ca^{2+} channels may control the hormonal function of some cells (e.g., hepatocytes), there has been little work done that explores the possibility that Ca^{2+} signaling or Ca^{2+} channels may be targets of anti-diabetic drugs.

1.8 Models for lipid accumulation

1.8.1. *In vitro* cell culture models

1.8.1.1. Induction of steatosis by pre-treatment with amiodarone

Amiodarone induces intracellular lipid accumulation by inhibition of lipid oxidation in cells (Fromenty et al., 1990; Yu et al., 2010)) and this amiodarone induced lipid-loaded cell model was previously used by Antherieu et al. (2011) in HepaRG cells.

1.8.1.2. Induction of steatosis by pre-treatment with palmitate

Palmitate, a saturated fatty acid, can also be used to induce lipid accumulation and model insulin resistance in a cell culture. Results have shown that free fatty acids, especially palmitate, can cause reactive oxygen species production by the mitochondrial respiratory chain and oxidative stress in H4IIEC3 hepatocytes. This leads to the accumulation of lipids within the cells (Nakamura et al., 2009).

1.8.2. *In vivo* rat and mouse models

1.8.2.1. Obese (fa/fa) Zucker rat, obese mouse models and high-fat fed rodent

At present, several types of animal models are used for modelling NAFLD and hepatic steatosis. One of these is dietary-based animal models, such as methionine- and choline-deficient diet fed rodents, high-fat-diet fed rodents (Hebbard and George, 2011). Other types of animal models used are genetic models such as obese *ob/ob* mice (Ingalls et al., 1950), Alms1$^{foz/foz}$ mice (Arsov et al., 2006), obese *db/db* mice (Hummel et al., 1966) and the commonly used obese Zucker rat (Gilbert et al., 2003; Phillips et al., 1996)).

1.9 Aims of the present study

As indicated in the review of the literature above, insulin resistance and NASH arising from liver steatosis are serious health problems. The mechanisms by which steatosis leads to insulin resistance are not well understood. Moreover, there is evidence that steatosis leads to altered intracellular Ca^{2+} regulation and subsequently altered endoplasmic reticulum function. Since store-operated Ca^{2+} entry plays an essential role in the hormonal regulation of liver metabolism and in the maintenance of optimum ER luminal Ca^{2+}, the specific aims of this thesis are to:

1. Determine if store-operated Ca^{2+} entry (SOCE) is altered in steatotic liver cells.

2. Investigate the role of protein kinase C (PKC) in impaired SOCE, if any, induced by steatosis.

3. Test if GLP-1 analogue exendin-4 reverses altered SOCE in lipid-loaded liver cells.

4. Evaluate the consequences of lipid-induced inhibition of SOCE on hormonal regulation of glucose metabolism and the development of steatosis.

CHAPTER II: GENERAL MATERIALS AND METHODS

2.1 Materials

Fura-2 AM (acetoxymethyl ester form), Dulbecco's Modified Eagles Medium (DMEM), F-12 (Ham) nutrient mixture (F-12), and pluronic acid F-127 were purchased from Invitrogen (Mt Waverley, Victoria Australia); Fetal bovin serum (FBS) was purchased from Bovogen Biologicals, Keilor East VIC, Australia; Collagenase (Type IV) was obtained from Worthington Biochemical Corporation (Lakewood, NJ, USA); Penicillin-Streptomycin (5,000 U/mL) (Catalogue Number: 15070-063), Lipofectamine RNAiMAX Reagent, Opti-MEM Medium, Amplex® Red Glucose/Glucose Oxidase Assay Kit from Life Technologies; ionomycin, Ethylene Glycol-bis(b-aminoethyl ether)-*N,N,N´N´*-Tetraacetic Acid (EGTA), 9-diethylamino-5-benzo[α]phenoxazinone (Nile red), 2,2',2",2'"-(Ethane-1,2-diyldinitrilo)tetraacetic acid (EDTA), trypsin solution, phorbol 12-myristate 13-acetate (PMA), 2-aminoethoxydiphenyl borate (2-APB), Adenosine triphosphate (ATP) and YM-58483/BTP-2 from Sigma-Aldrich (Castle Hill, N.S.W., Australia); calphostin C and GF109203X from Tocris Bioscience (UK); 2,5-di-(tert-butyl)-1,4-benzohydro-quinone (DBHQ) from Sapphire Bioscience (Redfern, N.S.W., Australia); and glass coverslips from Menzel-Glaser (GmgH, Braunschweig, Germany).

GF109203X (GFX) was dissolved in dimethylsulphoxide (DMSO) (0.2% (v/v) final DMSO concentration), amiodarone in methanol (0.05% (v/v) final methanol

concentration), PMA in DMSO (final DMSO concentration 0.008% (v/v), palmitate in hot water, and 2-APB and YM-58483/BTP-2 in DMSO (0.02% (v/v) final DMSO concentration).

The source of other materials, reagents or chemicals used in different experiments will be stated where appropriate throughout the thesis.

2.2 Cell culture

2.2.1. H4IIE rat liver cell culture

H4IIE rat hepatoma cells (ATCC CRL-1548) (Darlington, 1987) were routinely cultured in 75cm^2 (and 25 cm^2 where appropriate) sterile flasks in Dulbecco's Modified Eagles Medium (DMEM), supplemented with fetal bovine serum (10% (v/v)), penicillin (100 U/ml), streptomycin (100 µg/mL) in 5% (v/v) CO_2 (pH 7.4) at 37°C. Cells were passaged twice a week. The cells were subcultured to another new sterile flask. On the day before the experiments (in particular, for calcium imaging experiments), cells were subcultured to individual 35mm sterile petridishes containing No. 1 glass coverslips. The round glass coverslips (22 mm diameter) were previously pre-treated with concentrated hydrochloric acid to enhance their attachment to the cells. In addition, just immediately before the subculture of cells, the coverslips were sterilised by immersion in 100% ethanol and subsequently flamed.

After 48 h of cell subculture, the medium was replaced with fresh medium (DMEM medium was used for no longer than 4 weeks and was stored at 4^0C). The cell subculture was performed by washing cells 3 times with Phosphate Buffered Saline (PBS) followed by addition of 1ml of trypsin 0.25% plus 1mM EDTA solution, and left for 3-5 min at 37°C to detach the cells. Once the cells were detached, 9ml of

DMEM medium was added and the cells were resuspended by aspiration using a 10 ml pipette. Finally, 3ml of that suspension (just prepared) was transferred to another flask to which 10ml of fresh DMEM medium was added. The H4IIE cell line was subcultured no more than 25 passages to preserve the morphological/functional characteristics of the cell line. The compositions of PBS was (in mM): NaCl, 136; KCl, 4.7; KH_2PO_4, 1.3; Na_2HPO_4, 3.2; adjusted to pH 7.4 with NaOH.

2.2.2. Differentiation of H4IIE rat liver cells

H4IIE rat liver cells were cultured in 25 cm^2 sterile flasks in Dulbecco's Modified Eagles Medium (DMEM) with high glucose, supplemented with fetal bovine serum (10% (v/v)), penicillin (100 U/ml), streptomycin (100 µg/mL), insulin (100 nM final concentration) and dexamethasone (100 nM final concentration) for 12 to 14 days in 5% (v/v) CO_2 (pH 7.4) at 37°C to obtain differentiated H4IIE cells as described previously (Aromataris et al., 2006).

2.2.3. Isolation and culture of rat hepatocytes

Hepatocytes were isolated from rat (Hooded Wistar and Zucker) liver by the collagenase perfusion method, as described previously (Castro et al., 2009). The cells were suspended in DMEM medium with a concentration of ~ 10 x 10^6 cells/ml, kept on ice and cultured within 10 to 30 min. Cell viability was approximately 85 to 90% and above for all concentrations. The hepatocytes were plated on 35mm sterile petridishes containing glass coverslips pre-treated with concentrated hydrochloric acid to enhance their attachment to the coverslips. The hepatocytes were plated for 4 hours in "attachment medium" (Attachment medium was prepared as: DMEM / F12 supplemented with 10% (v/v) fetal bovine serum plus penicillin/streptomycin, insulin

100nM (final insulin concentration) and 100nM dexamethasone (final dexamethasone concentration) and kept in the cell culture incubator (at 5% (v/v) CO_2, at 37°C). After this period (4 hours), the "attachment medium" was replaced by "growth medium" (DMEM supplemented with 10% (v/v) fetal bovine serum plus penicillin/streptomycin) and then cultured for 24-72h in 5% (v/v) CO_2 (pH 7.4) at 37°C as described previously (Castro, 2008).

Animals received humane care in compliance with the Flinders University Animal Welfare Committee, and all the associated experimental protocols were conducted according to the guidelines outlined in the "Australian Code of Practice for the Care and Use of Animals for Scientific Purposes" (National Health and Medical Research Council of Australia). For this project, the Animal Welfare Committee approval number is 701/09.

2.2.4. Measurement of cell viability

In the case of H4IIE cells, after the treatment, normal incubation or expected confluence, cells were harvested with trypsin-EDTA solution and assayed for cell viability using 1:1 Trypan Blue staining, with 50 µl of cell suspension and 50 µl of 0.4% (w/v) Trypan Blue solution. From this trypan blue stained cell suspension, 10 µl of stained cells was added onto a haemocytometer plate, and viewed under a light microscope. Viable and non-viable cells were then counted, as per the methods described by Abcam (2014). The percentage of viable cells in relation to the total cell number was calculated. For primary rat hepatocytes, just after completion of isolation procedures, the viability assay was done using 1:1 Trypan Blue staining and the percentage of viable cells was determined in the same way as mentioned above.

2.2.5. Preparation of HCl-treated sterilized glass coverslips

To sterilize the coverslips for growing freshly-isolated hepatocytes or H4IIE liver cells, concentrated HCl (from Sigma-Aldrich) was added in an appropriate open container (container was made of glass or other acid/heat resistant material) under the chemical fume hood with the respective precautions and 1 whole box of coverslips (~100 coverslips) was carefully added into the HCl and left overnight under the chemical fume hood.

Then the coverslips (in the container) were washed with normal water (with running water in the sink) followed by washing several times with distilled water. After removal of the water, the container was covered with aluminium foil and placed in an oven for 4 h at 90ºC to sterilize the coverslips. Then the container containing sterilised coverslips was placed under the laminar hood for future use.

2.3 Induction of lipid accumulation using amiodarone or palmitate

2.3.1. Principles of Nile red use

The amount of cytoplasmic lipid within the cell can be measured by using the Nile red fluorescent dye and fluorescence microscopy (Greenspan et al., 1985). The procedure of amiodarone pre-incubation and determining the extent of lipid accumulation using Nile Red fluorescence has been demonstrated by Puljak et al. (2005), using a HTC rat liver cell line. Greenspan et al., (1985) first demonstrated the efficiency of using Nile red to identify cytoplasmic lipid droplets in cells, containing DAGs, TAGs and cholesterol esters. Nile red is poorly soluble in water but highly soluble in a wide variety of organic solvents, and exhibits the properties of a fluorescent hydrophobic probe (Fowler et al. 1985). Some of the benefits described for the use of Nile red as an intracellular lipid stain are that the fluorescence is

inactivated in an aqueous environment and is therefore seen only in lipids, without dissolving the lipids it binds (Greenspan et al. 1985). The properties of the binding of Nile red to lipids within the cell is different for cytoplasmic lipid droplets and phospholipids in the membrane. Viewing at a wavelength corresponding to yellow fluorescence (excitation: 450-500nm, emission: >528nm) allows the observation of only cytoplasmic lipid droplets (Greenspan et al., 1985). In addition, when viewed for red fluorescence (excitation: 515-560nm, emission: >590 nm) Nile red shows total lipid content, both phospholipids and cytoplasmic lipid droplets (Greenspan et al., 1985).

2.3.2. Cell culture for lipid accumulation

H4IIE cells (or primary hepatocytes) were seeded at $2x10^4$ cells in culture medium totalling 2 ml in 35mm petri- dishes containing 22mm round glass coverslips (HCl pre-treated) and incubated for 24 hours. Culture medium was replaced with 2ml fresh medium plus 4µl methanol (vehicle treatment) and 4µl 10mM amiodarone in methanol (20µM arniodarone treatment) to three petri-dishes (triplicate) per treatment. Control samples were incubated in fresh culture medium only. Cells were incubated in amiodarone or methanol treatment for 24 hours. In the case of palmitate, 10 mM stock solution was prepared by dissolving palmitate in hot water (double de-ionized H_2O) in a heat-resistant small beaker. Heating chamber (e.g, heat block) was used to slowly warm up the palmitate and water mixture for 7 to 10 min up to 65 to 70°C, and a clear solution of palmitate was obtained. Then the solution was taken at room temperature under laminar hood. After 2 or 3 minutes cooling, appropriate volume of palmitate solution (stock) was added to cell culture medium to get final culture medium containing 500 µM palmitate (Nakamura et al., 2009). Cells were seeded using that medium containing palmitate as above-mentioned procedure and

incubated for 24 hours. In trial experiments, we tried to use a mixture of palmitate and oleate, and in various proportions (e.g., Palmiate:Oleate:: 500 µM: 200µM) according to Listenberger et al. (2003) and lipid loading was examined by Nile red Fluorescence microscopy. In our conditions, however, a consistent lipid loading was not obtained with a mixture of fatty acids in liver cells. Then according to Nakamura et al. (2009), palmitate was used to load lipids into cells and it gave a consistent lipid-loading in H4IIE cells.

2.4 Measurement of lipid accumulation using Nile red

After 24 hours pre-incubation, medium was removed and cells were washed three times with 1ml PBS. Coverslips were incubated, in petri dishes, in 300 µl of 0.1 µg/ml Nile Red in PBS for 15 minutes at 37°C, 5% (v/v) CO_2. Nile red fluorescent stain was immediately removed and coverslips washed once with l ml PBS. Then the coverslips were incubated in 300 µl PBS and protected from light until use. Coverslips were viewed under a Cy3 filter (maximum excitation wavelength: 552nm, maximum emission wavelength: 570nm) to observe red fluorescence, and an Endow GFP filter (maximum excitation wavelength: 480nm, maximum emission wavelength: 503nm) to observed yellow fluorescence using a Fluorescence Microscope (Nikon Eclipse TE 300) with a 40X objective.

Images were acquired in monochrome, and the monochrome images quantified using MetaFluor software (Molecular Devices). To display images in the figures, the images were colour coded (lipid as green) using MetaFluor "Look-Up" Table. For each experimental condition, Nile red fluorescence was measured in 3-4 independent experiments employing 3 coverslips for each condition. For each coverslip, the fluorescence of two separate regions (each containing about 15 cells) was measured.

Background noise was, in each experiment, subtracted from each individual ROI by selecting and setting a reference ROI in a region where no cells were present.

2.5 Measurement of Ca^{2+} in the cytoplasmic space using fluorescent dye fura-2 AM

2.5.1. Principles of fluorescence dye fura-2 AM imaging

The principle for the measurement of cytoplasmic Ca^{2+} using this Ca^{2+} fluorescent dye is that the acetoxymethyl ester (AM) form of the fluorescent dyes can diffuse passively across the cell membrane (and intracellular membranes), and once the dye is inside the cell, esterases cleave off the AM groups (Bootman et al., 2013). Intracellular or cytoplasmic Ca^{2+} binds to the fura-2 free acid, and provides fluorescence intensity. Determination of Ca^{2+}-induced fluorescence at both 340nm and 380nm (excitation wavelengths of fura-2) permits for further calculation of calcium concentrations based on 340/380 ratios. The intracellular localisation of the fura-2 may depend on time and temperature of loading Fura-2 AM (Bootman et al., 2013). The schematic figure 2.1. illustrates the basic principle of fura-2 AM calcium imaging.

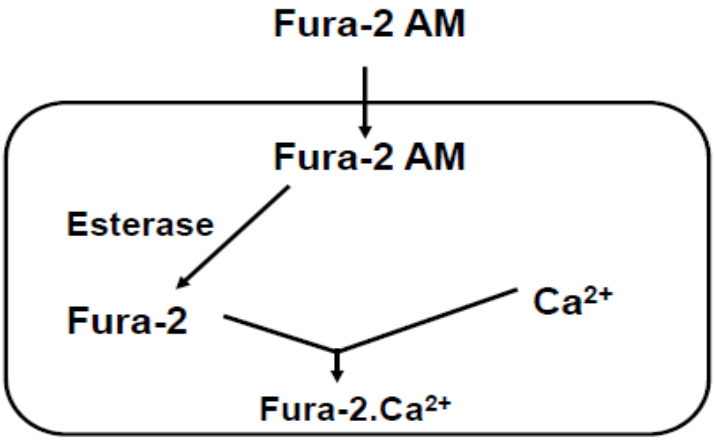

Fig. 2.1. Principles of fluorescence dye fura-2 AM imaging. Once the Fura-2 AM dye is inside the cell, intracellular esterases cleave off the AM groups (Bootman et al., 2013). Intracellular or cytoplasmic Ca^{2+} binds to the fura-2 free acid, and provides fluorescence intensity. Figure adapted from: http://img.springerimages.com/Images/SpringerBooks/BSE.

2.5.2. Loading of liver cells (and primary hepatocytes) with fura-2 fluorescent dye

H4IIE rat liver cells attached to 22mm No. 1 glass coverslips were incubated with 20 μM fura-2 AM in Krebs-Ringer-HEPES buffer (KRH) containing 0.02% (v/v) pluronic acid for 30 min. The concentration of fura-2 AM which we employed is in the range used by others (Castro, 2008; Christopher et al., 1998). Pluronic acid was used to facilitate the loading of the dye by enhancing the dispersal of the hydrophobic fura-2 AM (Conn, 2012). After the loading period, the cells were washed twice with KRH and then incubated for a further 10 to 20 min at room temperature to permit de-esterification of the acetoxymethylester by intracellular esterases. In our experiments, the Krebs-Ringer-HEPES solution contained (mM): NaCl, 136; KCl, 4.7; $CaCl_2$, 2.4; $MgCl_2$, 1.25; glucose, 10; and HEPES, 10; pH of

the solution was adjusted to 7.4 with NaOH. KRH buffer was prepared with or without Ca^{2+} ($CaCl_2$) according to the experimental need.

Primary hepatocytes isolated from Hooded Wistar or Zucker rats were loaded with fura-2 for 1 h at 37^0C in an atmosphere of 5% CO_2. After the loading period, the cells were washed twice with KRH and then incubated for a further 10 to 20 min at 37^0C to permit de-esterification of the acetoxymethylester by intracellular esterases.

2.5.3. Measurement of cytoplasmic fura-2 fluorescence in liver cells

After completion of the loading of fura-2 into cells, cells were placed in an open working chamber (metal incubation chamber) containing KRH buffer, for the measurement of the fura-2 dye fluorescence. Fluorescence of the Ca^{2+}-fura-2 complex was measured with a Nikon TE300 Eclipse inverted microscope. The microscope is connected with a Sutter Lambda DG-4/OF wavelength switcher (Sutter Instrument Company, Novato, CA, USA) and the temperature of the microscope stage was maintained at 37°C with a temperature controller device (Warner Instruments, Hamden, CT, USA). For Ca^{2+} measurement, fluorescence measurements were done using ratiometric acquisition of fura-2 fluorescence (excitation wavelengths of 340 nm and 380 nm) (Bootman et al., 2013). The fluorescence emission was measured at a wavelength of 510 nm. The images were acquired every 10 seconds using a 40x objective. The changes of fluorescence emissions over time, in each experimental condition, were measured with the Photonic Science ISIS-3 ICCD camera (under appropriate settings of intensifier and video gain for the CCD camera) controlled by a computer running UIC MetaFluor software (Molecular Devices Co., USA). Experimental agents were added directly to

the working chamber and mixed three times by gently drawing buffer-and-agents solution into the pipette tip (P200) and gently ejecting back into the chamber.

In order to acquire the fluorescence of fura-2, regions of interest (ROI) at the cytoplasmic regions were selected. Background noise was, in each experiment, subtracted from each individual ROI by selecting and setting a reference ROI in a region where no cells were present. The cells having a fluorescence intensity below the saturation set point of the camera, as well as homogeneous fluorescence, were selected for the experiments. The cells having diffuse fluorescence were carefully excluded. In this way, normally 15-20 out of 30 cells in a field or coverslip were chosen.

The total fluorescence intensity within each ROI was analysed with the MetaFluor software (version 6.0) and stored as text files or Microsoft Excel files. Using the data obtained, all the graphs were generated by GraphPad prism 5 software (GraphPad Software, Inc., San Diego, CA., USA). The results of the individual experiments are expressed as means ± SEM (between 10 and 20 cells for each experiment).

2.5.4. Conversion of fura-2 dye fluorescence ratio into cytoplasmic Ca^{2+} concentration

The ratio of fluorescence intensity at 340 nm and 380 nm (340nm/380nm) was converted to cytoplasmic calcium concentration ($[Ca^{2+}]_{cyt}$) using the equation given below (Grynkiewicz et al., 1985).

$$[Ca^{2+}]_{cyt} = k_d \times (F_{380\ unbound} / F_{380\ bound}) \times (r - R_{min}) / (R_{max} - r) \quad \text{--- (i)}$$

Where, k_d is the binding affinity of fura-2 to Ca^{2+}, r is ratio at any given time.

In the calibration experiment, the values of different parameters for the above equation were determined. In brief, for the calibration experiments, in the presence of Krebs-Ringer-HEPES buffer containing 5mM extracellular Ca^{2+}, fura-2 loaded cells were exposed to the Ca^{2+} ionophore, ionomycin (10μM), to obtain the equilibrium of cytoplasmic Ca^{2+} with extracellular Ca^{2+}. The given values of fluorescence intensity obtained at 380nm excitation correspond to the fura-2 emission fluorescence when fully bound to Ca^{2+} ($F_{380\ bound}$). After the plateau was reached, 20mM EGTA in 0.15 M Tris buffer (pH 8.7) was added to the bath (replacing the previous buffer (KRH buffer containing 5mM $CaCl_2$)) and, thereby, Ca^{2+} was chelated. The values of fluorescence intensity attained at 380nm would represent fura-2 emission fluorescence when unbound to Ca^{2+} ($F_{380\ unbound}$).

Subsequently from the calibration assay, the ratio of 340nm/380 nm fluorescence was determined. The maximum ratio (R_{max}) and minimum ratio (R_{min}) were achieved after ionomycin and EGTA addition respectively. The k_d for binding of fura-2 to Ca^{2+} is 224 nM (Conn, 2012). The calibration for dual wavelength (fura-2) data was performed using Ca^{2+} ionophore in our microscopy setup. The dissociation constant, k_d, for binding of Fura-2 to Ca^{2+} for our experimental set up was taken from literature (Castro et al., 2009; Grynkiewicz et al., 1985; Conn 2012). Considering the buffer pH 7.05 at 37°C, Grynkiewicz et al., (1985) determined the k_d value is to be 224 nM for fura-2. In our experimental procedure, associated buffer (KRH) was adjusted to 7.4 and during experiment, the temperature of buffer was kept at 37°C in the incubation chamber (with the help of appropriate temperature controller). Numerous groups used k_d = 224 nM (fura-2) for primary hepatocytes and liver cells lines (Malhi et al., 2000; Castro et al., 2009). Using the above equation (i) and given values,

where needed, fura-2 fluorescence were converted to cytoplasmic Ca^{2+} concentration ($[Ca^{2+}]_{cyt}$).

2.5.5. Quantification of Ca^{2+} release from the stores and the initial rate of Ca^{2+} entry across the plasma membrane

DBHQ-induced "Ca^{2+}-add back" protocol (illustrated in Fig. 2.2.) was employed for the determination of the amount of the agonist-induced Ca^{2+} release from intracellular stores and Ca^{2+} entry across the plasma membrane. In this experimental protocol, in the absence of extracellular Ca^{2+} (Ca^{2+}_{ext}) a specific agonist called DBHQ (Castro et al., 2009; Parekh et al., 1997), in this case, was added to induce Ca^{2+} release from ER stores. Extracellular Ca^{2+} was added back to the bath after the $[Ca^{2+}]_{cyt}$ returned to the basal levels, creating a second increase in the $[Ca^{2+}]_{cyt}$ until a new plateau was established. This second increase in $[Ca^{2+}]_{cyt}$ is due to store-operated Ca^{2+} entry across the plasma membrane.

Figure 2.2 is a representative plot of Ca^{2+}_{cyt} as a function of time for cells incubated in the absence of Ca^{2+}_{ext}, and subsequent addition of DBHQ and Ca^{2+}_{ext}. The plots of fura-2 fluorescence as a function of time are the means ±SEM (n = 10-20 cells) for one representative experiment. The frequency of the image acquisition was every 10 seconds. The quantity of Ca^{2+} released were estimated by measuring the height of the peak of the agonist-induced increase in $[Ca^{2+}]_{cyt}$. The SLOPE function of MS Excel 2010 was used to determine the initial rate of Ca^{2+} entry.

Calculating the difference between the maximum $[Ca^{2+}]_{cyt}$ observed after Ca^{2+}_{ext} addition and the value of $[Ca^{2+}]_{cyt}$ obtained immediately before Ca^{2+}_{ext} addition

determined the values of the peak of Ca^{2+} entry observed after Ca^{2+}_{ext} addition, as shown in the figure 2.2.

For each experimental condition, fura-2 imaging was performed on a total of 5-10 coverslips on 3-5 separate days (3-5 independent experiments).

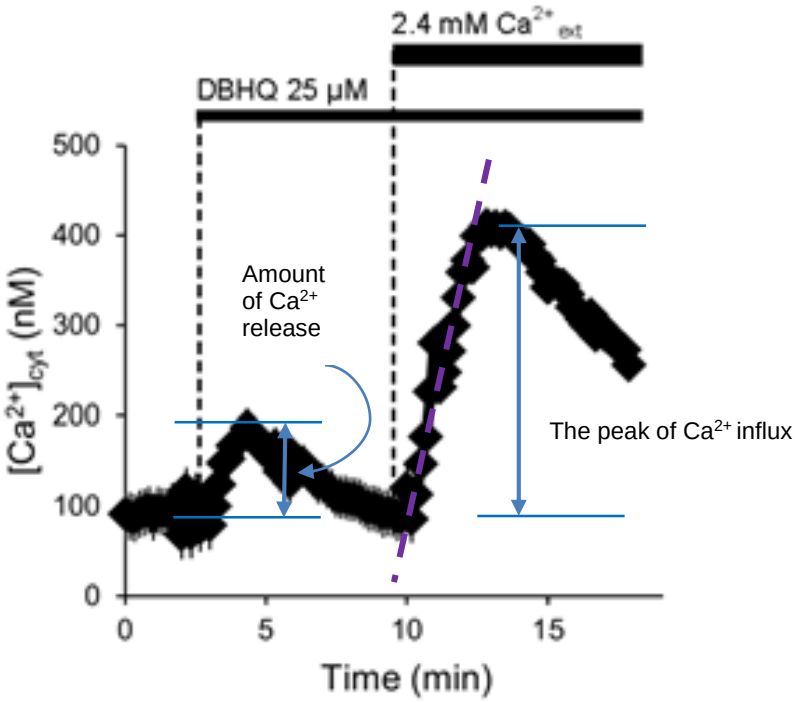

Fig. 2.2. Quantitation of the amount of Ca^{2+} released from ER and Ca^{2+} entry through SOCs with the "Ca^{2+}-add back" protocol. A representative trace (averaged for 15 cells on a coverslip) is presented, showing the alterations in $[Ca^{2+}]_{cyt}$ resulting from the release of Ca^{2+}, by DBHQ in the absence of Ca^{2+}_{ext}, from DBHQ-sensitive stores and Ca^{2+} entry (through SOCs) by subsequently Ca^{2+} re-addition into the working solution in the incubation chamber.

2.6 Determination of the amount of glucose release into cell culture medium

Differentiated H4IIE cells were used to measure the hormone-initiated glucose release into cell culture medium (Aromataris et al., 2008; Aromataris et al., 2006). During hormonal treatment of the cells, FBS- and glucose-free medium was used. After the treatment of cells with hormones (dbcAMP, phenylephrine), samples of extracellular media were collected in eppendorf tubes at different time intervals. The collected samples of medium were stored at -20°C until assayed.

The hormone-induced glucose release into cell culture medium was determined with the Amplex® Red Glucose/Glucose Oxidase Assay Kit (Life Technologies) according to the manufacturer's protocol (Liu et al., 2014). In principle, in this method, glucose oxidase reacts with d-glucose to produce H_2O_2 and d-gluconolactone. The H_2O_2 then reacts with the Amplex® Red reagent, in the presence of horseradish peroxidase, to produce resorufin, which fluoresces. This fluorescence can be measured with a fluorescence microplate reader (Liu et al., 2014).

For the assay, diluting the appropriate amount of the glucose stock solution into Reaction Buffer produced different concentrations of glucose and a glucose standard curve was prepared. The glucose-containing samples were diluted in Reaction Buffer. Then, 50 µL of the standard curve samples, controls, and experimental samples were loaded into individual wells of a 96 well microplate. A working solution of 100 µM Amplex® Red reagent, 0.2 U/mL HRP and 2 U/mL glucose

oxidase was prepared. Working solution of 50 µL of the Amplex® Red reagent/HRP/glucose oxidase was added to each microplate well containing the standards, controls, and samples to begin the reactions. The reactions were incubated for 30 min and protected from light. Fluorescence was then measured with a fluorescence BMG FLUOstar Galaxy microplate reader using an excitation filter of 544 nm and fluorescence emission detection at 590 nm. The fluorescence values were converted to glucose concentrations by reference to the standard curve.

2.7 Transfection with siRNA to knockdown STIM1 and Orai1 expression

H4IIE cells attached to coverslips were transfected with Silencer® Select Pre-Designed siRNA (Life Technologies™) targeting rat STIM1 (Catalog #: 4390771) or rat Orai1 (Catalog #: 4390771) using Lipofectamine® RNAiMAX transfection reagent (Life Technologies™) as per manufacturer's instructions. As a negative control, cells were also transfected with Silencer® Select Negative Control No. 1 siRNA (Life Technologies™).

For the transfection, the diluted siRNA (added 9µl into 150 µl Opti-Mem medium) and diluted Lipofectamine RNAiMAX reagent (added 3µl into 150 µl Opti-MEM medium) were mixed (1:1) properly. After mixing, this mixture was incubated for 5 min at room temperature under the laminar hood. For knockdown of genes, the Silencer® Select Predesigned and Validated siRNA for STIMI and Orai1; and Silencer® Select negative control siRNA were used.

At the same time, H4IIE cells growing in a 75 cm^2 culture flask (~ 90% confluence) were detached by adding 1ml of 1 mM EDTA in PBS (incubated in the incubator for 7 mins to detach) and then resuspended in 9 ml DMEM medium (antibiotic free).

After 5 min incubation for the siRNA (siRNA against STIM1 and Orai1 together)/transfection reagent mix, this 'transfection cocktail' was added to the cell suspension, and then mixed by pipetting up and down. After this, 1 ml of the siRNA/cells mixture was placed at the centre of sterile coverslips (previously positioned into sterile 35mm petridishes). The petridishes were then placed into the incubator at 5% (v/v) CO_2 and 37^0C. The cells incubated for 72 h before use. After 48 hours (out of 72 h), Amiodarone and methanol (vehicle) were carefully added to the cells, and the petridish contents gently swirled to mix properly. After 24 h incubation, the cells were stained with Nile Red without fixing (Nile red staining has been described above in the subsection 2.4.).

2.8 Real-time quantitative PCR (qPCR)

Total RNA was prepared from control and transfected H4IIE cells using TRIzol reagent (Invitrogen). Briefly, for the isolation of total RNA, after harvesting of H4IIE cells, an appropriate volume of cell suspension containing $10x10^6$ cells was transferred to a 10 ml tube and centrifuged for 5 min, 1,500g. The cells were re-suspended in 1 ml Trizol reagent. The tube was incubated at room temp for 5 min, then centrifuged at 12,000g for 10 min at 4°C. The supernatant was transferred to a fresh tube and 200 µl chloroform was added before being shaken by hand vigorously

for 15 sec. Then the tube was incubated at room temperature (RT) for 3 min and centrifuged at 12,000g for 15 min at 4°C.

The supernatant (~500µl), top aqueous phase containing RNA, was transferred to a fresh 1.5 ml tube, and 600 µl of isopropyl alcohol (for the precipitation of RNA) was added and vigorously shaken by hand for 10 sec. Then, the tube was incubated at RT for 10 min followed by centrifugation at 12,000g at 4°C for 10 min. The supernatant was decanted, and the RNA was washed with pre-chilled 75% ethanol and further centrifuged at 7,500g for 5 min at 4°C. Supernatant was decanted and RNA was dried in air at RT for 3-5 min and the pellet was dissolved in nuclease free water. The RNA was aliquoted and/or stored at -80°C for further use.

The RNA concentration in the aliquotes was determined using a Nanodrop spectophotometer and a sample run on a 1% (w/v) agarose gel to ensure the quality of the RNA obtained. The RNA was treated with DNAse I, and subsequently cDNA was prepared with the treatment of oligo-dT and reverse transcriptase enzyme. Complementary DNA (cDNA) was synthesized as described previously (Wilson et al., 2011). mRNA was quantified by qPCR using TaqManTM probe technology, a Rotor-Gene 3000 (Qiagen) and the $2^{-\Delta\Delta CT}$ method (Livak and Schmittgen, 2001).

Rat specific TaqMan® Gene Expression assays (primer and probe pairs) were purchased from Applied Biosystems. These include: STIM1 (assayID: Rn01506502_m1). Sequences of rat Orai1 primers and probes are: 5’ CATGGTAGCGATGGTGGAAG 3’ (forward), 5’ CAGCCTCGATGTTGGGCAG 3’ (reverse) and 5’ CCTGTTCGCCCTCATGAT- CAGTACCTG3’ (probe). Primer

and probe sequences for β-actin were selected as previously mentioned by Scrimgeour et al. (2009). The 5' FAM reporter dye and the 3' black hole quencher dyes were used to label the probes.

2.9 Statistical analysis

Data were entered into a standard spread-sheet (Excel 2010, Microsoft Corporation) or GraphPad Prism 5 (La Jolla, CA, USA) and the statistical significance of two groups was compared using Student's t-test (unpaired and two tailed). The statistical significance between multiple groups was compared using Analysis of Variance (ANOVA) followed by the Bonferroni post hoc test or by Newman-Keus multiple comparison post hoc test (GraphPad Prism 5). Unless otherwise indicated, the data are expressed as means ± standard error of the mean (SEM). Differences between means were considered significant at $P < 0.05$.

CHAPTER III: EFFECT OF LIPID ACCUMULATION IN LIVER CELLS ON STORE-OPERATED Ca^{2+} ENTRY AND ENDOPLASMIC RETICULUM Ca^{2+} RELEASE

3.1 Introduction

As described in the Introduction, the liver plays a critical role in different aspects of lipid metabolism and provides the appropriate concentrations of lipids in the blood. While lipid metabolism is one of the fundamental functions of liver, an excess amount of intracellular lipid accumulation in liver cells may cause liver pathology and can lead to non-alcoholic fatty liver disease, acute fatty liver in pregnancy (Bechmann et al., 2012; Canbay et al., 2007), altered insulin clearance, insulin resistance and type 2 diabetes (Kotronen et al., 2008a; Kotronen et al., 2008b). It is also known that excessive accumulation of intracellular lipid in the cytoplasmic space can lead to reduced endoplasmic reticulum Ca^{2+} content in steatotic liver cells (Park et al., 2010; Wei et al., 2009). However, the effect of excess lipid accumulation or steatosis on Ca^{2+} entry pathways and intracellular Ca^{2+} signalling in the liver is currently unknown. In addition, the effect of extra lipid accumulation on ER Ca^{2+} release *in vivo* is yet to be determined.

Store-operated Ca^{2+} channels are the main Ca^{2+} entry channels, located on the hepatocyte plasma membrane and can be activated by hormones (Castro et al., 2009). Ca^{2+} entry through SOCs plays an important role in the maintenance of cytoplasmic and ER Ca^{2+} homeostasis (Parekh and Putney, 2005; Targos et al., 2005) and spatial

correlation of cytoplasmic Ca^{2+} oscillations (Di Capite et al., 2009) in different cell types, in general.

Given the evidence from others summarised above that lipid accumulation or steatosis alters Ca^{2+} homeostasis and leads to decreased ER Ca^{2+}, and given that SOCE re-fills the ER with Ca^{2+}, the first aim was to determine if accumulated lipids or steatosis inhibits SOCE in steatotic liver cells. To test the hypothesis, H4IIE cells and hepatocytes isolated from Hooded Wistar rats were loaded with lipid by incubation with amiodarone or palmitate. After that, steatotic hepatocytes isolated from obese Zucker rats were employed to verify the observations *in vivo*.

3.2 Results

3.2.1. Amiodarone pre-treatment induces steatosis in H4IIE rat liver cells

The intracellular lipid-accumulation in amiodarone pre-treated H4IIE liver cells was observed and confirmed by fluorescence microscopy. The cells were observed under the Endow GFP filter for yellow fluorescence for observation of DAGs, TAGs, and cholesterol esters within the cell cytoplasmic space (Greenspan et al., 1985). In the case of yellow fluorescence, Greenspan et al. (1985) demonstrated that the intensity of Nile red fluorescence is directly proportional to the amount of intracellular lipid droplets present inside the cells. In our experiments, amiodarone pre-treated cells showed a significant increase in intensity when compared to vehicle and controls cells. Pre-treatment of H4IIE rat liver cells with amiodarone (20 µM) for 24 hours led to the accumulation of intracellular lipid droplets (Fig. 3. 1 A and B).

As shown in Fig 3.1 A (left panel), unlike vehicle and control cells, the pre-treatment of H4IIE cells with amiodarone (20 µM) resulted in intracellular lipid droplets in the cell cytoplasm. In many cases, by visual perception, cytoplasmic lipid accumulation displaced the nucleus in amiodarone pre-treated cells. H4IIE cells pre-incubated for 24 h with amiodarone exhibited substantially increased Nile red fluorescence whereas vehicle (methanol) treated cells showed almost the same degree of fluorescence as untreated control H4IIE cells.

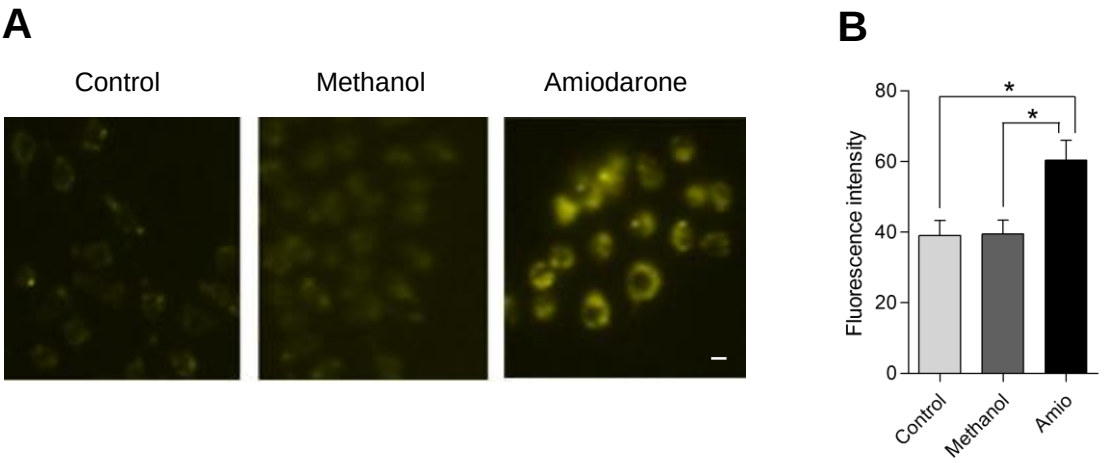

Fig. 3.1. Amiodarone pre-treatment (24 h) induces steatosis in H4IIE rat liver cells. Before imaging, H4IIE cells were incubated with a lipid indicator Nile red (0.1 μg/ml) for 15 min. (**A**) Representative fluorescent images of control (cells were pre-treated with no reagent; at left), methanol pre-treated cells (0.05% v/v overnight exposure) (in middle) and amiodarone pre-treated cells (20 μM overnight exposure) are shown. For each experimental condition, Nile red fluorescence was measured in 3-4 independent experiments (done on separate days) employing 3 coverslips for each condition. For each coverslip, the fluorescence of two separate regions (each containing about 10 – 15 cells) was measured. Yellow-gold fluorescence (excitation, 450-500 nm; emission > 528 nm) was used to view the cytoplasmic loaded lipid droplets using Endow GFP-BP filter. (**B**) The values are the means ± SEM of 3-4 experiments similar to the ones shown in panel **A**. In **B**, degree of significance between control and amiodarone, and amiodarone and methanol, determined using ANOVA followed by Newman-Keuls multiple comparison *post hoc* test, are $P < 0.05$). Image bar 5μm.

The quantified fluorescence intensity results suggest that 20 µM amiodarone pre-treatment provides approximately a 50% increase in yellow fluorescence intensity compared to control and vehicle pre-treated cells, producing a steatotic *in vitro* cell model.

3.2.2. Palmitate pre-treatment induces steatosis in H4IIE rat liver cells

In has been demonstrated that palmitate can induce intracellular lipid accumulation in different cells types. For example, Nakamura et al. (2009) used palmitate to induce lipid accumulation in H4IIEC3 cells to develop an *in vitro* steatotic cell culture model. In our experiments, pre-incubation of H4IIE cells with 500 µM palmitate for 24 hours induced lipid accumulation (Fig. 3.2 A and B) as shown by Nile red fluorescence microscopy.

Some researchers suggest that amiodarone and its principle metabolite desethylamiodarone can inhibit respiratory chain enzymes and β-oxidation of fatty acids and may adversely affect other signalling cascades in the cells (Bolt et al., 2001; Fromenty et al., 1990; Yasuda et al., 1996). To overcome these situations, we used the palmitate-induced lipid-loaded model, in parallel. Both models (amiodarone or palmitate), however, under our conditions, showed similar responses or a similar pattern of responses in our different experiments, e.g., Ca^{2+} add-back experiments or protocols.

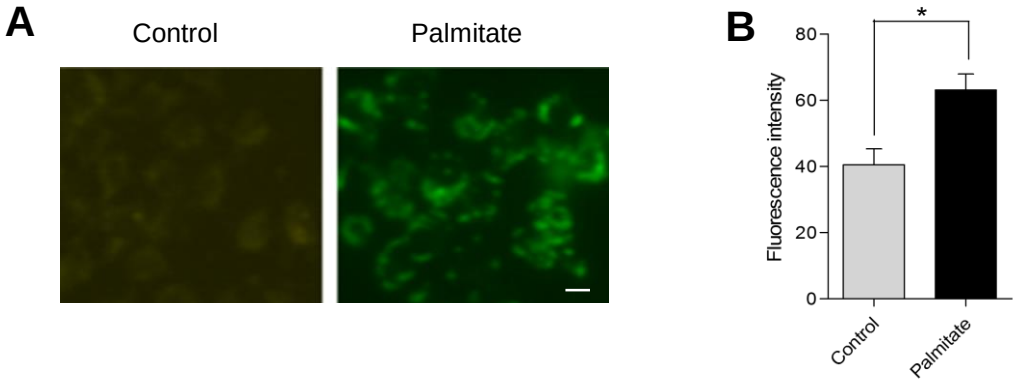

Fig. 3.2. Effects of palmitate on the amount of lipids in H4IIE rat liver cells. Before Nile red fluorescence imaging, H4IIE cells were incubated with a lipid indicator Nile red (0.1 μg/ml) for 15 min as described in Materials and Methods. (**A**) Representative fluorescent images of control (cells were pre-treated with no reagent; at left), and palmitate pre-treated cells (500 μM overnight exposure) are shown. For each experimental condition, Nile red fluorescence was measured in 3 independent experiments (done on separate days) employing 2 coverslips for each condition. For each coverslip, the fluorescence of two separate regions (each containing about 10 – 15 cells) was measured. (**B**) The values are the means ± SEM of 3 experiments similar to the ones shown in panel **A**. In **B**, the degree of significance between control and palmitate, determined using student *t* test, is $P < 0.05$. Image bar, 5 μm.

3.2.3. Amiodarone or palmitate pre-treatment (24 h) and cell viability in H4IIE rat liver cells

As both amiodarone and palmitate can affect a number of cell functions (Anderson and Borlak, 2006; Halliwell, 1997; Nakamura et al., 2009) pre-treatment of cells with amiodarone or palmitate may affect cell viability.

To test the effects of amiodarone or palmitate on cell viability, cells were pre-treated with amiodarone or palmitate for 24 h, and cell viability was determined using Trypan blue exclusion assay. Fig. 3.3 shows the percentage viability of H4IIE cells. After 24 hour, both un-treated (control) cells and methanol pre-treated cells showed about 99% viability whereas amiodarone or palmitate caused about 2% decrease in cell viability compared to control or methanol pre-incubated cells.

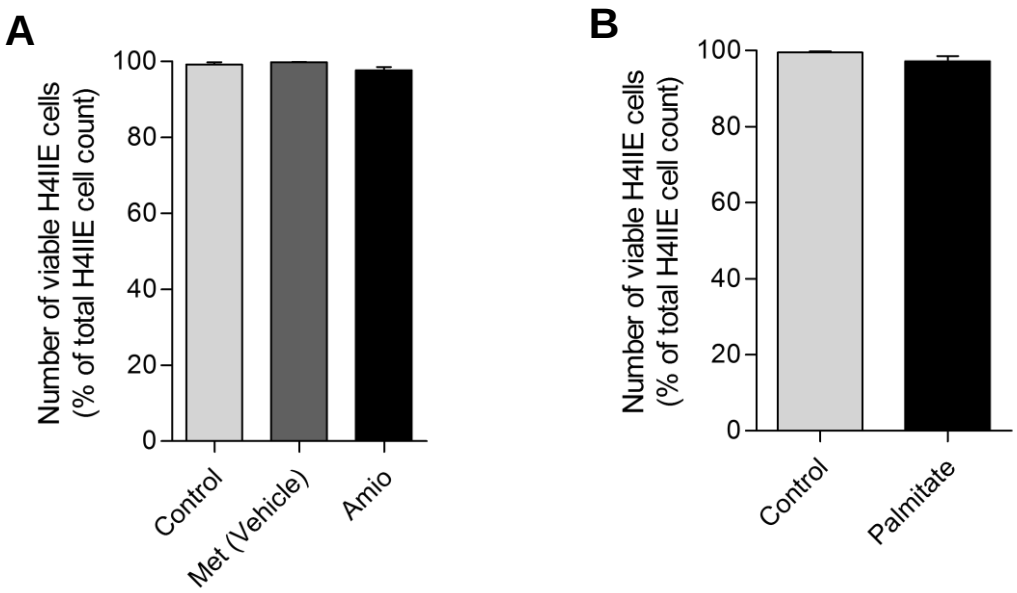

Fig. 3.3. Effect of 24 hour pre-treatment of amiodarone (20 µM) or palmitate (500 µM) on the viability of H4IIE liver cells grown in T25 tissue culture flask. A. The number of viable cells (as a percentage of total cell number) after 24 hour pre-treatment with amiodarone or methanol (0.05% (v/v) final methanol concentration). **B**. The number of viable cells (as a percentage of total cell number) after 24 hour pre-treatment with palmitate. Data are expressed as means ± SEM of 3 independent experiments (done on 3 separate days), duplicate T25 flasks in each condition. Applying ANOVA followed by Newman-Keuls Multiple Comparison *post hoc* test, it was found that the decrease of cell viability in 24h amiodarone pre-treated H4IIE cells was not significantly different compared with vehicle or control cells. Again, the reduction of cell viability in 24h palmitate pre-treated H4IIE cells was not significantly different (two tailed unpaired t test) when compared with non-treated control cells.

3.2.4. Activation of SOCs by SERCA inhibitor DBHQ, and the effect of DBHQ in the presence of extracellular Ca^{2+}

In experimental conditions, as mentioned in the Introductory chapter, ER Ca^{2+} release can be induced by inhibition of the SERCA with thapsigargin, DBHQ and other SERCA inhibitors (Hoth and Penner, 1992, 1993; Lewis, 1999) or by hormone-initiated IP_3 generation within cells (Castro et al., 2009). Both receptor agonists and Ca^{2+}-depleting reagent (e.g., DBHQ) induce a biphasic increase in cytoplasmic Ca^{2+} in the presence of extracellular Ca^{2+} (Bird et al., 2008; Putney, 2010).

To test the effect of lipid accumulation on SOCE in the presence of extracellular Ca^{2+}, addition of DBHQ to fura-2 loaded cells showed a biphasic Ca^{2+} signal (Fig. 3.4), indicating an initial release of ER Ca^{2+} (release phase) followed by a continuous phase of steady Ca^{2+} entry (entry phase), which is of a very similar pattern to the results of Putney (2010); (Putney et al., 1981).

In our present work, when DBHQ was added to cells initially in the presence of $[Ca^{2+}]_{ext}$, the heights of the Ca^{2+} release peak and plateau induced by DBHQ were substantially decreased in lipid-loaded H4IIE cells compared to control and vehicle treated cells (Fig. 3.4. A-C). The reduction in the height of the plateau indicates reduced SOCE in lipid-loaded H4IIE cells.

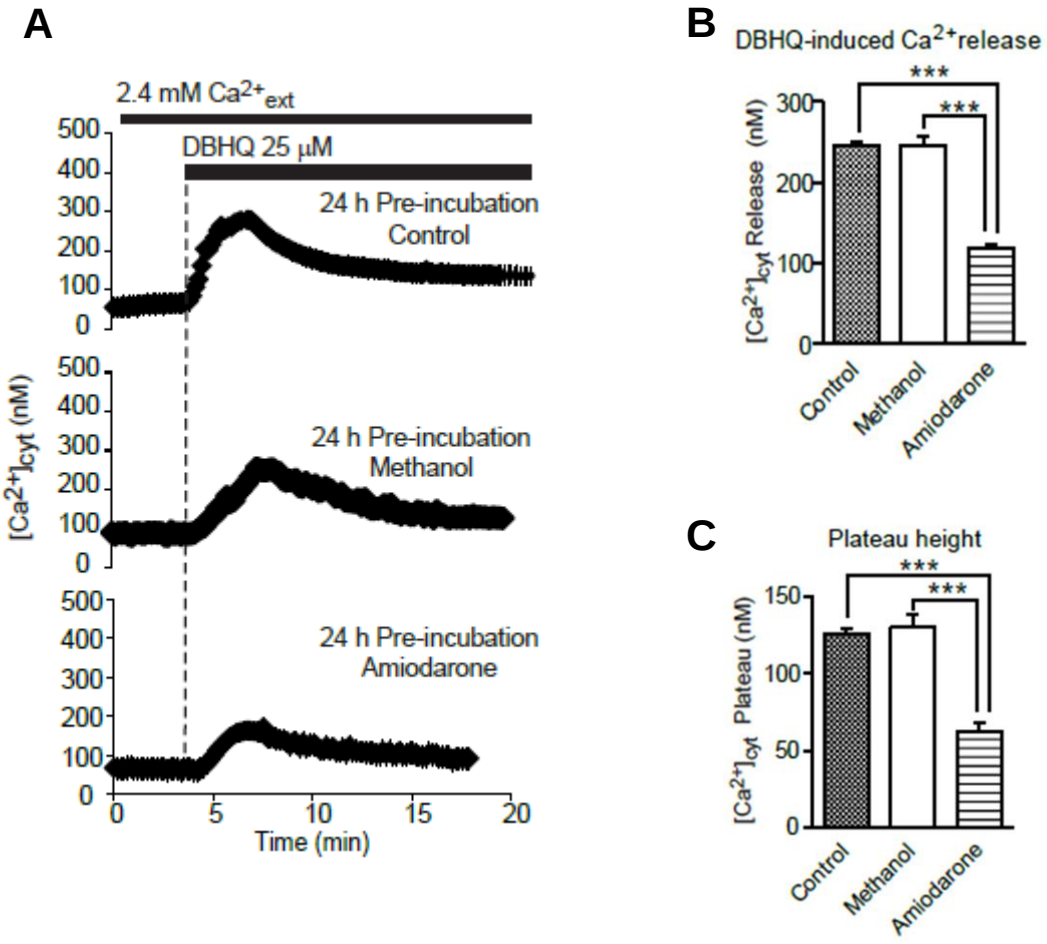

Fig. 3.4. Lipid-accumulation in H4IIE liver cells induced by pre-treatment with amiodarone leads to a substantial decrease in the response to DBHQ added in the presence of extracellular Ca^{2+}. (A) Representative traces showing effects of DBHQ on $[Ca^{2+}]_{cyt}$. **(B**) Ca^{2+} released by DBHQ. **(C)** Plateau height (t=15min) of $[Ca^{2+}]_{cyt}$ following DBHQ addition. $[Ca^{2+}]_{cyt}$ was measured as a function of time in H4IIE cells loaded with fura-2, as described in Methods. Each data point is the mean ± SEM of the values of $[Ca^{2+}]_{cyt}$ obtained for 10-15 cells. The values are the means ± SEM of 3 independent experiments similar to the one shown in panel A. In B and C, degrees of significance between amiodarone and control, and methanol and amiodarone, determined using ANOVA followed by Newman-Keuls multiple comparison *post hoc* test, are *** P<0.001.

3.2.5. Store-operated Ca^{2+} entry (SOCE) is substantially impaired in amiodarone-induced lipid-loaded H4IIE liver cells

H4IIE liver cells were pre-incubated with 24h amiodarone (20µM) to develop intracellular lipid accumulation into the cells (Puljak et al., 2005), and lipid accumulation was confirmed by Nile red staining (Fowler and Greenspan, 1985; Greenspan et al., 1985). In order to investigate whether amiodarone-induced lipid accumulation inhibits store-operated Ca^{2+} entry, after loading with fura-2, cells were incubated in the absence of extracellular Ca^{2+}, treated with DBHQ, and then extracellular Ca^{2+} was added to allow store-operated Ca^{2+} entry (see "Ca^{2+} addback protocol' in Methods section). Amiodarone-induced lipid-loaded cells showed a significant reduction in store-operated Ca^{2+} entry (the initial rate of Ca^{2+} entry) (Fig. 3.5. A, C) and DBHQ-induced ER Ca^{2+} release (Fig. 3.5. A, B). The peak value of Ca^{2+} entry was also substantially reduced in lipid-loaded H4IIE cells compared to control or vehicle control cells (Fig. 3.5. A, D). The results from this study suggest that amiodarone-induced lipid-loading can be linked to a significant inhibition of SOCE and ER Ca^{2+} release.

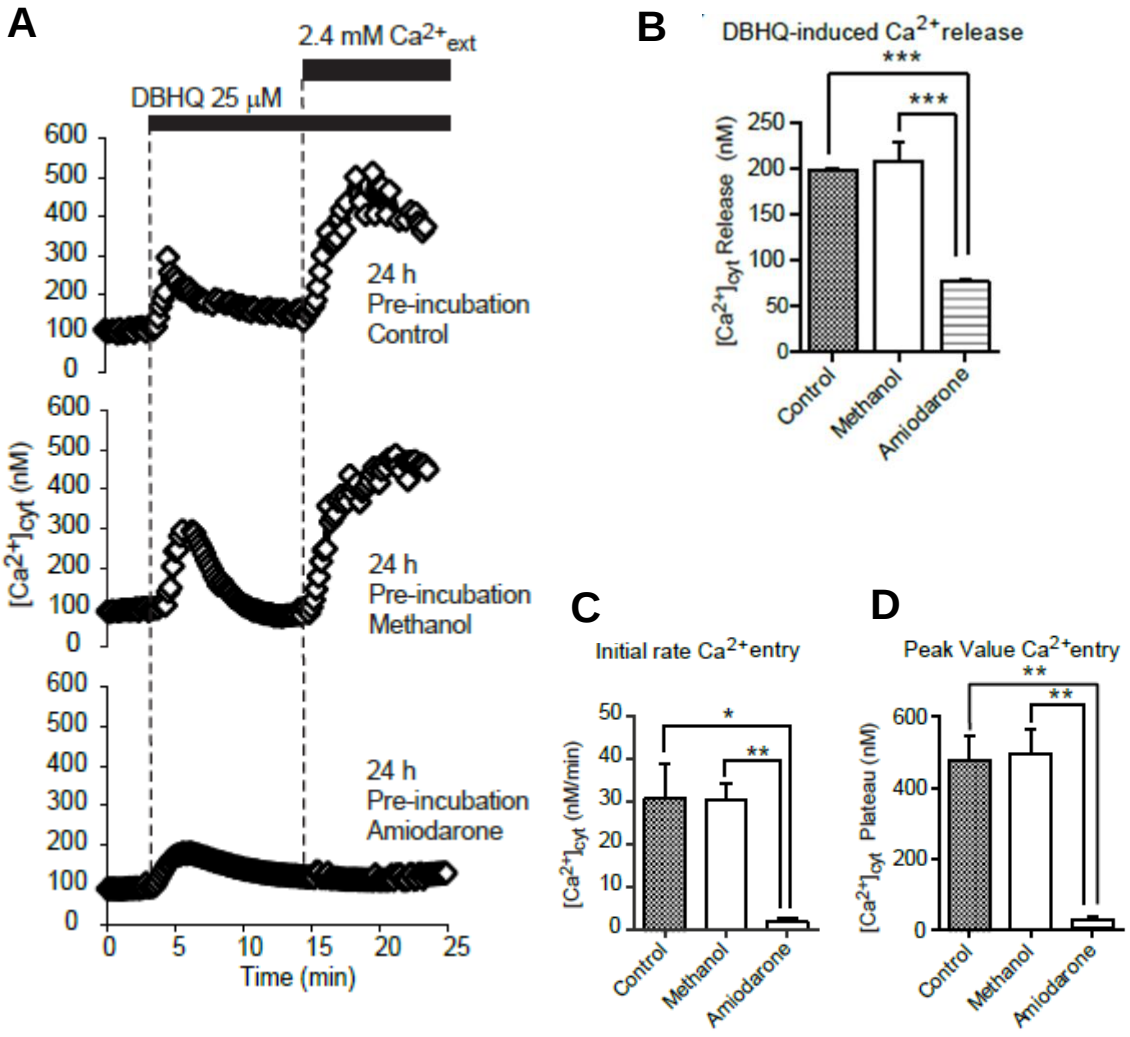

Fig. 3.5. Store-operated Ca^{2+} entry (SOCE) is substantially impaired in steatotic H4IIE liver cells. (A) The addition of the SERCA inhibitor DBHQ (25µM) to H4IIE cells loaded with fura-2, in the absence of Ca^{2+}_{ext}, induces the release of Ca^{2+} form ER Ca^{2+} stores. When Ca^{2+} was added back to the bath an increase in $[Ca^{2+}]_{cyt}$ was observed. $[Ca^{2+}]_{cyt}$ was measured as a function of time in H4IIE cells loaded with fura-2, as described previously. Each data point is the mean ± SEM of the values of $[Ca^{2+}]_{cyt}$ obtained for 10-15 cells. **(B)** Amounts of Ca^{2+} released (peak height) by DBHQ in normal (non-treated), methanol pre-treated and amiodarone pre-treated cells. **(C)** Initial rates of Ca^{2+} entry and **(D)** peak (maximum) values of $[Ca^{2+}]_{cyt}$ following Ca^{2+}_{ext} addition, determined as described previously. The values are the means ± SEM of 3 experiments similar to the one shown in panel A. In B and C, degrees of significance between amiodarone and the control, and methanol and the amiodarone, determined using ANOVA followed by Newman-Keuls multiple comparison *post hoc* test, are * P<0.05, ** P<0.01 and *** P<0.001.

3.2.6. SOCE and ER Ca^{2+} release are impaired in cells loaded with lipid by incubation with palmitate

As for amiodarone pre-incubation, H4IIE cells were pre-treated with 500 µM palmitate for 24 hours and lipid-loading was checked and confirmed with Nile red staining (Fig. 3.2) by fluorescence microscopy.

Palmitate-induced lipid loaded H4IIE cells showed inhibition of DBHQ-induced Ca^{2+} entry through SOCs and of Ca^{2+} release from ER stores when compared to control cells (Fig. 3.6 A-D). In palmitate pre-treated cells, similar patterns of results were obtained as for amiodarone-induced lipid-loaded cells.

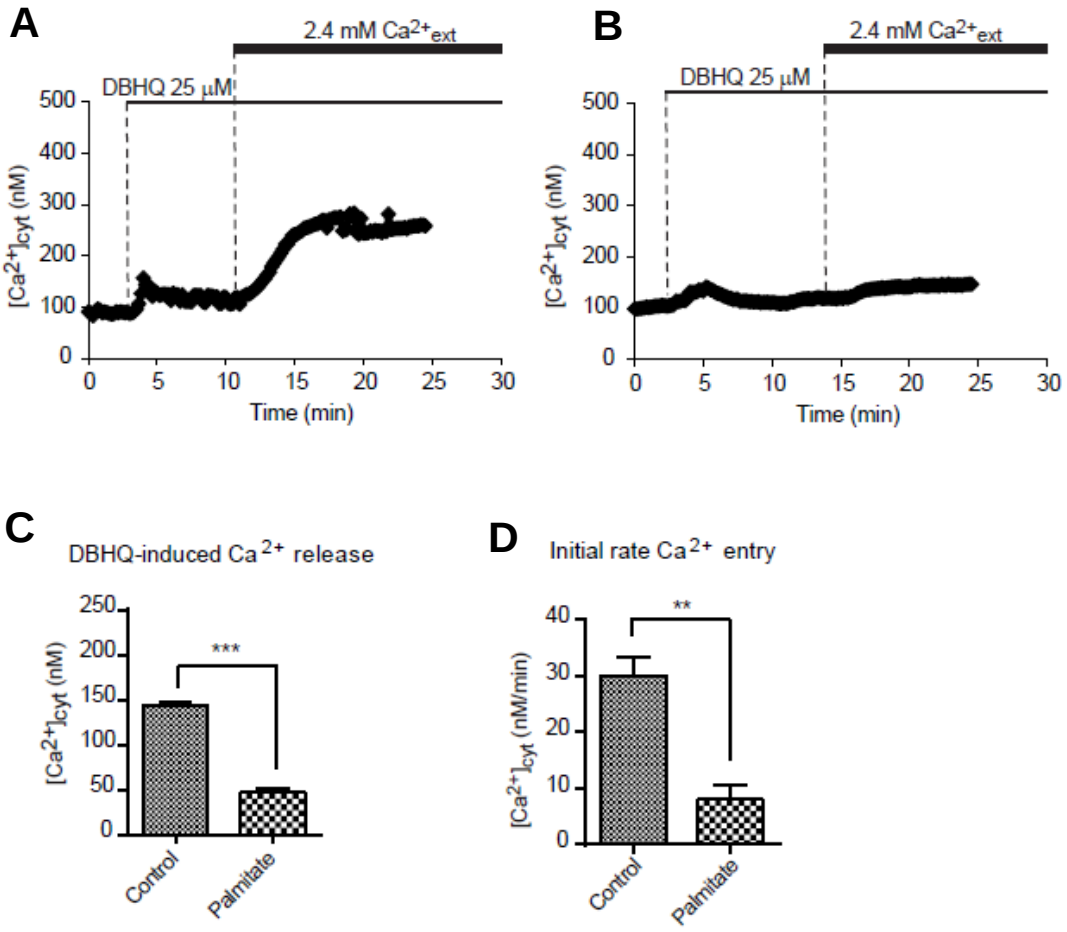

Fig. 3.6. Palmitate 24 h pre-incubation, inhibits DBHQ-induced Ca^{2+} entry through SOCs and Ca^{2+} release from intracellular stores in H4IIE liver cells. (**A, B**) The addition of the SERCA inhibitor DBHQ (25 µM) to H4IIE cells loaded with fura-2, in the absence of Ca^{2+}_{ext}, induces the release of Ca^{2+} form intracellular stores. When Ca^{2+} was added back to the bath a DBHQ-dependent increase in $[Ca^{2+}]_{cyt}$ was observed. Both, the DBHQ-induced Ca^{2+} release and Ca^{2+} entry, were decreased in cells pre-treated for 24 h with 500µM of palmitate. (**C**) Amounts of Ca^{2+} released (peak height) by DBHQ in the presence and absence of palmitate. (**D**) Initial rates of Ca^{2+} entry following Ca^{2+}_{ext} addition, determined as described in Method Section. The values are the means ± SEM of 3 independent experiments (done on three separate days) similar to the one shown in panel A and B. In C and D, degrees of significance between Palmitate and control, determined using student t test, are ** P<0.01 and *** P<0.001.

3.2.7. Evidence that amiodarone does not directly inhibit SOCE

As amiodarone may have some Ca^{2+} channel blocking activity (Lubic et al., 1994), there was a possibility that the observed SOCE inhibition resulted from a direct effect of amiodarone on SOCs located on the plasma membrane. Consequently, the effect of amiodarone (5 µM), added to fura-2 loaded cells immediately before the measurement of $[Ca^{2+}_{cyt}]$, was investigated. Cells incubated in the absence of Ca^{2+}_{ext} and in the presence of 5 µM amiodarone exhibited no change in DBHQ-induced Ca^{2+} release compared to control cells incubated in the presence of vehicle (Fig. 3.7). Using the DBHQ-induced Ca^{2+} add-back protocol, around 24% inhibition of Ca^{2+} entry was observed in 5 µM amiodarone treated cells (Fig. 3.7).

To determine the direct effect of amiodarone on SOCs in the plasma membrane, H4IIE cells were incubated with amiodarone for 10 min, then washed using the same protocol as for the 24h pre-treatment. The DBHQ-induced 'Ca^{2+} add-back protocol' was then performed. The results showed that there was no change in DBHQ-induced Ca^{2+} release and SOCE compared to controls (Fig. 3.8 A-C). These results indicate that under the conditions of our experiment there was no evidence for a direct effect of amiodarone on the inhibition of SOCE. This result further indicates that the detected inhibition of SOCE induced by amiodarone pre-treatment for 24 hours is not due to direct effects of this compound on SOCs components in the plasma membrane.

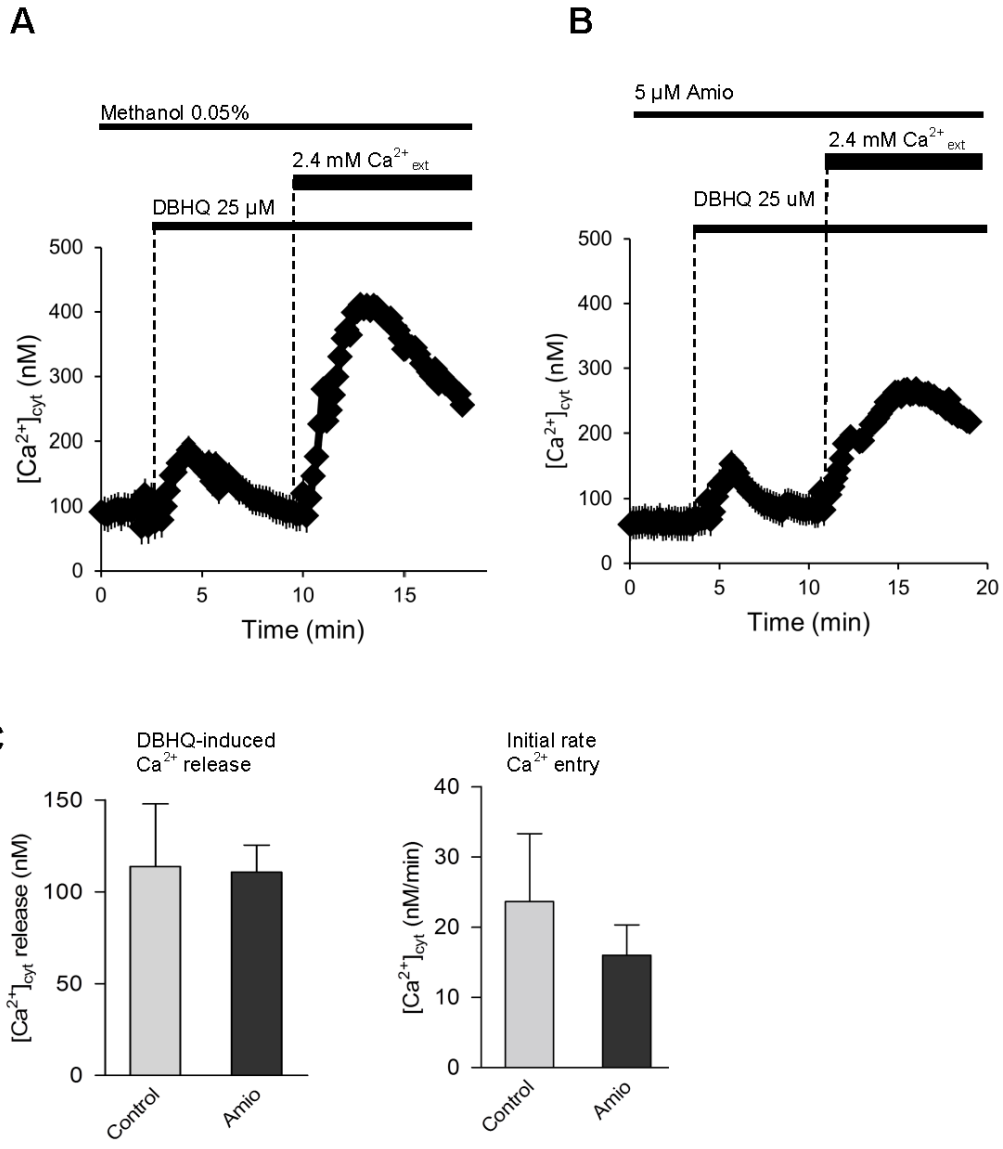

Fig. 3.7. Incubation of H4IIE rat liver cells with low concentrations of amiodarone shows inhibition of Ca^{2+} entry but no effect of DBHQ-induced Ca^{2+} release. The figure shows the effects of amiodarone, added at the beginning of the measurement of $Ca^{2+}{}_{cyt}$, on Ca^{2+} release from the ER initiated by DBHQ and Ca^{2+} entry initiated by addition of extracellular Ca^{2+} following addition of DBHQ. Direct addition of 5 µM Amio, shows a degree of inhibition (~ 24%) of DBHQ-induced Ca^{2+} entry through SOCs in H4IIE liver cells. (**A**), **(B)**, The addition of the SERCA inhibitor DBHQ (25 µM) to H4IIE cells loaded with fura-2, in the absence of Ca^{2+}ext, induces the release of Ca^{2+} form ER stores. Each data point is the means ± SEM of the values of $[Ca^{2+}]_{cyt}$ obtained for 10 - 20 cells. (**C**) Amounts of Ca^{2+} released (peak height) by DBHQ in control (directly treated with 0.05% methanol) and 5µM amiodarone (prepared in 0.05% methanol) direct-treated cells are unchanged. The values are the means ± SEM of 5 experiments those in panel **A** and **B**.

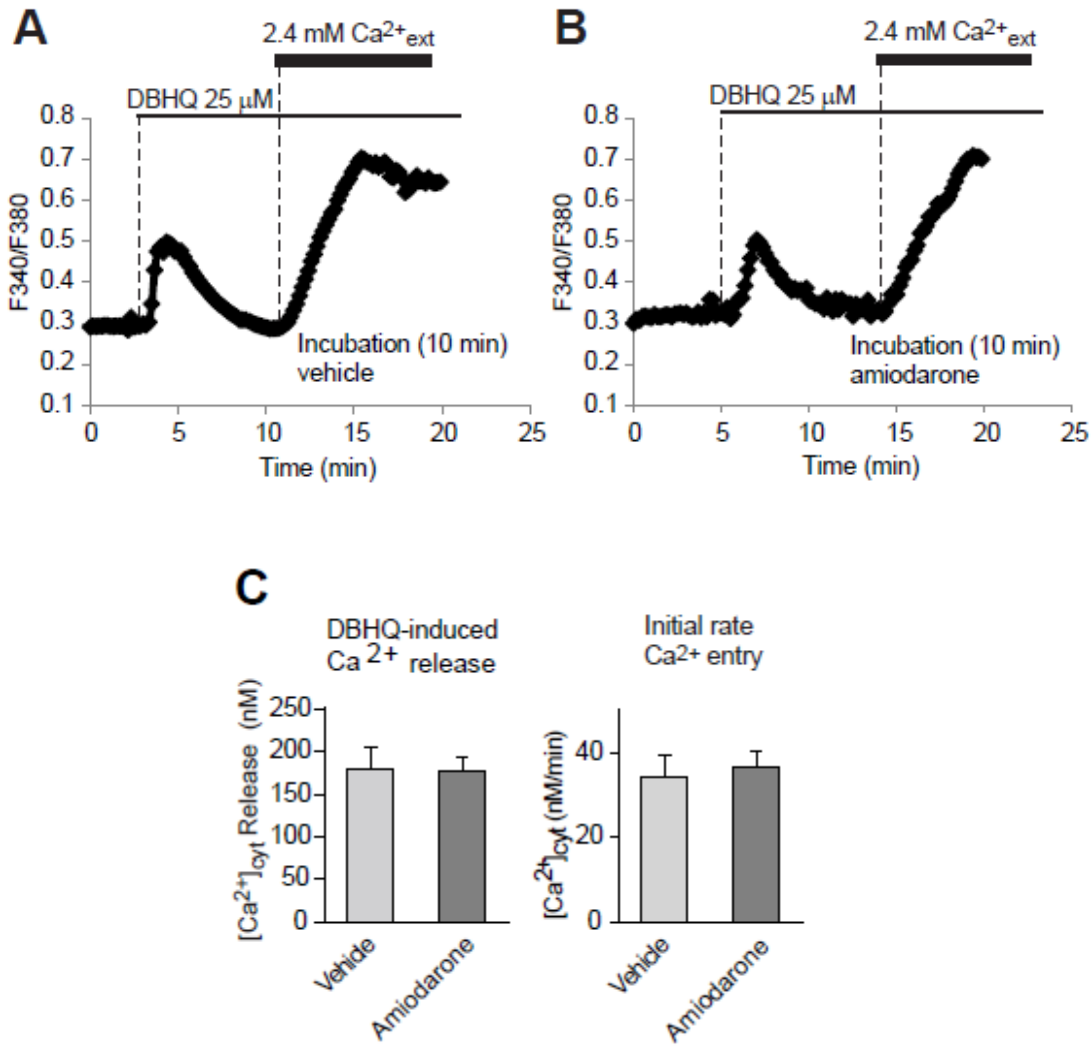

Fig. 3.8. The addition, and subsequent wash-out of amiodarone, does not inhibit store-operated Ca^{2+} entry. (**A, B**) Representative traces showing the effects of the addition of DBHQ in the absence of Ca^{2+}_{ext} and the subsequent addition of 2.4 mM Ca^{2+}_{ext} on $[Ca^{2+}]_{cyt}$, measured using Fura-2, in H4IIE cells following washout (as done for 24 h amiodarone experiments) after incubation for 10 min with 0.05% (v/v) methanol (vehicle) (**A**) and 20 μM amiodarone (**B**). The additions to the bath are indicated by the horizontal bars. (**C**) Amounts of Ca^{2+} released (peak height) by DBHQ and initial rates of Ca^{2+} entry following Ca^{2+}_{ext} addition (means ± SEM (n = 6 coverslips, 2 independent experiments)).

3.2.8. Ionomycin-induced Ca^{2+} release in the absence of extracellular Ca^{2+} is reduced in lipid-loaded H4IIE rat liver cells

In order to confirm that lipid loading in the liver cells reduces the amount of Ca^{2+} in intracellular stores or ER stores, cells were loaded with fura-2, and treated with 15 µM ionomycin in the absence of extracellular Ca^{2+}. At 15 µM of ionomycin treatment, the amount of intracellular Ca^{2+} released by ionomycin in lipid-loaded cells was found to be less than that of control cells (Fig. 3.9 A-C).

Similarly, in the absence of extracellular Ca^{2+}, as above, a higher concentration of ionomycin (50 µM) was used to confirm the maximum ER membrane ion permeability where maximum ER Ca^{2+} was released. In the case of this high concentration of ionomycin, the amount of ER Ca^{2+} release was significantly reduced in lipid-loaded H4IIE rat liver cells (Fig. 3.9. E-G). Using ionomycin-induced Ca^{2+} add-back protocol, SOCE in lipid-loaded cells was also found to be less than that of control cells (Fig A-H).

Overall, the study shows that lipid-loading reduces the amount of ionomycin-releasable Ca^{2+} from intracellular stores. The results may further suggest that lipid-loading in liver cells is linked to a reduction in the ER and/or intracellular Ca^{2+} amount.

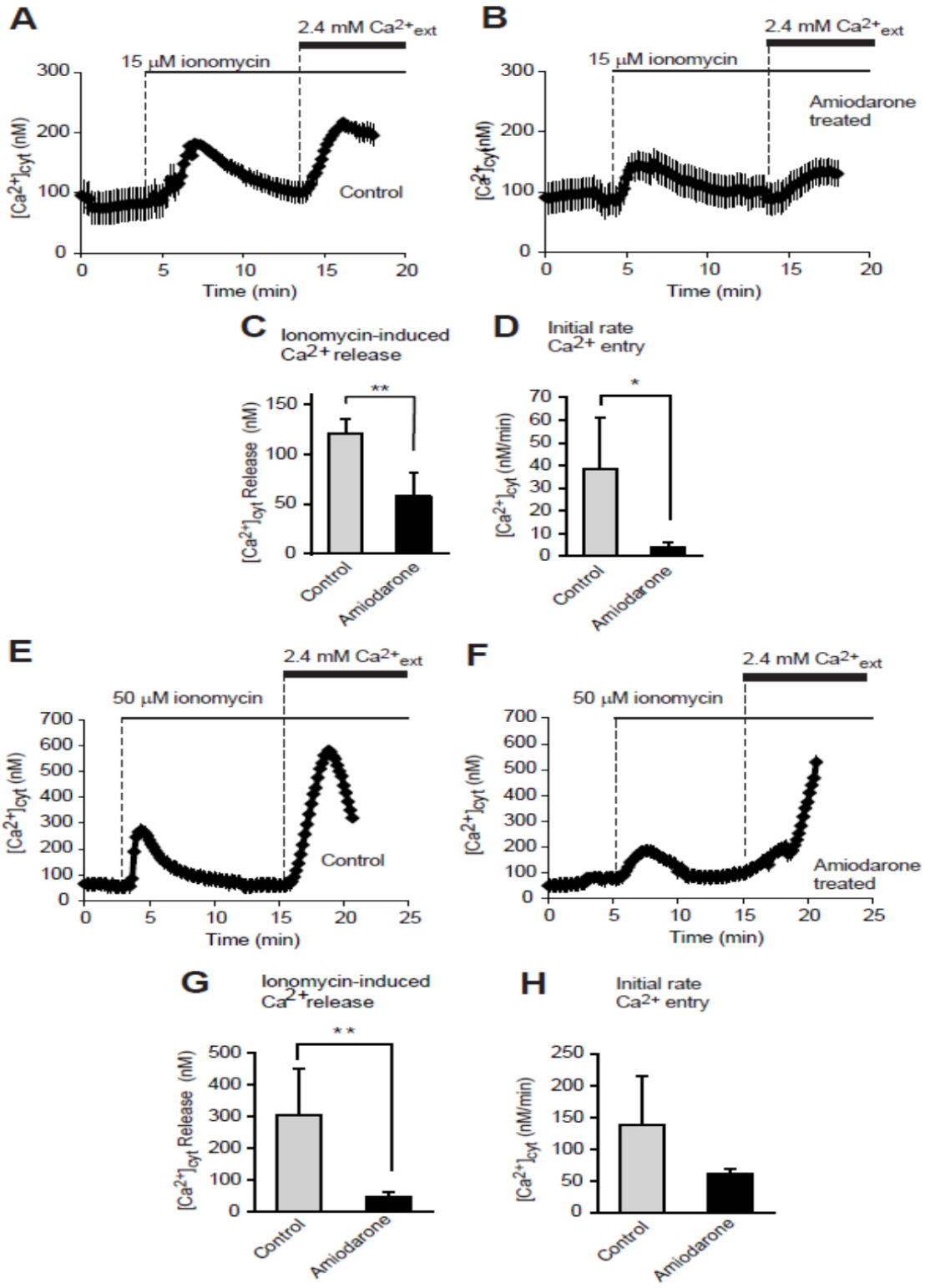

Fig. 3.9. Ionomycin-induced Ca^{2+} release in the absence of extracellular Ca^{2+} is reduced in lipid-loaded H4IIE rat liver cells. (A,B,E,F) Representative traces showing the effects of 15 µM (A,B) and 50 µM (E,F) ionomycin in the absence of added Ca^{2+}_{ext} and of the subsequent addition of 2.4 mM Ca^{2+}_{ext} on $[Ca^{2+}]_{cyt}$, on control (A,E) and lipid-loaded (B,F) cells. (**C,G**) Amounts of Ca^{2+} released (peak height) by ionomycin. (**D,H**) Initial rates of Ca^{2+} entry following Ca^{2+}_{ext} addition. Means ± SEM (n= 4-5). Degree of significance: * P<0.05, and ** P<0.01.

3.2.9. SOCE and ER Ca^{2+} release are substantially impaired in lipid-loaded primary hepatocytes isolated from Hooded Wistar rats.

To determine whether lipid accumulation is associated with alterations in SOCE in lipid-loaded primary hepatocytes, fresh hepatocytes isolated from Hooded Wistar rats were incubated with amiodarone for 24 hours to induce lipids into cells; lipid induction was confirmed by Nile red fluorescence spectroscopy. Lipid-induced primary hepatocytes were loaded with fura-2, incubated in the absence of extracellular Ca^{2+} (Ca^{2+}_{ext}), exposed to DBHQ to release Ca^{2+} from the ER, then Ca^{2+}_{ext} (2.4 mM final concentration) was added to permit Ca^{2+} entry (Ca^{2+} add-back protocol).

Hepatocytes isolated (freshly) from Hooded Wistar rats loaded with lipid by pre-treatment with 20 μM amiodarone exhibited decreased Ca^{2+} release from the ER and decreased Ca^{2+} entry initiated by DBHQ (Fig. 3.10.).

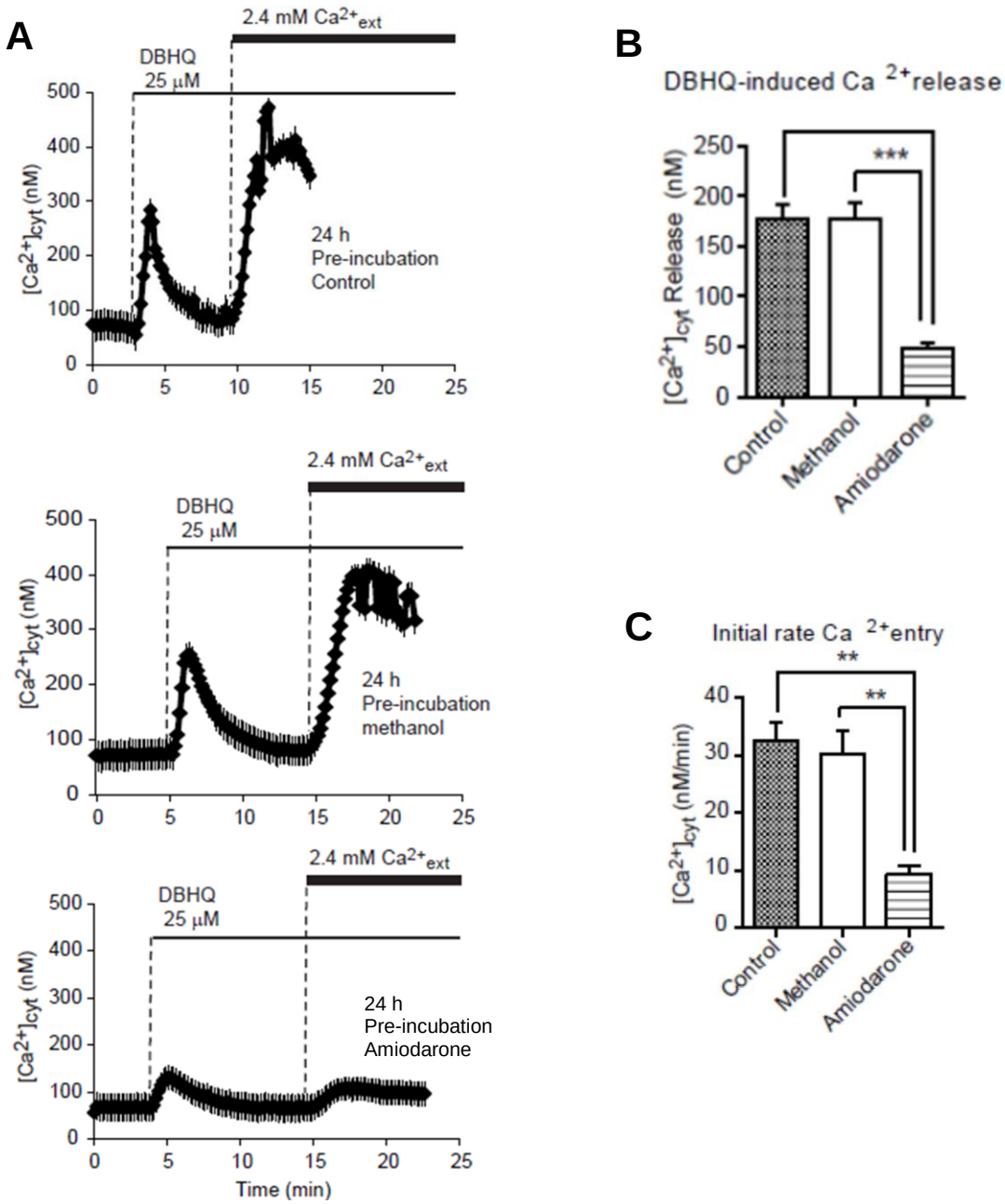

Fig. 3.10. Store-operated Ca^{2+} entry and Ca^{2+}_{er} are substantially altered in lipid-loaded primary hepatocytes isolated from Hooded Wistar rats. In **A,** Hepatocytes isolated from Hooded Wistar rats loaded with lipid by pre-treatment with 20 µM amiodarone exhibit decreased Ca^{2+} release from the ER and decreased Ca^{2+} entry initiated by DBHQ. $[Ca^{2+}]_{cyt}$ was measured as a function of time in primary rat hepatocyes loaded with fura-2, as described in Methods section. Each data point is the mean ± SEM of the values of $[Ca^{2+}]_{cyt}$ obtained for 10-20 cells. The values are the mean ± SEM of 3 independent experiments similar to the one shown here. In **B** and **C**, degrees of significance between amiodarone and control, and methanol and amiodarone, determined using ANOVA followed by Newman-Keuls multiple comparison *post hoc* test, are ** P<0.01 and *** P<0.001.

3.2.10. SOCE and ER Ca^{2+} release are substantially impaired in primary hepatocytes isolated from Obese Zucker rats

To determine the effect of steatosis on SOCE in a more physiological environment, primary hepatocytes isolated from obese Zucker and lean Zucker rats were employed. Using the DBHQ-induced Ca^{2+}-add-back protocol, it was shown that primary hepatocytes freshly isolated from obese Zucker rats exhibited reduced Ca^{2+} release from the ER and decreased Ca^{2+} entry initiated by DBHQ, compared to hepatocytes isolated from lean Zucker rats (Fig. 3.11. A, B).

Primary hepatocytes isolated from lean Zucker rats were incubated with amiodarone for 24 hours to induce lipids into lean Zucker hepatocytes; lipid induction was confirmed by Nile red fluorescence spectroscopy. Lipid-induced primary hepatocytes were loaded with fura-2, incubated in the absence of extracellular Ca^{2+}, exposed to DBHQ to release Ca^{2+} from the ER, then Ca^{2+}_{ext} was added to permit extracellular Ca^{2+} entry. Hepatocytes isolated from lean Zucker rats loaded with lipid by pre-treatment with 20 μM amiodarone exhibited decreased Ca^{2+} release from the ER and decreased Ca^{2+} entry initiated by DBHQ, compared to controls (Fig 3.11. C, D).

In our experimental conditions, any significant change in basal $[Ca^{2+}]_{cyt}$ between normal and fatty liver cells was not observed. However, the 'unchanged or constant' concentration in basal free Ca^{2+} in obese Zucker hepatocytes or lipid-loaded H4IIE cells was not a consistent observation (e.g., Fig. 3.11 B vs D). In some experiments, the basal free Ca^{2+} was slightly altered. A statistical analysis of the basal $[Ca^{2+}]_{cyt}$ in fatty liver cells compared to vehicle pre-treated normal cells was undertaken, but found no significant difference in the mean values. No significant change in the basal value of $[Ca^{2+}]_{cyt}$ was observed in hepatocytes isolated from obese Zucker rats or palmitate/amiodarone pre-treated cells.

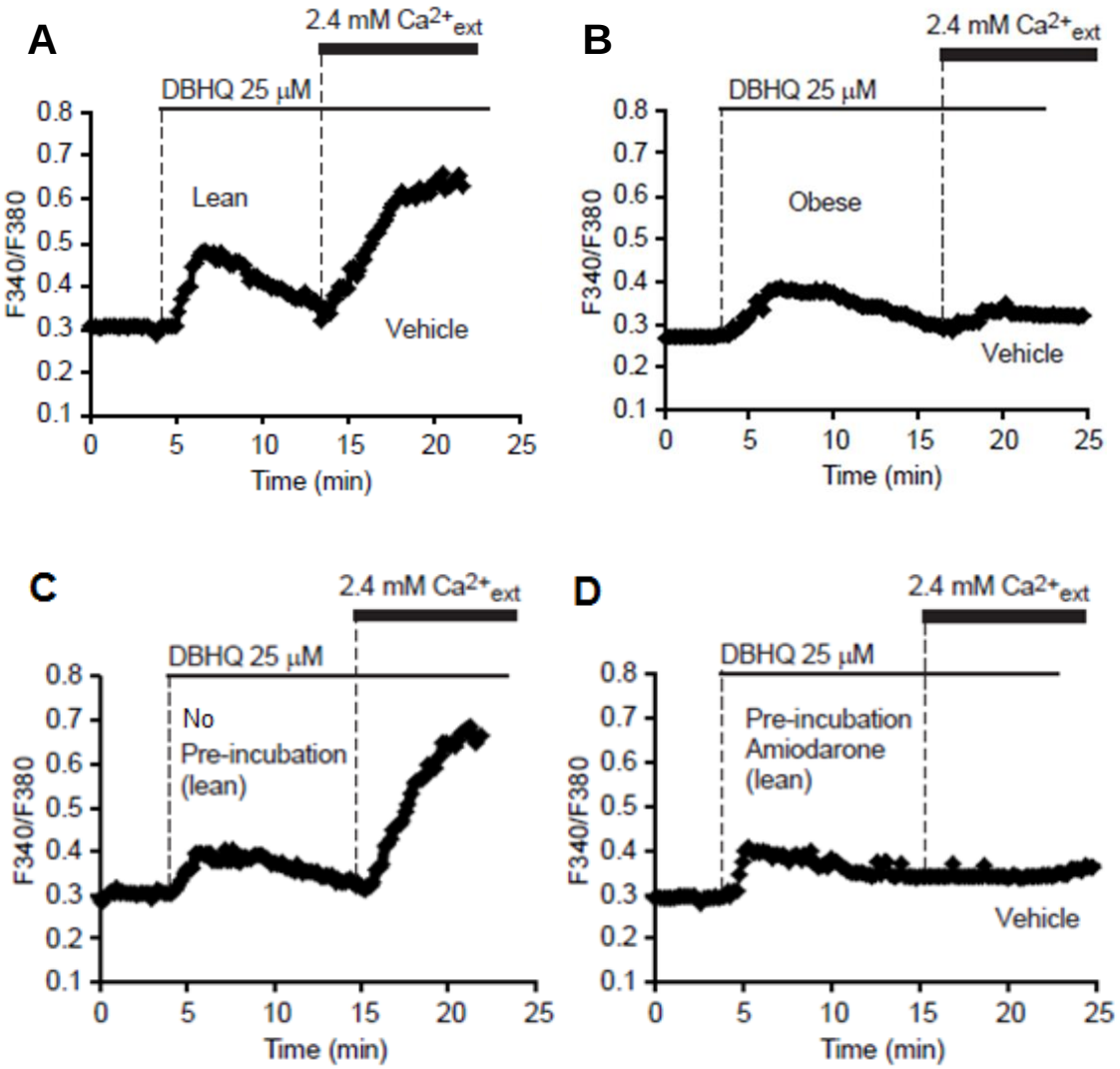

Fig. 3.11. ER Ca^{2+} release and SOCE are substantially impaired in steatotic primary hepatocytes isolated from obese Zucker rats. Steatotic hepatocytes isolated from Obese Zucker rats and amiodarone-induced lipid-loaded hepatocytes from lean Zucker rats exhibit decreased Ca^{2+} release from the ER and decreased Ca^{2+} entry initiated by DBHQ. $[Ca^{2+}]_{cyt}$ was measured as a function of time in primary rat hepatocytes loaded with fura-2, as described previously. The results shown here are representatives of those obtained for one of 2 independent experiments (done on two separate days, 6 coverslips for each condition) which each gave similar results.

3.3 Discussion

In this chapter, evidence was provided that pre-incubation with amiodarone or palmitate can induce lipid accumulation in H4IIE rat liver cells, and rat hepatocytes isolated from Hooded Wistar or lean Zucker rats. Lipid-loaded liver cells exhibited a substantial decrease in store-operated Ca^{2+} entry (SOCE) and impaired ER Ca^{2+} release compared to control cells. In order to determine the effects of steatosis on store-operated Ca^{2+} entry, three different models, amiodarone induced lipid-loaded cell culture model (Puljak et al., 2005), in vitro cell model developed by pre-incubation with palmitate (Nakamura et al., 2009) and *in vivo* obese Zucker rat hepatocytes (Buque et al., 2010) were used. All the models essentially showed a similar pattern of results, when the given results from the three models were compared for a particular experimental condition.

3.3.1. Amiodarone or palmitate induced lipid accumulation as a cell culture model for steatosis and further *in vivo* verification

In amiodarone or palmitate pre-treated cells, a small decrease in percentage of cell viability is likely due to the indirect effect of excess lipid accumulation during pre-incubation or a direct effect of amiodarone. As the relative number of damaged cells (compared to viable cells) was very low (around 2% only), it is unlikely that the given cell culture model could affect the calcium imaging experiments. Since it has been suggested by others that amiodarone may block ion channels, may perturb cytosolic Ca^{2+} homeostasis (Lubic et al., 1994), and excess palmitate in the cells may cause growth arrest (Listenberger et al., 2001), generate ROS (Nakamura et al., 2009), can be lipotoxic to cells of hepatic lineage *in vitro* by a JNK-dependent mechanism (Mei et al., 2011), the results obtained from these two *in vitro* models

were verified by using *in vivo* steatotic fresh primary hepatocytes isolated from obese Zucker rats, and similar results were obtained. As the three different models showed a similar pattern of results, it may indicate that the results obtained from our studies are independent of the models used.

3.3.2. Evidence that the lipid accumulation in the cells reduces ER Ca^{2+} and inhibits SOCE

The results of this study have demonstrated that lipid-loaded liver cells exhibit substantial decreases in SOCE and ER Ca^{2+} release. The observation that in the absence of extracellular Ca^{2+}, DBHQ-induced or ionomycin-releasable ER Ca^{2+} release is decreased indicates that lipid accumulation is associated with a decrease in the amount of ER Ca^{2+}. Future experiments are needed to directly measure ER Ca^{2+} using an ER targeted fluorescent dye.

As stated before, there is much evidence to suggest that the action of store-operated Ca^{2+} channels is crucial to replenish the ER Ca^{2+} stores (Gaspers and Thomas, 2005; Parekh and Putney, 2005). So, it can be speculated that in steatotic hepatocytes, the reduced SOCE and altered SERCA2b activity (Park et al., 2010) may be linked to the decreased amount of ER luminal Ca^{2+} in steatotic liver cells. Another possibility is that in the excess intracellular lipid-loaded condition, the ER membrane, having a high cholesterol environment, can influence the impaired conformational state of SERCA thereby decreasing Ca^{2+} transport into the ER lumen (Lee, 2002; Vangheluwe et al., 2005).

3.3.3. The possible mechanisms for inhibition of SOCE in lipid-loaded liver cells

The mechanisms by which lipid accumulation inhibits store-operated Ca^{2+} entry in liver cells likely involves the decrease in the expression of STIM1 and/or Orai1, as well as decreased movement of STIM1 to the plasma membrane. While it has recently been reported that some fatty acids may inhibit the coupling between STIM1 and Orai1, thereby inhibiting SOCE in mast cells (Holowka et al., 2014), this mechanism may also be present in liver cells. Additionally, as in other cell types (Parekh and Penner, 1995), protein kinase C (PKC) mediated phosphorylation of Orai1 and/or STIM1, and inhibition of Ca^{2+} entry through Orai1 can be some likely mechanisms for the inhibition of SOCE in lipid-loaded liver cells.

Lipid accumulation in liver cells is linked to the activation of several isoforms of protein kinase C (Huang et al., 2009). One recent study shows that PKC-β mediated phosphorylated Orai1 can inhibit the activity of Orai1 thereby inhibiting SOC channels in HEK293 cells (Kawasaki et al., 2010). Whether protein kinase C enzymes play a role in the mechanism of lipid induced inhibited Ca^{2+} entry in liver cells and primary hepatocytes, was investigated further as described in the next chapter.

CHAPTER IV: ROLE OF PROTEIN KINASE C IN LIPID-INDUCED INHIBITION OF STORE-OPERTAED Ca^{2+} ENTRY

4.1 Introduction

In the previous chapter (chapter 3), it was shown that lipid accumulation in liver cells causes a substantial reduction in store-operated Ca^{2+} entry (SOCE). As discussed at the end of the last chapter, the likely mechanisms underlying inhibition of SOCE in steatotic liver cells may include inhibited SERCA2b activity (Park et al., 2010), altered release of Ca^{2+} from ER store and impaired activation or movement of STIM1. Additionally, protein kinase C (PKC) mediated phosphorylation (and inhibition) of Orai1 may play a role in the mechanism of inhibited SOCE (Kawasaki et al., 2010) in steatotic liver cells.

There is some clear evidence to suggest that intracellular lipid accumulation in liver cells is linked with the activation of PKCε and other isoforms of protein kinase C (Huang et al., 2009; Jornayvaz and Shulman, 2012). Some results also have indicated that protein kinase C can inhibit store-operated Ca^{2+} entry in some other cell types via pre-mediated phosphorylation of SOC components (Kawasaki et al., 2010; Parekh and Penner, 1995; Yazaki et al., 2014). However, it is not clearly established whether protein kinase C is involved in the inhibition of SOCE in hepatocytes. The evidence for PKC involvement in SOCE inhibition has been discussed in details in Introduction chapter (subsection: *1.5.2.3.*)

Considering the evidence mentioned above, the specific aim of the experiments described in this chapter is to test whether PKC contributes to SOCE inhibition in lipid-loaded rat liver cells. If PKCs are involved in SOCE inhibition, an additional aim was to investigate the extent of the degree of inhibition (e.g., partial inhibition or full inhibition) of store-operated Ca^{2+} entry.

To evaluate the role of PKC in the mechanism of inhibited SOCE in steatotic hepatocytes, short-term use of PMA (for PKC activation) (Lu et al., 1998), long-term incubation of PMA for PKC down-regulation/degradation (Lu et al., 1998), and two different PKC inhibitors GF109203X (Toullec et al., 1991) and calphostin C (Kobayashi et al., 1989) were employed. PMA, in short-term incubation, activates PKC by binding to the C1 domain, cysteine-rich zinc finger-like subdomain of PKC (Zhang et al., 1995). In HEK293 cells, Kawasaki and colleagues demonstrated that during the activation of PKCs, Orai1 polypeptide can be phosphorylated and subsequently can cause inhibition of SOCE (Kawasaki et al., 2010). In our experiment, the idea was to activate PKCs and to understand the association of activated PKC with store-operated Ca^{2+} entry into normal H4IIE cells.

4.2 Results

4.2.1. Short-term incubation (15 min) of normal (non lipid-loaded) H4IIE cells with PMA substantially decreases store-operated Ca^{2+} entry

In order to activate various PKC isoforms, normal H4IIE cells were treated with phorbol 12-myristate 13-acetate (PMA) for 15 min (Lu et al., 1998). The incubation of H4IIE cells with PMA (4 µM) for 15 min, caused a significant inhibition of Ca^{2+} entry (Fig. 4.1. A, C) suggesting that the activation of PKC inhibits store-operated Ca^{2+} entry in control (non lipid-loaded) cells. This large inhibition of Ca^{2+} entry is comparable to that observed in lipid-loaded cells in Figure 3.5A.

In addition to the inhibition of SOCE, short-term incubation of normal H4IIE cells with PMA (4 µM) caused a slight decrease in the amount of ER Ca^{2+} (Fig. 4.1. A, B). In our experiments, the amount of Ca^{2+} in the ER store in liver cells was not measured directly with the ER dye. This observed alteration or reduction in ER Ca^{2+} has been inferred from the ER Ca^{2+} release or uptake experiments.

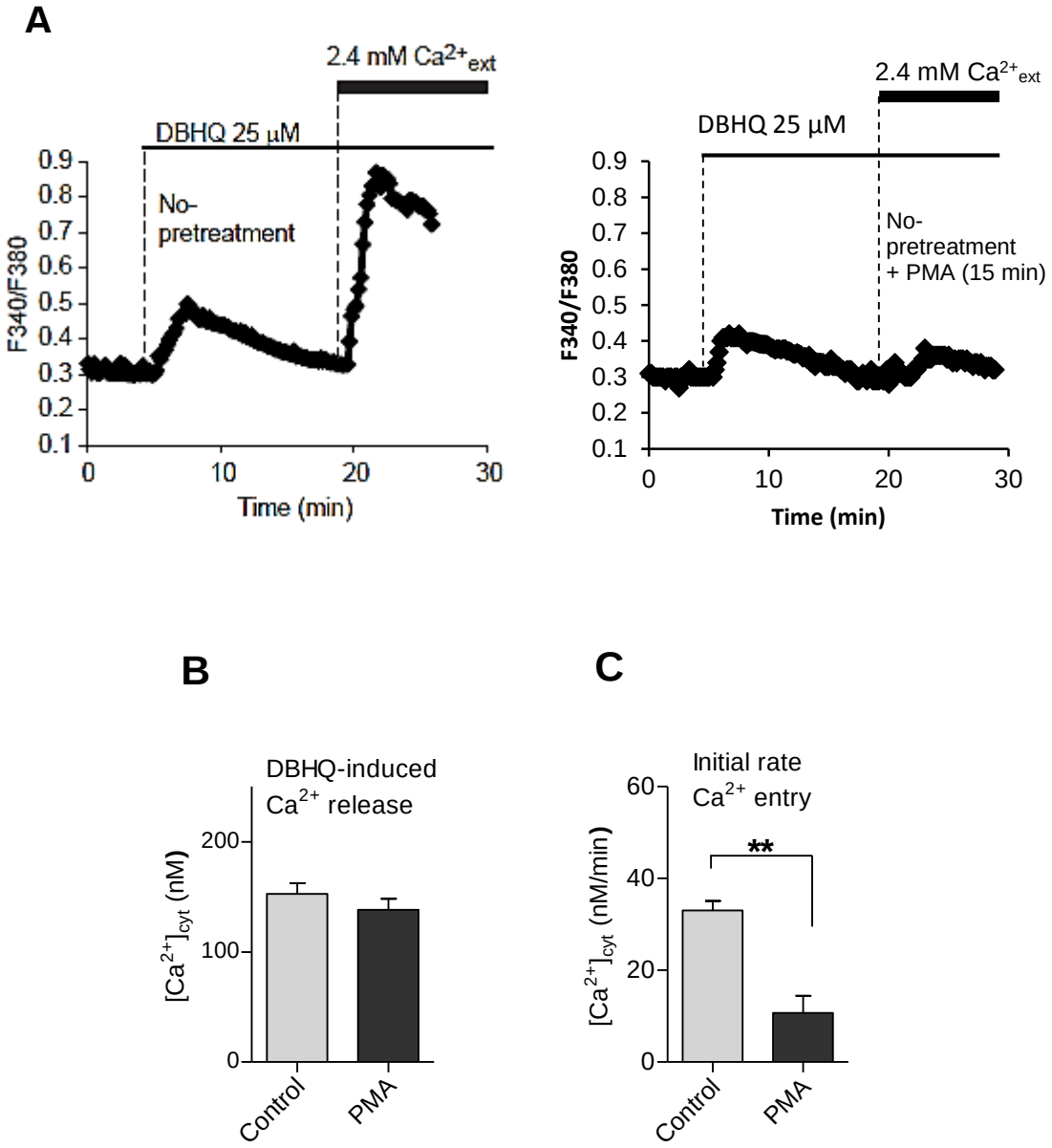

Fig. 4.1. Effect of pre-incubation of H4IIE cells for 15 min with PMA (4 µM) on DBHQ-initiated Ca^{2+} entry. (A) Representative traces showing the effects of the addition of DBHQ in the absence of added Ca^{2+}_{ext} and subsequent addition of 2.4 mM Ca^{2+}_{ext} on $[Ca^{2+}]_{cyt}$. Each data point is the mean of the values of $[Ca^{2+}]_{cyt}$ obtained for 10-20 cells. (**B, C**) Amounts of Ca^{2+} released (peak height) by DBHQ and initial rates of Ca^{2+} entry following Ca^{2+}_{ext} addition. Means ± SEM (n = 3). Degrees of significance: ** P<0.01.

4.2.2. Long-term (24 h) incubation of cells with PMA reverses the lipid-induced impaired Ca^{2+} entry

To reduce the concentration of PKC isoforms by activation and subsequent proteasomal degradation, cells were pre-incubated with PMA (4 μM) for 24h (Lu et al., 1998). Lipid-loaded cells pre-treated with PMA exhibited much greater rates of Ca^{2+} entry than lipid-loaded cells pre-treated with vehicle, while pre-treatment of control cells with PMA caused very little change in Ca^{2+} entry (Fig. 4.2 and Fig. 4.3).

The rate of Ca^{2+} entry in lipid-loaded cells treated for 24h with PMA was similar to the rates of Ca^{2+} entry in untreated control cells and in control cells pre-treated for 24h with PMA (Fig. 4.2 *cf* Fig. 4.3).

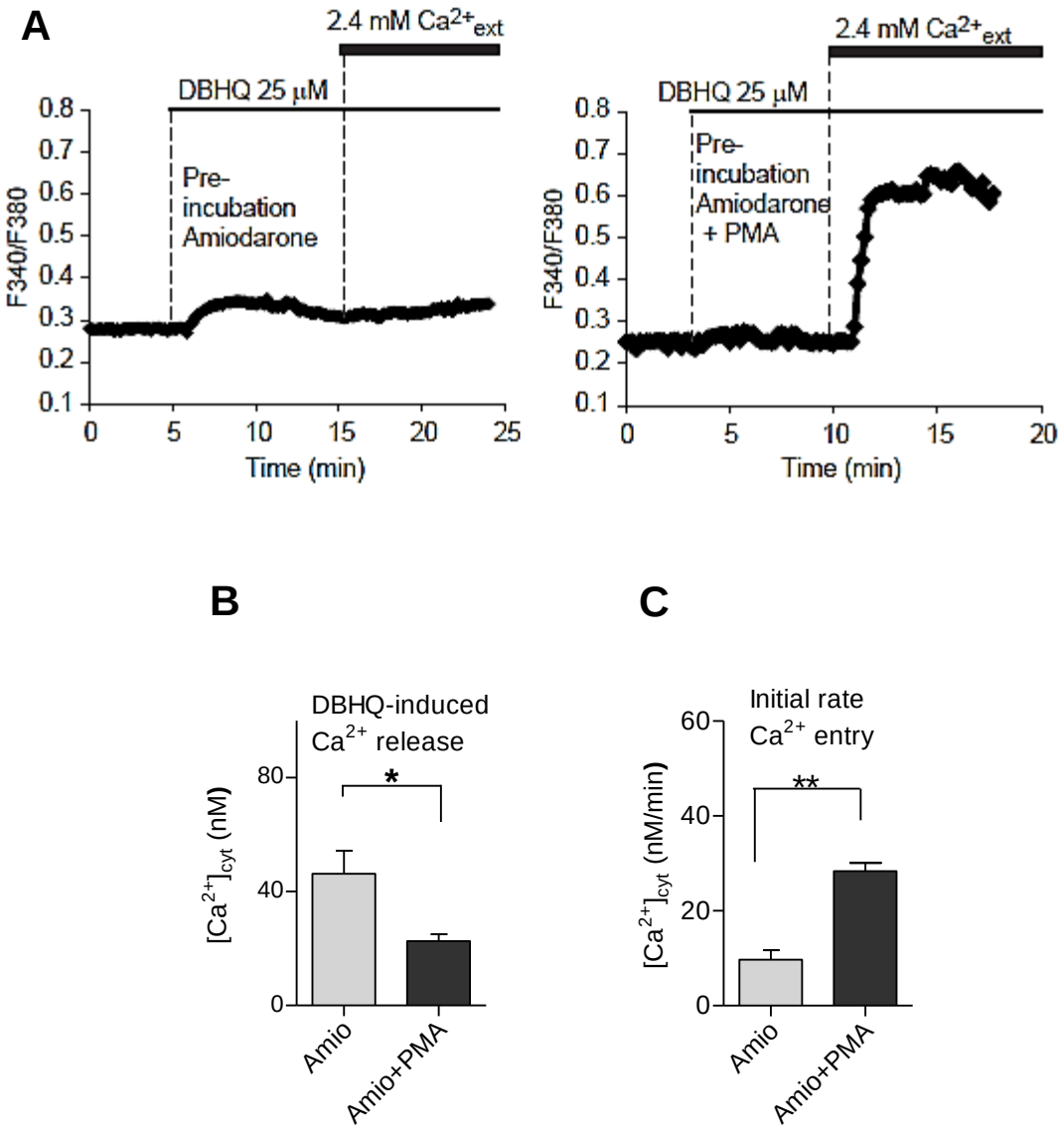

Fig. 4.2. Effect of pre-incubation of H4IIE cells for 24h with PMA (4 µM) (added with amiodarone) on lipid-loaded cells, and effect of PMA (4 µM) on DBHQ-initiated Ca^{2+} entry. (**A**) Representative traces showing the effects of the addition of DBHQ in the absence of added Ca^{2+}_{ext} and subsequent addition of 2.4 mM Ca^{2+}_{ext} on $[Ca^{2+}]_{cyt}$. Each data point is the mean of the values of $[Ca^{2+}]_{cyt}$ obtained for 10-20 cells. (**B, C**) Amounts of Ca^{2+} released (peak height) by DBHQ and initial rates of Ca^{2+} entry following Ca^{2+}_{ext} addition. Means ± SEM (n= 3). Degrees of significance: * P<0.05, and ** P<0.01.

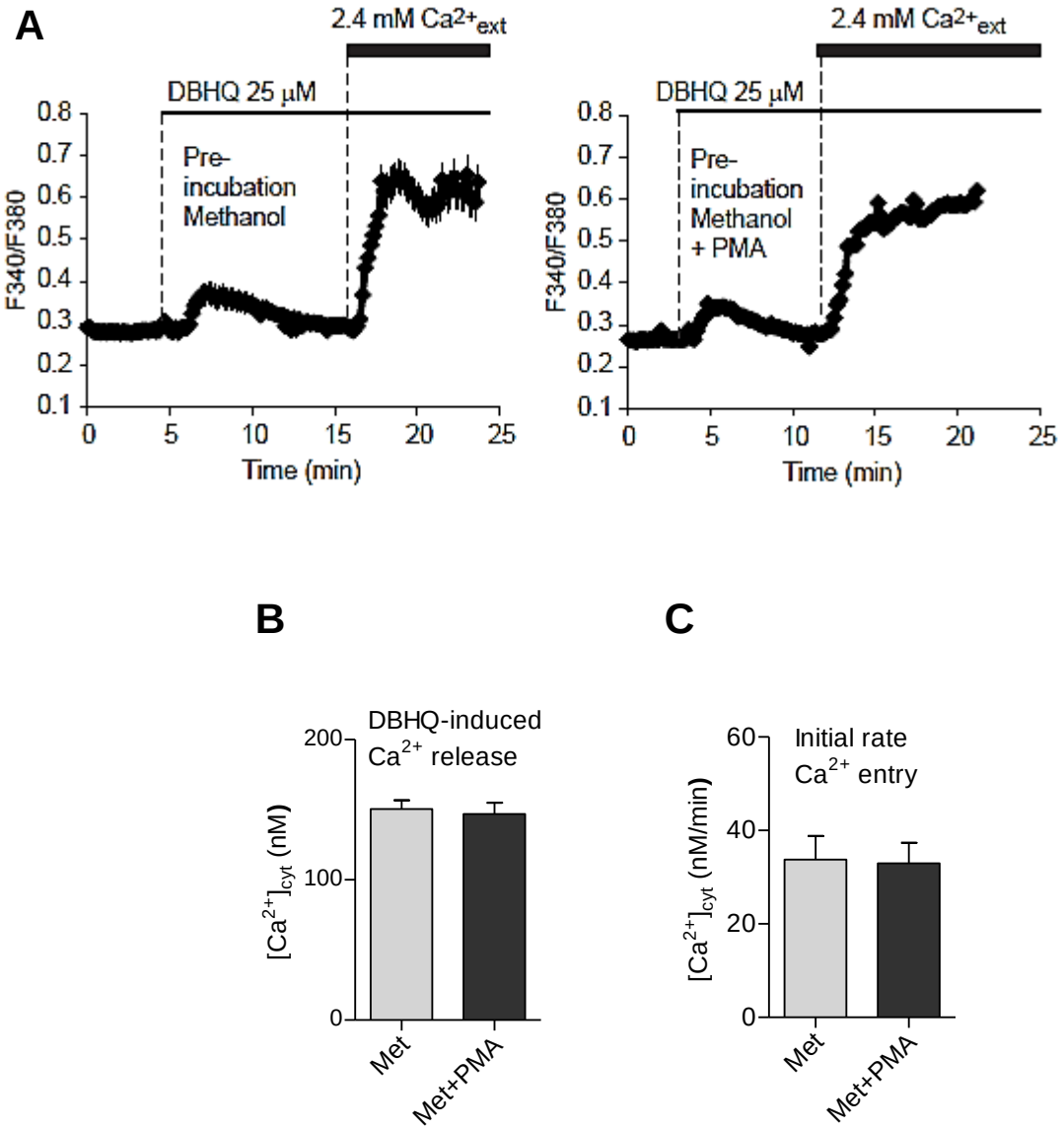

Fig. 4.3. Effect of pre-incubation of H4IIE cells for 24h with PMA (4 µM) (added with vehicle methanol) on control cells, and effect of PMA (4 µM) on DBHQ-initiated Ca^{2+} entry. (**A**) Representative traces showing the effects of the addition of DBHQ in the absence of added Ca^{2+}_{ext} and subsequent addition of 2.4 mM Ca^{2+}_{ext} on $[Ca^{2+}]_{cyt}$. Each data point is the mean of the values of $[Ca^{2+}]_{cyt}$ obtained for 10-20 cells. (**B, C**) Amounts of Ca^{2+} released (peak height) by DBHQ and initial rates of Ca^{2+} entry following Ca^{2+}_{ext} addition. Means ± SEM (n= 3). Degrees of significance: $P>0.05$.

4.2.3. The dose-response data for the protein kinase C inhibitor, GFX, to reverse impaired Ca^{2+} entry in steatotic liver cells

In the initial trials, in order to determine the effective concentration of GFX needed for inhibition of various isoforms of PKC in lipid-loaded liver cells, as well as determining the PKC isoforms specificity, different concentrations of GFX were tested. While 500 nM GFX did not reverse the lipid-induced SOCE inhibition markedly, 5 μM and 10 μM of GFX were able to reverse impaired SOCE by 20% and 35% respectively (Fig. 4.4.). Within the range of GFX concentrations tested here (500 nM to 10 μM), presumably, the inhibition of PKCs by GFX was not complete.

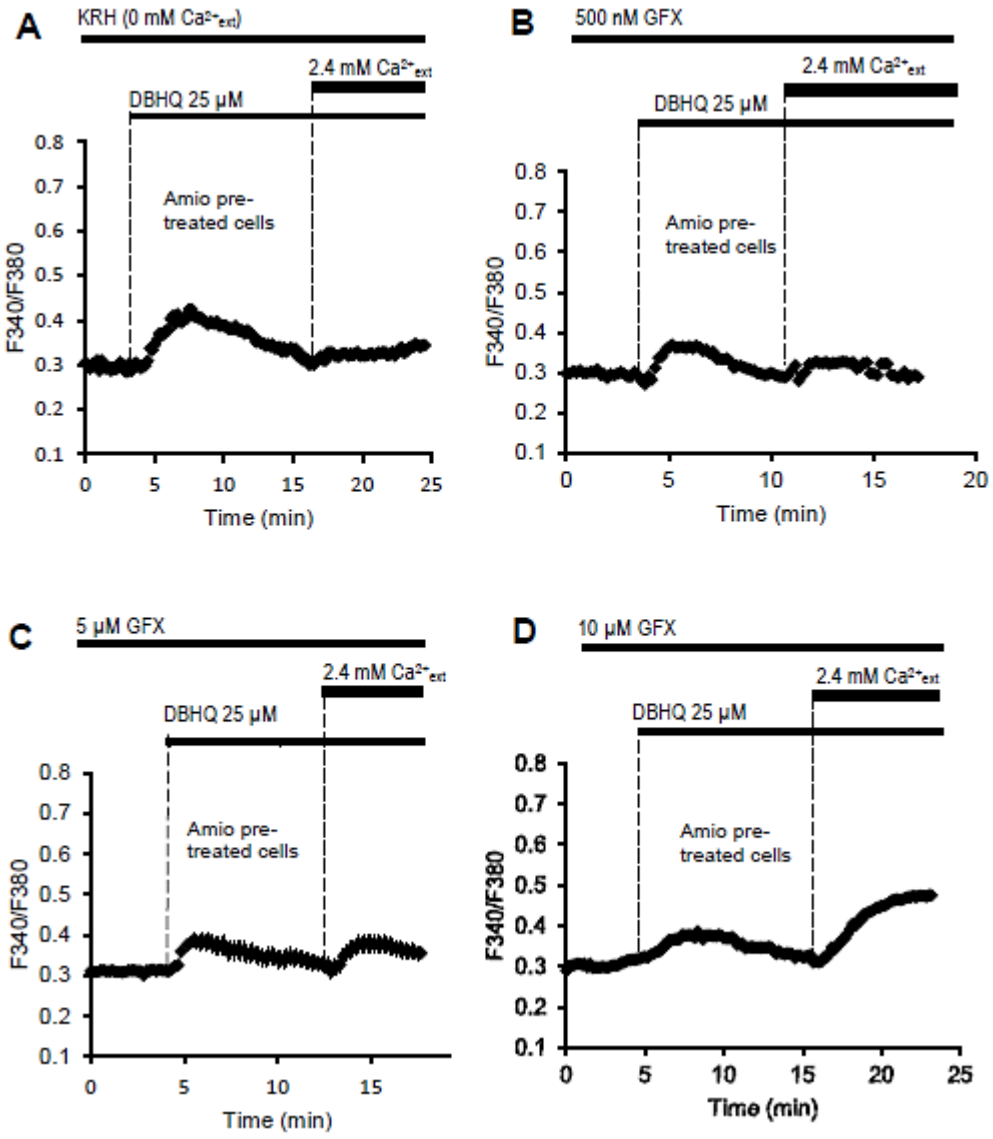

Fig. 4.4. The effects of GF109203X (GFX) at different concentrations to reverse the inhibition of SOCE in lipid-loaded H4IIE liver cells. (A) Amiodarone induced lipid-loaded H4IIE cells shows impaired SOCE. (**B, C, D**) Effect of GFX 500nM, 5 µM and 10 µM respectively, added at the beginning of the measurement of Ca^{2+} imaging to lipid-loaded H4IIE cells. Representative traces shown here. Each data point is the mean of the values of $[Ca^{2+}]_{cyt}$ obtained for 10-20 cells. Results are one of 3 experiments, each showed similar results.

4.2.4. The protein kinase C inhibitor, GFX (20 µM), reverses impaired Ca^{2+} entry in steatotic liver cells

To test whether PKC is involved in SOCE inhibition in lipid-loaded cells, Ca^{2+} entry was measured in H4IIE cells in the presence of the PKC inhibitor GF109203X (GFX) (Toullec et al., 1991) (20 µM) added immediately before $[Ca^{2+}]_{cyt}$ measurement. We employed DBHQ-induced 'Ca^{2+} add-back protocol' and GFX (20µM) was added at the beginning of the period over which $[Ca^{2+}]_{cyt}$ was measured (5 min before DBHQ). The results showed that GFX increased the rate of Ca^{2+} entry in lipid-loaded (Fig. 4.5.) but not in control (Fig. 4.6) cells, and reduced the height of the initial peak indicating ER Ca^{2+} release (Fig. 4.5. and 4.6.).

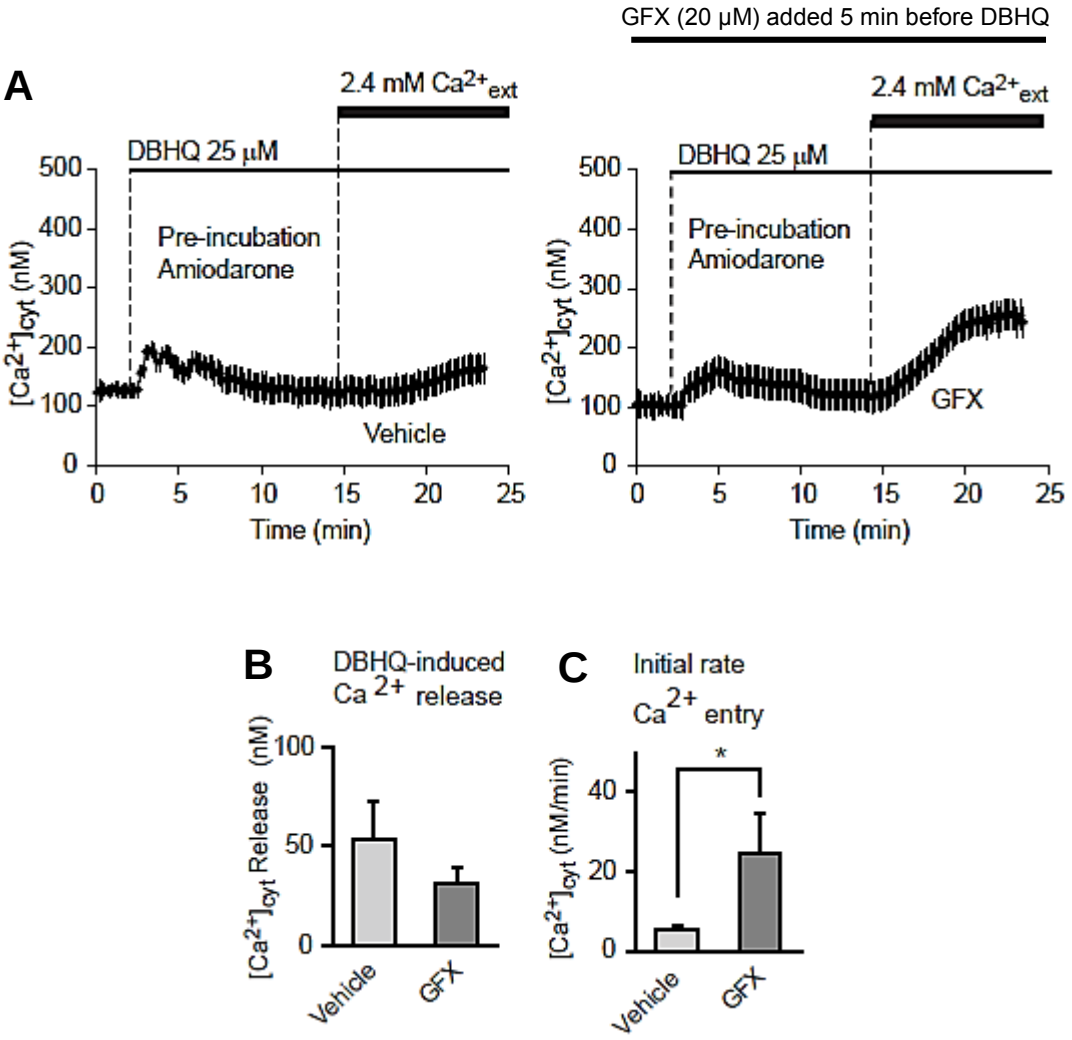

Fig. 4.5. The protein kinase C inhibitor GF109203X (GFX) reverses the inhibition of store-operated Ca^{2+} entry induced by lipid accumulation in H4IIE liver cells. (A, B, C) Effect of GFX (20 µM), added at the beginning of the measurement of Ca^{2+} imaging to lipid-loaded cells. Horizontal bars indicate the additions to the bath. The results shown in (A) are representative of those obtained in 3 to 4 similar experiments. In each experiment, the fluorescence of 10-15 cells was measured. **(B)** and **(C)** show the amount of Ca^{2+} released (peak height) by DBHQ and initial rates of Ca^{2+} entry following Ca^{2+}_{ext} addition. Means ± SEM (n=3-4). Degrees of significance: * $P<0.05$.

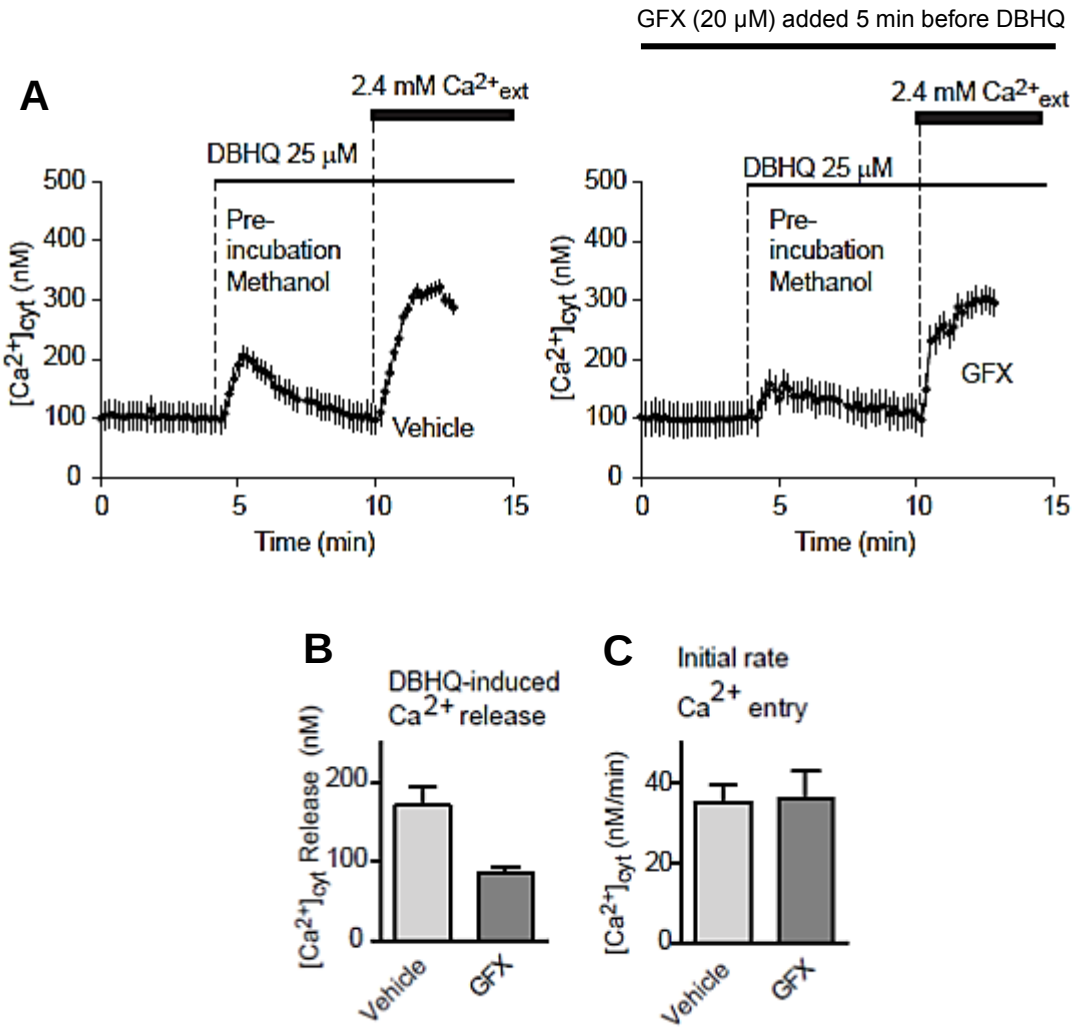

Fig. 4.6. GFX (20 µM) does not have any significant effect on SOCE in vehicle pre-treated H4IIE liver cells. (A, B, C) Effect of GFX (20 µM), added at the beginning of the measurement of Ca^{2+} imaging to vehicle pre-treated H4IIE cells. $[Ca^{2+}]_{cyt}$ was measured as a function of time in fura-2 loaded H4IIE cells, as described in Materials and Methods section (in sub-section 2.5.3). The results shown in **(A)** are representative traces from one of 3 independent experiments (done on separate days), employing 3 coverslips for each condition, which showed similar results. **(B)** and **(C)** graphs show the amount of Ca^{2+} released (peak height) by DBHQ and initial rates of Ca^{2+} entry following Ca^{2+}_{ext} addition. Means ± SEM (n=3-4). The values in **B** and **C** are the means of 3 to 4 experiments (P>0.05).

4.2.5. The effect of GFX (20 µM) when added 30 min before DBHQ or added after release of Ca^{2+} from the ER in lipid-loaded H4IIE liver cells

To further determine the response of GFX and whether GFX needs a longer time of pre-incubation, GFX was added 30 min before DBHQ in the experiments. Addition of GFX to lipid-loaded cells around 25 min before the beginning of $[Ca^{2+}]_{cyt}$ measurement also resulted in an increased rate of Ca^{2+} entry in lipid-loaded cells when compared to control cells (Fig. 4.7). Ca^{2+} entry in lipid-loaded cells pre-treated with GFX was 70% of that in control cells pre-treated with GFX (Fig. 4.7.A *cf* Fig. 4.6.A).

Addition of GFX to lipid-loaded cells after the addition of DBHQ also caused a rise in the rate of Ca^{2+} entry (Fig. 4.8). This was about 84% of the rate when GFX was added to lipid-loaded cells 30 min before DBHQ addition (Fig. 4.8 *cf* Fig. 4.7). These results indicate that the action of GFX in enhancing Ca^{2+} entry is independent of the effects of lipid on the amount of Ca^{2+} in intracellular stores.

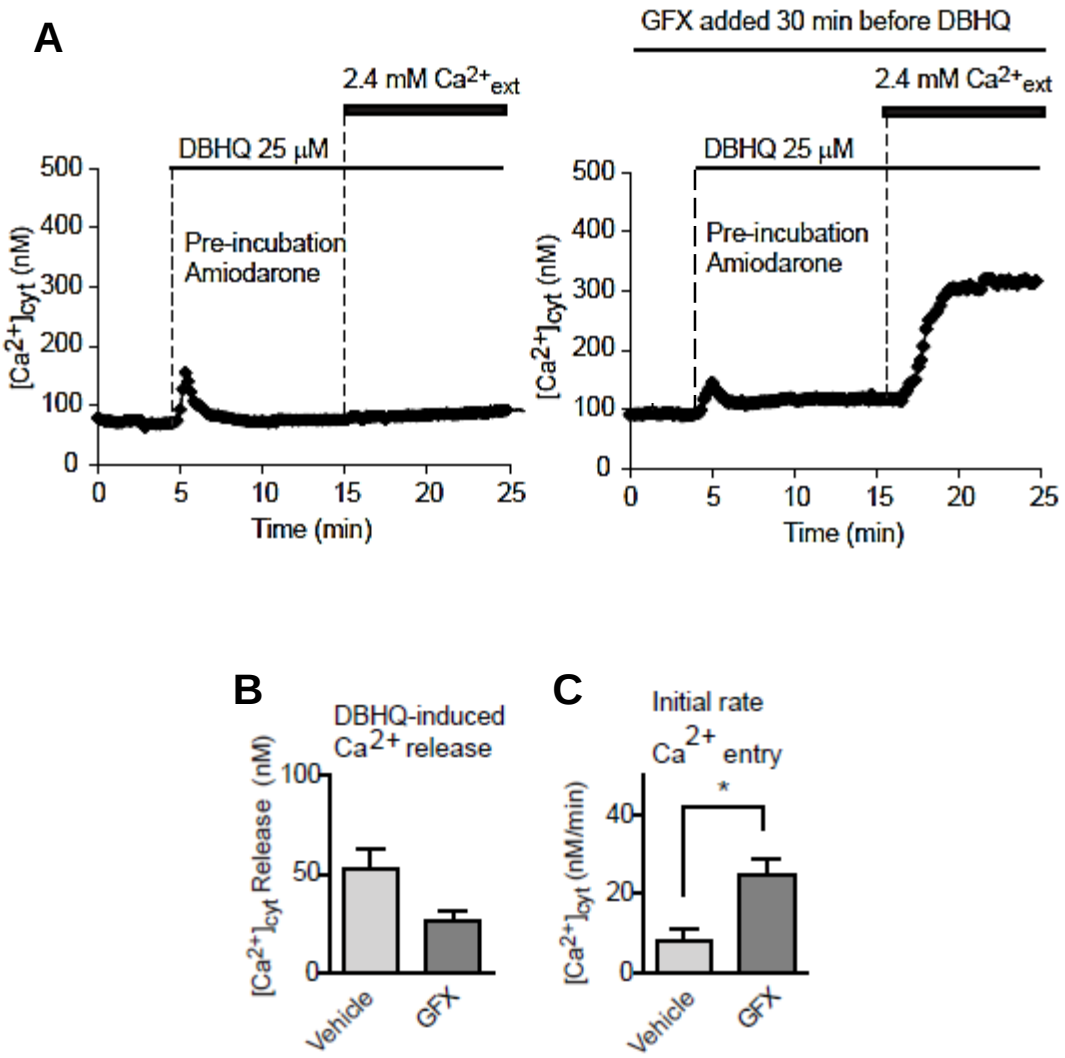

Fig. 4.7. GFX (20 µM), added 30 min before DBHQ, reverses the impaired SOCE induced by lipid accumulation in H4IIE liver cells. (A, B, C) Effect of GFX (20 µM), added at 30 min before DBHQ during the measurement of Ca^{2+} imaging to lipid-loaded H4IIE cells. (**A**) Representative traces are shown here. Each data point is the mean of the values of $[Ca^{2+}]_{cyt}$ obtained for 10-15 cells. (**B, C**) Column graphs show the amount of Ca^{2+} released (peak height) by DBHQ and initial rates of Ca^{2+} entry following Ca^{2+}_{ext} addition. Means ± SEM (n=3-4). Degrees of significance: * P<0.05.

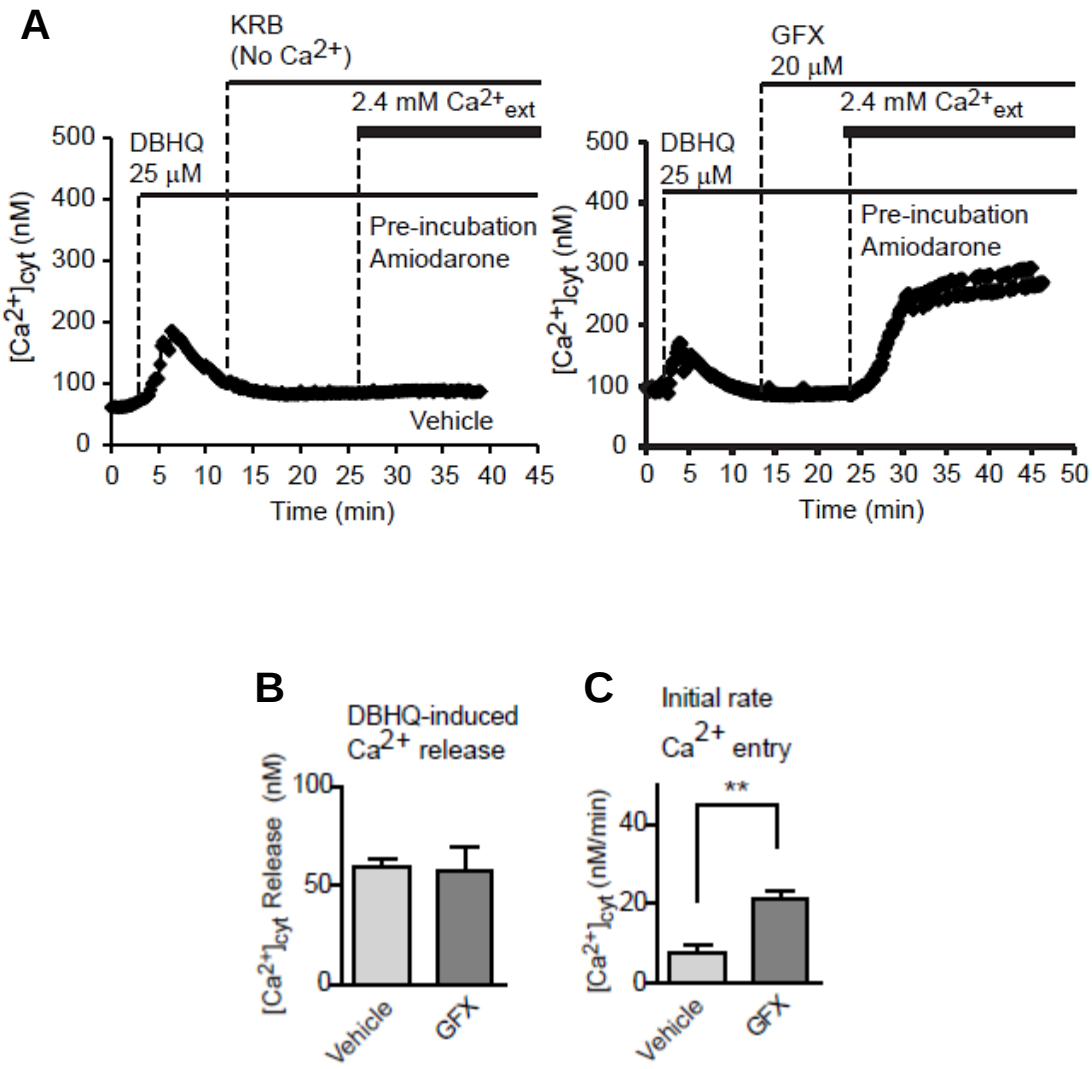

Fig. 4.8. GFX, added after release of Ca^{2+} from the ER in lipid-loaded H4IIE liver cells, reverses lipid-induced impaired SOCE. (**A, B, C**) Effect of GFX (20 µM), added after release of Ca^{2+} from the ER in lipid-loaded H4IIE liver cells. (**A**) Representative traces are shown here. Each data point is the mean of the values of $[Ca^{2+}]_{cyt}$ obtained for 10-15 cells. (**B, C**) Graphs show the amount of Ca^{2+} released (peak height) by DBHQ and initial rates of Ca^{2+} entry following Ca^{2+}_{ext} addition. Means ± SEM (n=3-4). Degrees of significance: ** P<0.01.

4.2.6. GFX, over time, decreases the amount of Ca^{2+} in the intracellular stores

The results described above indicate that, in addition to reversing the lipid-induced inhibition of Ca^{2+} entry, GFX decreases (but not statistically significant) the height of the peak of the DBHQ-induced increase in $[Ca^{2+}]_{cyt}$. To further investigate the action of GFX on intracellular Ca^{2+} stores, the effect of GFX on ionomycin-releasable Ca^{2+} was investigated. Control (non lipid-loaded) H4IIE cells loaded with Fura-2 were incubated with vehicle or with GFX (20 μM) added 1 min before or 30 min before ionomycin (50 μM). $[Ca^{2+}]_{cyt}$ was measured as a function of time, and the peak height of the ionomycin-induced increase in $[Ca^{2+}]_{cyt}$ determined (Fig. 4.9.). These results indicate that GFX does, over time, decrease the amount of Ca^{2+} in intracellular stores.

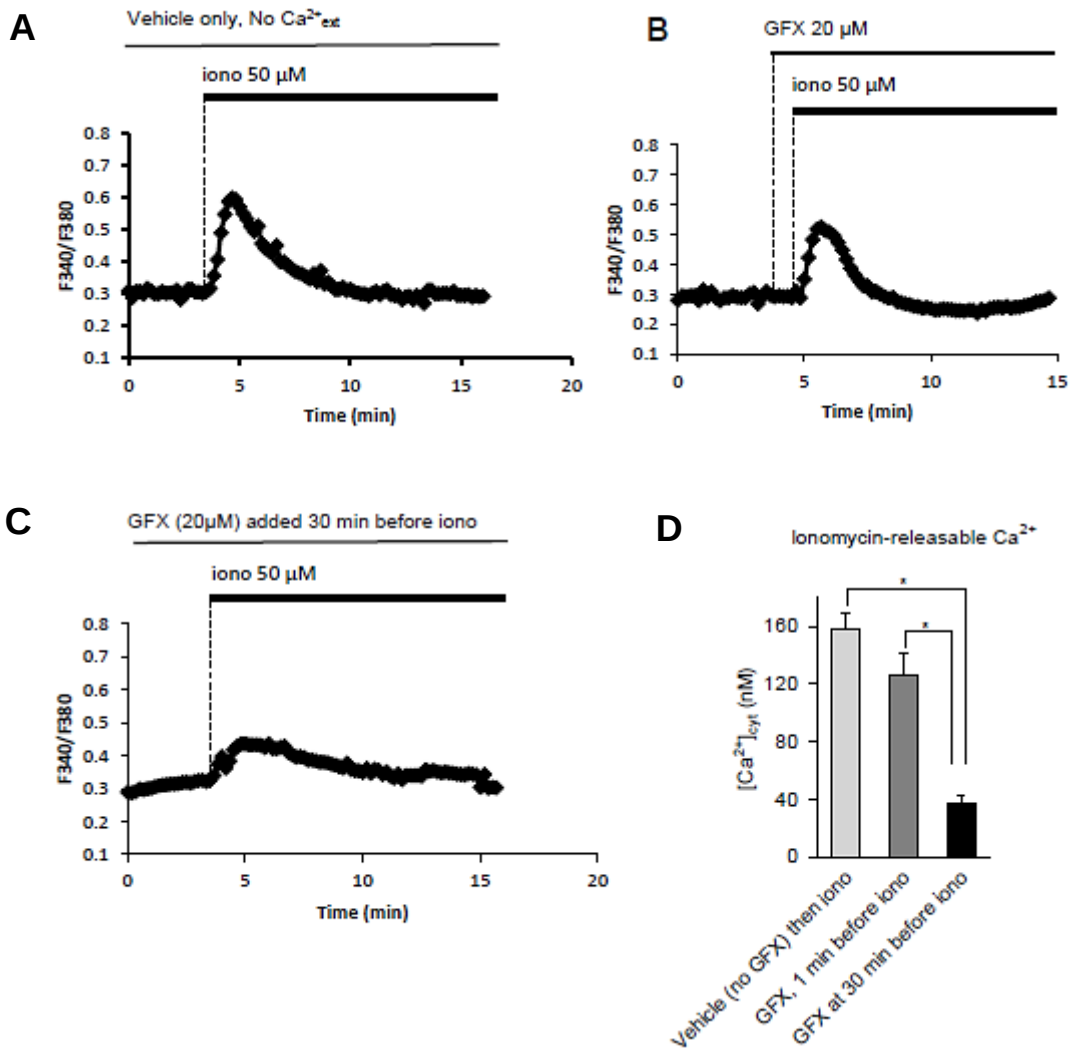

Fig. 4.9. GFX decreases the amount of Ca^{2+} in intracellular stores in H4IIE liver cells. The peak height values for vehicle, and GFX added at 1 and 30 min before ionomycin were 157 ± 12, 126 ± 15 and 37 ± 5 nM (means ± SEM n=3). In **A, B, C,** The results shown are representative traces of those obtained for 3 separate experiments (done on separate days) in which each gave similar results.

4.2.7. GFX (20 µM) increases the rate of Ca^{2+} entry in hepatocytes isolated from Obese Zucker rats

To test the effect of GFX in more physiological conditions, hepatocytes were isolated from obese Zucker rats, cultured and subsequently GFX was tested on primary cultured hepatocytes. Using the DBHQ add-back protocol, protein kinase C inhibitor GFX, added at the beginning of the experiments, substantially increased the rate of Ca^{2+} entry compared to control experiments in obese Zucker hepatocytes (Fig. 4.10 A). The results also demonstrated that DBHQ-induced ER Ca^{2+} release was slightly decreased in GFX-incubated obese hepatocytes when compared to vehicle control obese hepatocytes (Fig. 4.10. B, C.).

In the case of primary hepatocytes isolated from lean Zucker rats, interestingly, GFX did not increase the rate of Ca^{2+} entry in lean Zucker hepatocytes when compared to vehicle incubated lean Zucker hepatocytes (Fig. 4.11). In addition, as shown in the Fig 4.12, when intracellular lipid was loaded (amiodarone induced) in hepatocytes isolated from lean Zucker rats, GFX substantially increased the rate of Ca^{2+} entry in lipid-loaded lean hepatocytes.

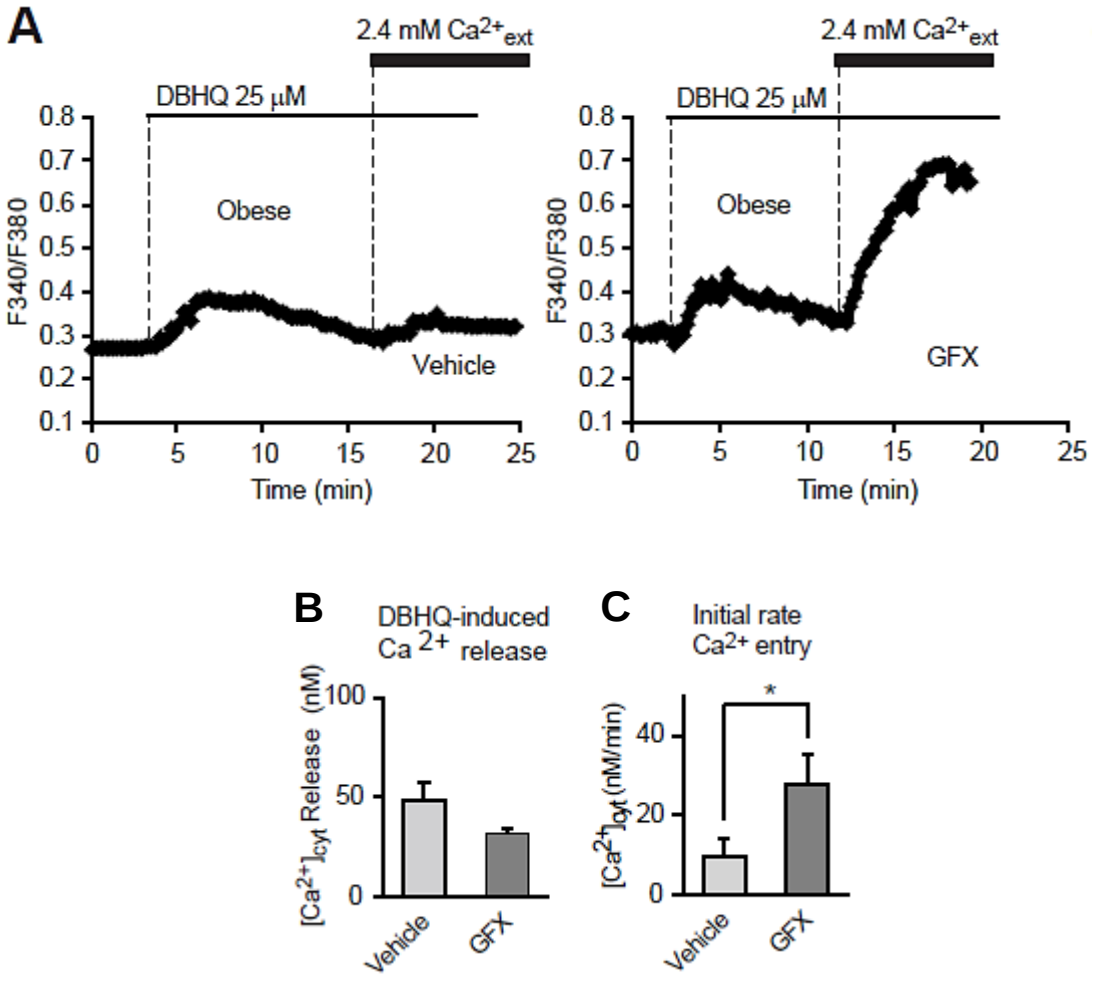

Fig. 4.10. GFX reverses the impaired store-operated Ca^{2+} entry in primary hepatocytes isolated from obese Zucker rats. (A, B, C) Effect of GFX (20 μM), added at the beginning of the measurement of Ca^{2+} imaging, on freshly isolated hepatocytes from Obese Zucker rats. (**A**) Representative traces shown here. Column graphs **B** and **C** show the amount of Ca^{2+} released (peak height) by DBHQ and initial rates of Ca^{2+} entry following Ca^{2+}_{ext} addition. Means ± SEM (n=3-4). Degrees of significance: * P<0.05.

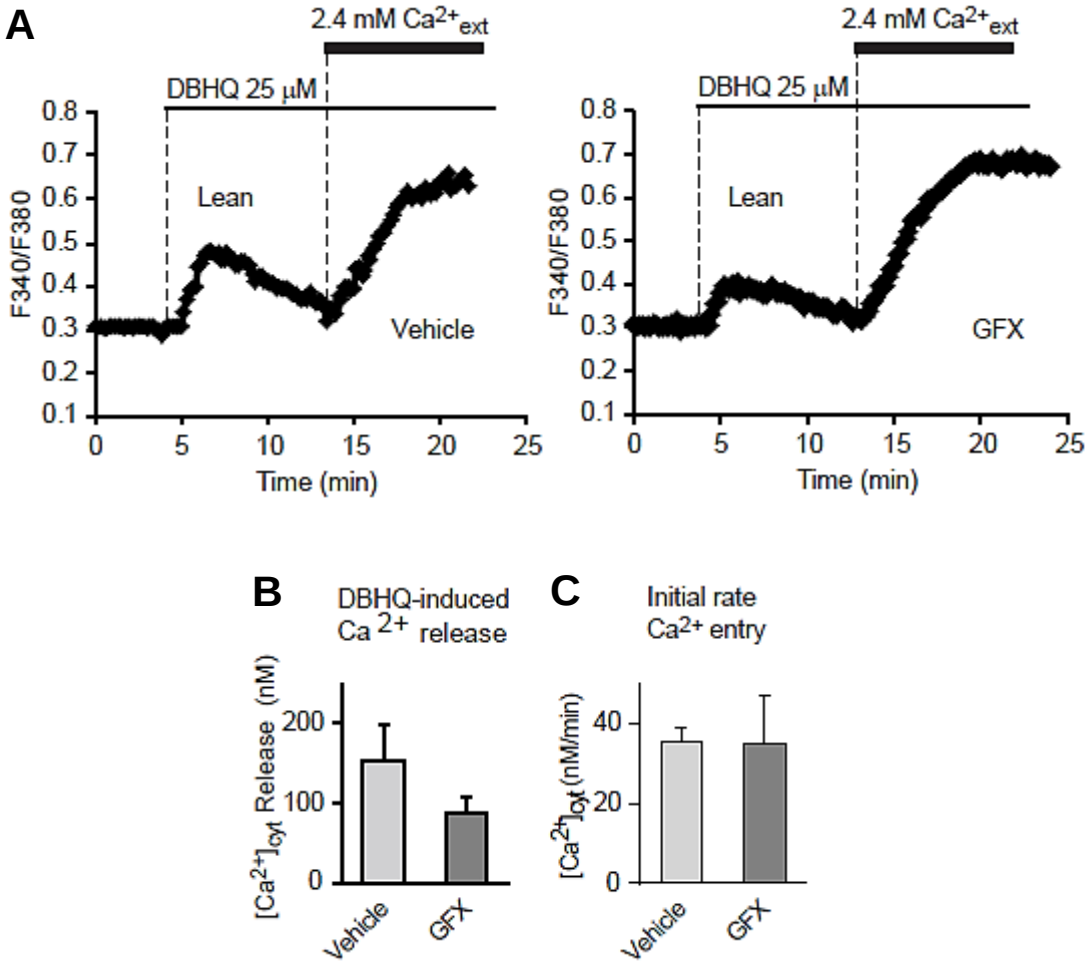

Fig. 4.11. GFX (20 µM), does not show any response in DBHQ-induced Ca^{2+} entry, but reduces (not statistically significant) ER Ca^{2+} release in primary hepatocytes isolated from lean Zucker rats. (A, B, C) Effect of GFX (20 µM), added at the beginning of the measurement of Ca^{2+} imaging to hepatocytes isolated from lean Zucker rats. (A) Representative traces shown here. In each experiment, the fluorescence of 10-15 cells was measured. **B** and **C** graphs show the amount of Ca^{2+} released (peak height) by DBHQ and initial rates of Ca^{2+} entry following Ca^{2+}_{ext} addition. Means ± SEM (n=3-4).

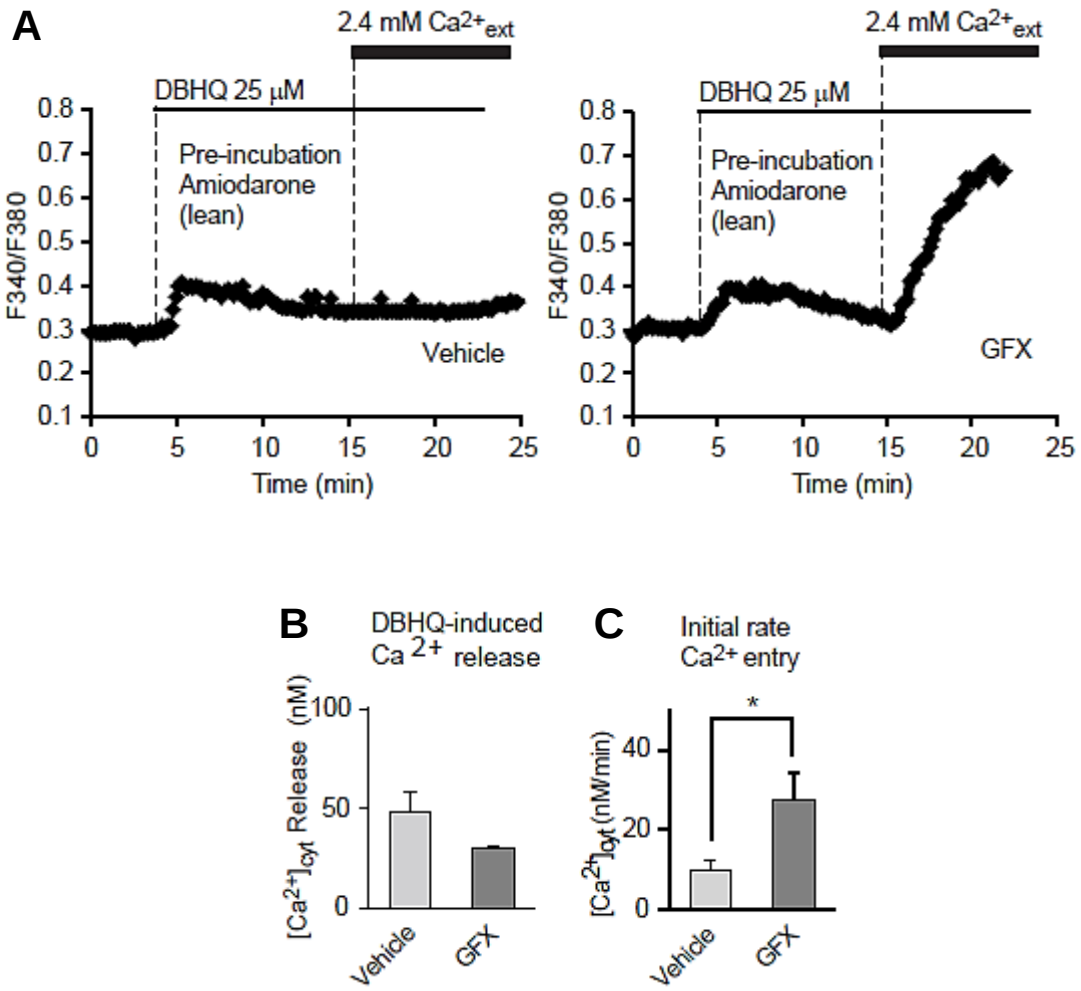

Fig. 4.12. GFX (20 μM) reverses impaired Ca^{2+} entry in amiodarone pre-treated (lipid-loaded) hepatocytes isolated from lean Zucker rats. (A, B, C) Effect of GFX (20 μM), added at the beginning of the measurement of Ca^{2+} imaging to lipid-loaded lean Zucker hepatocytes. Horizontal bars indicate the additions to the bath. The results shown in **(A)** are from a representative experiment, of those obtained in 3 to 4 similar experiments. In each experiment, the fluorescence of 10-15 cells was measured. **(B)** and **(C)** show the amount of Ca^{2+} released (peak height) by DBHQ and initial rates of Ca^{2+} entry following Ca^{2+}_{ext} addition. Means ± SEM (n=3-4). Degrees of significance: * P<0.05.

4.2.8. Calphostin C (20µM) reverses the impaired Ca^{2+} entry by 65% in lipid-loaded liver cells.

To confirm further whether activation of PKC is associated with lipid-induced inhibition of SOCE in lipid-loaded liver cells, another PKC inhibitor, calphostin C, was employed. It has been known that calphostin C inhibits PKC through the covalent modification of the lipid binding regulatory domain of PKC (Rao et al., 2013; Sciorra et al., 2001). Similar to the results obtained with GFX, Calphostin C (20 µM) also increased the rate of Ca^{2+} entry in amiodarone-induced lipid-loaded cells (Fig. 4.13).

This result provides additional evidence that activation of PKC contributes to the lipid-induced inhibition of SOCE in lipid-loaded liver cells.

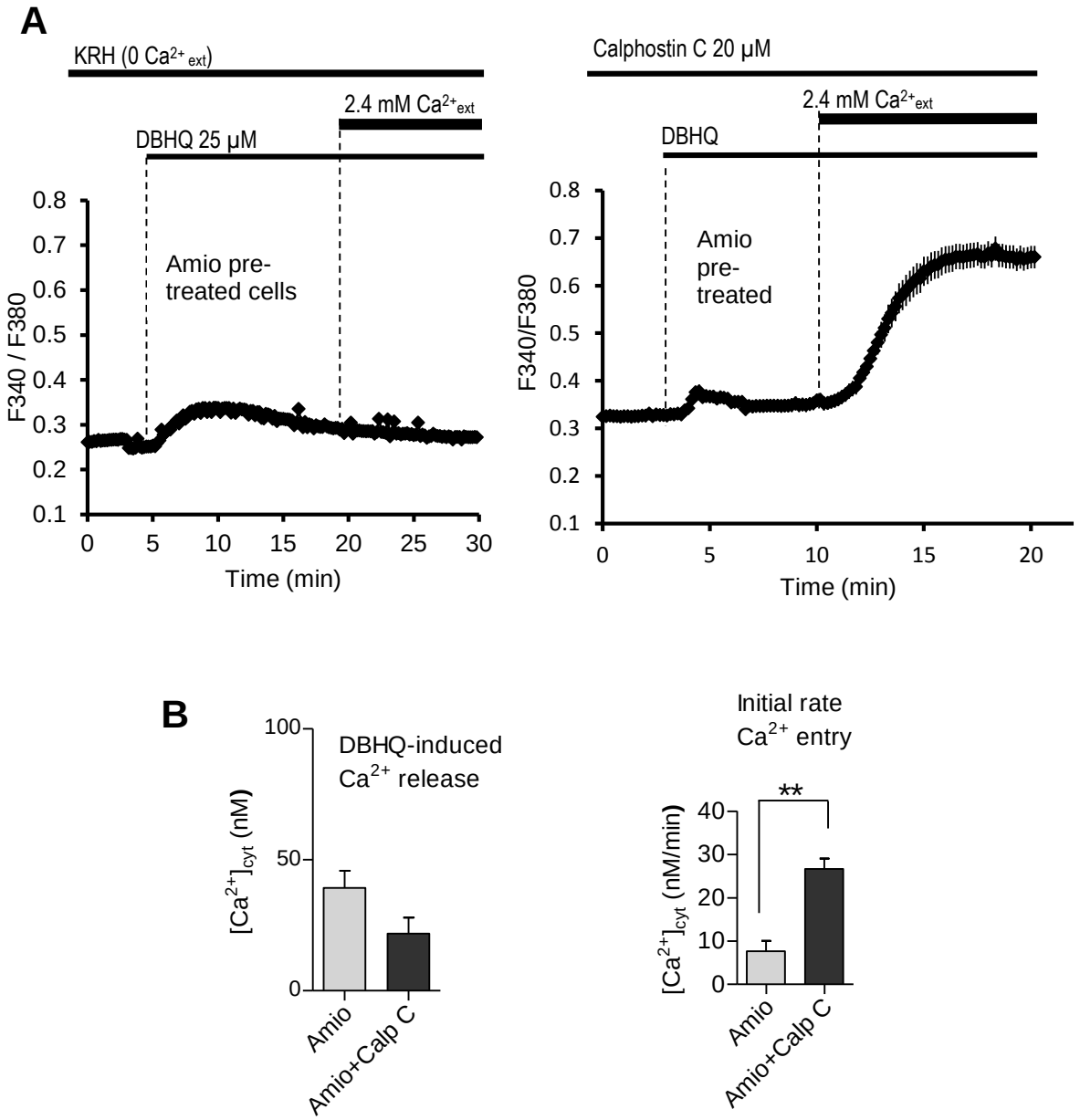

Fig. 4.13. The protein kinase C inhibitor Calphostin C reverses the inhibition of store-operated Ca^{2+} entry induced by lipid accumulation in H4IIE liver cells. Effect of calphostin C (20 µM), added at the beginning of the measurement of Ca^{2+} imaging to lipid-loaded H4IIE cells. Calphostin C (20 µM) increased the rate of Ca^{2+} entry in lipid-loaded cells from 8.0 ± 2.1 nM/min to 24.8 ± 2.9 nM/min (means ± SEM, n=3) in the absence and presence, respectively, of calphostin C. In **A**, the results shown are representative traces of those obtained in 3 separate experiments (done on separate days) in which each gave similar results. In each experiment, the fluorescence of 10-15 cells was measured. In **B**, degrees of significance: ** P<0.01.

4.3 Discussion

In this chapter, the results of the study have shown that short-term (15 min) incubation of control (non lipid-loaded) liver cells with phorbol 12-myristate 13-acetate (PMA) inhibits store-operated Ca^{2+} entry whereas pre-incubation (24h) of lipid-loaded liver cells with PMA reverses the lipid-initiated inhibition of store-operated Ca^{2+} entry. The protein kinase C inhibitors GF109203X (GFX), and calphostin C, independently, can reverse impaired Ca^{2+} entry in lipid-loaded or steatotic liver cells.

4.3.1. Evidence that PKC is involved in the lipid-initiated inhibition of SOCE

Evidence is provided by the results of these present experiments employing GFX and calphostin C, inhibitors of PKC, and PMA, an activator of PKC that PKC mediates the lipid-initiated inhibition of store-operated Ca^{2+} entry. Results from the work of others suggest that lipid accumulation in liver cell lines or hepatocytes is associated with the activation of PKCβ, PKCδ, and PKCε (Samuel et al., 2004; Samuel et al., 2007 (Kawasaki et al., 2010). Using inhibitors of PKC, *in vitro* kinase assays, and knockdown experiments in a HEK293 cell model, Kawasaki et al (2010) demonstrated that PKCβ can phosphorylate Orai1 leading to inhibition of SOCE. The activation of PKC inhibits SOCE (Kawasaki et al., 2010; Lee et al., 1997), and this was further confirmed for hepatocyte SOCE in the present results using phorbol 12-myristate 13-acetate (PMA). Therefore, the mechanism by which lipid accumulation inhibits SOCE may involve the activation of one or more isoforms of PKC by diacylglycerol and/or lipid droplets, phosphorylation of Orai1, and subsequent inhibition of Ca^{2+} entry through Orai1 pores.

The results obtained from the experiments where PKC was down-regulated by 24h pre-incubation with PMA, or inhibited by 30 min treatment with GFX, indicate that activation of PKC accounts for most of the observed lipid-induced inhibition of SOCE.

4.3.2. Action of GFX on the Ca^{2+} stores

In the present study it was observed that cells pre-treated (pre-treatment for 5 or 30 min) with protein kinase C inhibitor GFX showed reduced ER Ca^{2+} storage compared to non-treated control cells. A similar type of effect of GFX on the ER Ca^{2+} storage has been reported by Sipma et al. (1996). In addition to this, the results from experiments using ionomycin indicate that GFX does, over time, decrease the amount of Ca^{2+} in intracellular stores. The mechanisms by which incubation with PKC inhibitor(s) are contributing to reduced ER Ca^{2+} storage/release in cells need to be investigated in future. However, the decreased ER Ca^{2+} content in lipid-loaded liver cells is not likely to play a main role in the mechanisms by which lipid accumulation decreases SOCE. The observations, where GFX added after DBHQ (to initiate ER Ca^{2+} release) caused almost the same degree of reversal of SOCE inhibition as is shown when GFX is added before DBHQ may indicate that the step(s) involved in the inhibition of SOCE in lipid-loaded liver cells will be the downstream events of ER Ca^{2+} release.

4.3.3. Evidence that Orai1 is the likely target of PKC action

In the present study, the observation that GFX, when added after DBHQ-induced ER Ca^{2+} release, could reverse the lipid-initiated SOCE inhibition indicates that Orai1, rather than STIM1, can be the site of action of PKC. It has been suggested that, in liver cells, store-operated Ca^{2+} entry can be activated at around 3 min after the

initiation of the ER Ca^{2+} release (Wilson et al., 2014). In the experiment described in right-hand panel of Fig 4.8, in amiodarone-pre-treated lipid-loaded cells, GFX was added at 10 min after DBHQ. At this time (after 10 mins) STIM1 would have moved completely to the plasma membrane to activate SOCE. At this time point, the plot indicates the action of GFX and PKC is on the phosphorylation of Orai1 protein. Recent studies also show that the activity of STIM1 is regulated by phosphorylation (Pozo-Guisado et al., 2013; Pozo-Guisado and Martin-Romero, 2013; Smyth et al., 2009). Thus PKC-mediated phosphorylation of STIM1 may also play a role in the observed SOCE inhibition in the experiments. While Bruton's tyrosine kinase (Btk) (Lopez et al., 2012), and some extracellular-signal-regulated kinases (Pozo-Guisado et al. 2010) have been implicated in the phosphorylation of STIM1 in various cell types, no PKC-mediated phosphorylation of STIM1 has been reported yet (Srikanth et al., 2013).

4.3.4. Concentration on GFX needed to reverse the lipid-induced inhibition of SOCE

GFX has been shown to inhibit PKC isoforms with IC_{50} ranging from about 0.01 to 6 uM (Toullec et al., 1991). The concentrations of GFX we have used are consistent with those employed in many recent studies (Manna et al., 2007)(Abramian et al., 2014). In our experiments, the PKC isoforms likely to be activated in steatotic liver cells are beta, delta and epsilon. The last two isoforms have much higher IC_{50} for GFX (Jacobson et al., 1995; Toullec et al., 1991), and higher concentrations of GFX, therefore, were needed to inhibit those isoforms completely.

4.3.5. Further considerations and experiments to confirm the role of PKC

In our experiments, in lipid-loaded cells, long-term incubation of PMA reverses SOCE, probably, through the activation of PKCs and followed by ubiquitination and

proteolytic degradation of those PKCs (Kawasaki et al., 2010). Presumably, at this condition, cells may not have enough PKC to phosphorylate Orai1 (and/or STIM1), thereby lead to increase Ca^{2+} influx into cells. Inhibition of PKC by GFX or calphostin C also may increase Ca^{2+} influx into cells in lipid-loaded cells, as SOCs components may not be phosphorylated and inhibited during/after the treatment of PKC inhibitors. As in our experimental condition, PMA-mediated PKC degradation was not measured, further experiments such as measurement of (long term) PMA-mediated PKC degradation should be done in future. Apart from the time-dependent effect of phorbol ester (PMA) on store-operated Ca^{2+} entry, there might be some other mechanism(s) involved by which phorbol ester may have effect on Ca^{2+} entry in liver cells. However, in the case of liver cells, the hypothesis yet needs to be explored. Pozo-Guisado et al., (2010) reported that, in HEK293 cells, STIM1 can be a target of extracellular-signal regulated kinases 1 and 2 (ERK1/2), and subsequently ERK1/2-phosphorylated sites on the STIM1 sequence were defined. Activating ERK1/2, PMA (short-term) can modulate store-operated Ca^{2+} entry. We cannot eliminate the possibility that PMA may have (differential) effects (short vs long) on the expression of SOCs components in the liver cells. Elucidation of the precise mechanism(s) by which PMA treatment mediates the SOCE will require further study (including the measurement of activation or down-regulation of PKC) in liver cells. Activation of PKC can be identified by monitoring intracellular distribution of PKC via [^{3}H]phorbol ester binding activity assay (Brick-Ghannam et al., 1991). Once activated, the movement of PKC from the cytosol to the plasma membrane can be monitored by immunofluorescence (Beuers et al., 1999). siRNA knockdown strategies for PKC isoforms (e.g., PKCβ, PKCδ, and PKCε) are required to identify the involvement of specific PKC isoform(s) in the SOCE inhibition in steatotic liver

cells. In addition, further studies are required to determine the degree of PKC induced-phosphorylation of Orail in the lipid-loaded liver cells.

The results obtained in this chapter showed that activation of PKC is associated with reduced SOCE in steatotic liver cells. This impaired SOCE, in turn, may have different pathophysiological consequences for the cells. So, it is of great importance to search for compounds that might reverse impaired SOCE in steatotic liver cells. The next chapter presents investigations to determine whether this lipid-initiated SOCE impairment can be reversed by exendin-4, a member of the GLP-1 mimetic family of anti-diabetic drugs in frequent use for the treatment of insulin resistance.

CHAPTER V: EXENDIN-4, A GLUCAGON-LIKE PEPTIDE-1 ANALOGUE, REVERSES IMPAIRED SOCE IN STEATOTIC LIVER CELLS

5.1 Introduction

In chapter 3, it was demonstrated that excess lipid accumulation in immobilised liver cells and primary hepatocytes causes a substantial decrease in store-operated Ca^{2+} entry. As Ca^{2+} is a universal intracellular messenger for animal cells and SOCE maintains the ER Ca^{2+} contents (Parekh and Penner, 1997) and sustained cytoplasmic Ca^{2+} oscillations in the cells (Gaspers and Thomas, 2005), the disturbances in the entry of Ca^{2+} through the plasma membrane will be a huge pathological burden to the cells. Another recent observation involving Ca^{2+} indicates that genetic variation in one of the Ca^{2+}-permeable channels (TRPM5), is associated with increased risk of type 2 diabetes (Ketterer et al., 2011), an observation that may emphasize the potential importance of Ca^{2+} channels in fatty liver-associated diseases and insulin resistance. In this context, it was of similar necessity to identify or develop pharmacological agents which can reverse or improve the impaired store-operated Ca^{2+} entry in steatotic liver cells.

As described in the Introduction, therapeutic agents currently employed to treat metabolic abnormalities, insulin resistance and type 2 diabetes, in various indirect ways, interact with intracellular Ca^{2+} signaling pathways. Insulin, the glucagon-like peptide-1 (GLP-1) analogues, the thiazolidinediones, and the biguanides are the main therapeutic agents currently employed in the treatment of insulin resistance and type

2 diabetic patients (Chen et al., 2011). Among the drugs listed above, GLP-1 analogue (e.g., exendin-4) is a drug of major clinical significance, and may modulate insulin secretion in β cells through a Ca^{2+}-dependent pathway (Campbell and Drucker, 2013), as well as reversing steatosis in livers of obese mice (Ding et al., 2006; Meloni et al., 2013) and in an *in vitro* lipid-loaded Hep-G2 cell culture model (Gupta et al., 2010). Therefore, we aimed to test exendin-4 to see if it would reverse the inhibition of SOCE in steatotic liver cells.

Considering the evidence above, the specific aims of the experiments described in this chapter were: i) to test whether exendin-4 can act as an ER Ca^{2+} depleting agent and activate store-operated Ca^{2+} entry in non lipid-loaded liver cells, ii) to investigate if exendin-4 can reverse the lipid induced inhibition of SOCE in steatotic hepatocytes. To investigate whether exendin-4 has a DBHQ-like ER Ca^{2+} depleting effect, normal non lipid-loaded H4IIE cells and hepatocytes isolated from lean Zucker rats were used. To explore the effects of exendin-4 on inhibited SOCE, lipid-loaded H4IIE cells and hepatocytes isolated from obese Zucker rats were used.

5.2 Results

5.2.1. The glucagon-like peptide-1 (GLP-1) analogue exendin-4 does not affect Ca^{2+}_{cyt} or SOCE in untreated H4IIE cells

At first, to determine whether exendin-4 has any effect on normal non-steatotic cells, or on SOCE or ER Ca^{2+} release in normal H4IIE cells, cells were loaded with fura-2, incubated in the absence of extracellular Ca^{2+} (Ca^{2+}_{ext}), exposed to exendin-4 to determine whether any release of Ca^{2+} occurs from the ER, then Ca^{2+}_{ext} was added to permit Ca^{2+} entry. In normal (non lipid-loaded) H4IIE cells, exendin-4 alone did not have any effect on $[Ca^{2+}]_{cyt}$ in the absence of DBHQ (Fig. 5.1). This result may suggest that exendin-4 alone may not have a DBHQ-like effect in normal H4IIE liver cells.

As is shown in Fig. 5.2, in vehicle control cells, exendin-4 did not show any effect on the increase in $[Ca]^{2+}_{cyt}$ upon addition of extracellular Ca^{2+} (5.2 A *cf* B), while DBHQ-induced ER Ca^{2+} release was considerably reduced in exendin-4 treated cells (5.2 B *cf* A).

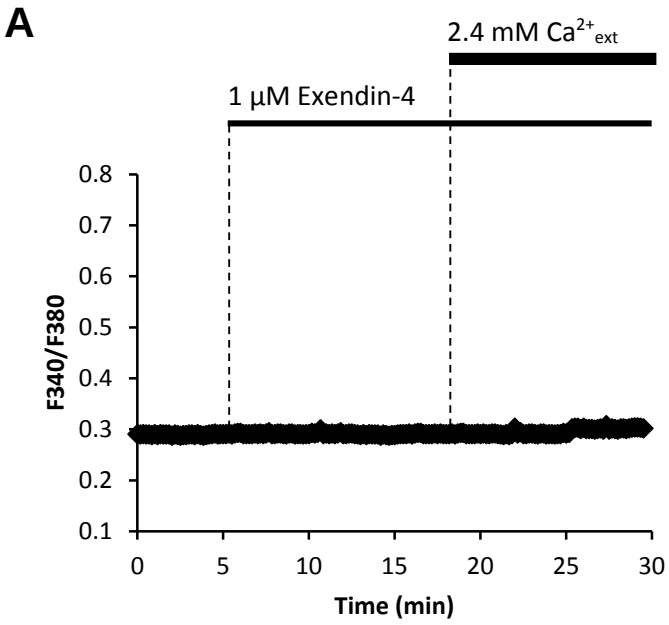

Fig. 5.1. Exendin-4 alone does not have any effect on $[Ca^{2+}]_{cty}$ in the absence of DBHQ. (A) H4IIE normal cells were incubated in the presence of vehicle KRH (without Ca^{2+}). After 5 min, Exendin-4 was added to cells initially in the absence of extracellular Ca^{2+}. Then extracellular 2.4 mM Ca^{2+} added back to the incubation chamber. The results shown are representative traces of those obtained for 3 separate experiments (done on separate days) in which each gave similar results. In each experiment, the fluorescence of 10-15 cells was measured.

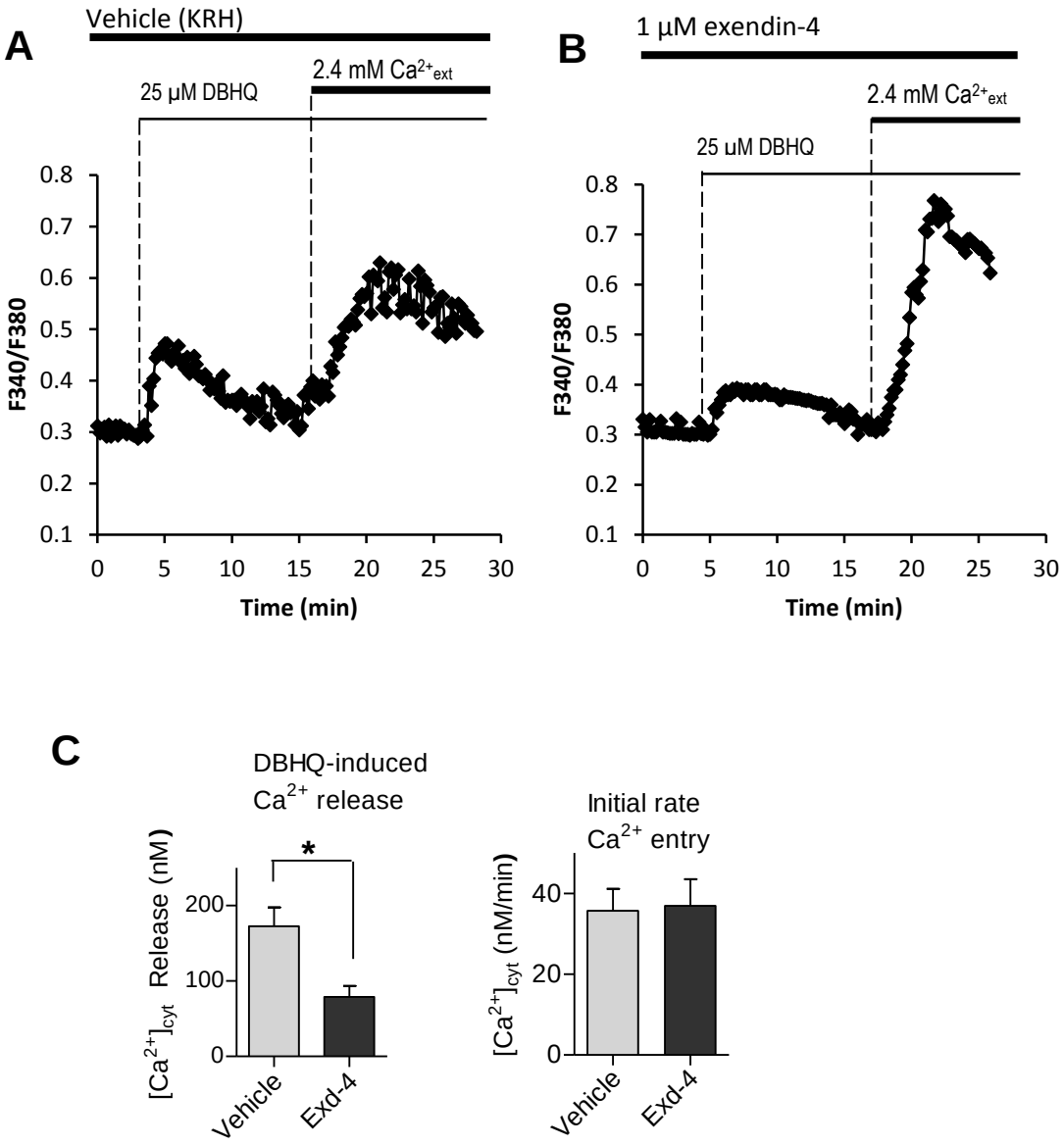

Fig. 5.2. Exendin-4 does not have any effect on SOCE in non-steatotic normal H4IIE cells. (A, B) H4IIE normal cells were incubated in the presence of vehicle (A) or exendin-4 (B). In each case DBHQ was added to cells initially in the absence of extracellular Ca^{2+}. The results shown are representative traces of those obtained for 3 to 4 separate experiments (done on separate days) in which each gave similar results. In each experiment, the fluorescence of 10-15 cells was measured. (**C**) DBHQ induced ER Ca^{2+} release (left panel) and the initial rate of Ca^{2+} entry upon addition of extracellular Ca^{2+} (right panel). The values in **C** are the means ± SEM of 3 or 4 experiments of the type shown in A and B. * $P<0.05$.

5.2.2. Exendin-4 reverses inhibited SOCE in lipid-loaded H4IIE liver cells

To determine whether exendin-4 increases Ca^{2+} entry in lipid-loaded liver cells, cells were loaded with fura-2, incubated in the absence of extracellular Ca^{2+} (Ca^{2+}_{ext}), exposed to the SERCA inhibitor DBHQ to release ER Ca^{2+}, then Ca^{2+}_{ext} was added to permit Ca^{2+} entry.

The results of this study showed that amiodarone induced lipid-loaded H4IIE cells exhibit markedly depressed DBHQ initiated Ca^{2+} entry, and the GLP-1 analogue exendin-4 increases Ca^{2+} entry initiated by DBHQ and decreases DBHQ-induced release of Ca^{2+} from intracellular stores in lipid-loaded cells (Fig. 5.3).

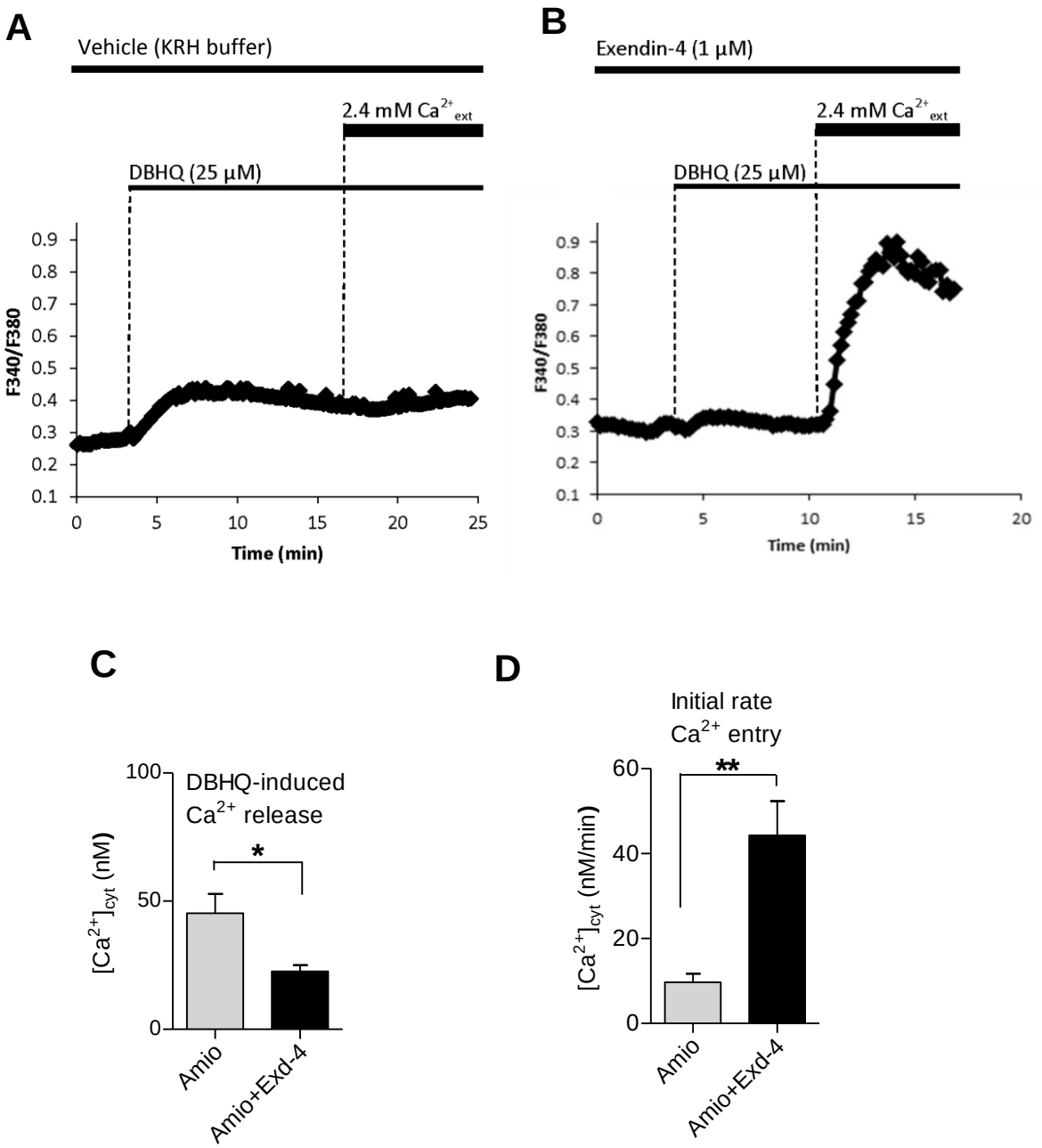

Fig. 5.3. Exendin-4 enhances DBHQ-induced Ca^{2+} entry in H4IIE rat liver cells loaded with lipid by pre-treatment with amiodarone. Lipid-loaded cells were incubated in the presence of vehicle (A) or exendin-4 (B). In each case DBHQ and Ca^{2+} were added to cells initially incubated in the absence of extracellular Ca^{2+}. The plots shown are each representative of those obtained in 5-6 similar experiments. In each experiment, the fluorescence of 10-15 cells was measured. (**C**) DBHQ-induced ER Ca^{2+} release and (**D**) the initial rate of Ca^{2+} entry upon addition of extracellular Ca^{2+}. The values in **C** and **D** are the means ± SEM of 5 or 6 experiments of those in A and B. * $P<0.05$ and ** $P<0.01$.

5.2.3. Dose response curve for effect of exendin-4 on SOCE in lipid-loaded cells

To determine the half maximal effective concentration of exendin-4 to reverse the inhibited SOCE in lipid-loaded H4IIE liver cells, a dose-response curve was constructed employing five different concentrations of exendin-4 and the corresponding responses. Lipid-loaded cells were loaded with fura-2, incubated in the absence of added extracellular Ca^{2+} (Ca^{2+}_{ext}), exposed to the SERCA inhibitor DBHQ to release ER Ca^{2+}, then Ca^{2+}_{ext} was added to permit Ca^{2+} entry. DBHQ-initiated Ca^{2+} entry (response) was recorded for each corresponding concentration of exendin-4. Fig 5.4 shows that the effective dose of exendin-4 that caused half-maximal reversal of the inhibited SOCE in lipid-loaded cells, as judged by $[Ca^{2+}]_{cyt}$ (nM/min), is ~ 100 nM.

The concentration of exendin-4 (1 μM) which we employed is in the range used by others for the activation of liver cell metabolism (Flock et al., 2007) or metabolism of other cell types (Kuc et al., 2014). While it was intended to use low concentration of exendin-4, initial trial experiments using different concentrations showed that consistent reversal of impaired SOCE was observed with 1 μM exendin-4 in the case of hepatocytes isolated from Obese Zucker rats or lipid-loaded liver cells. So, this concentration of exendin-4 was used in all the experiments.

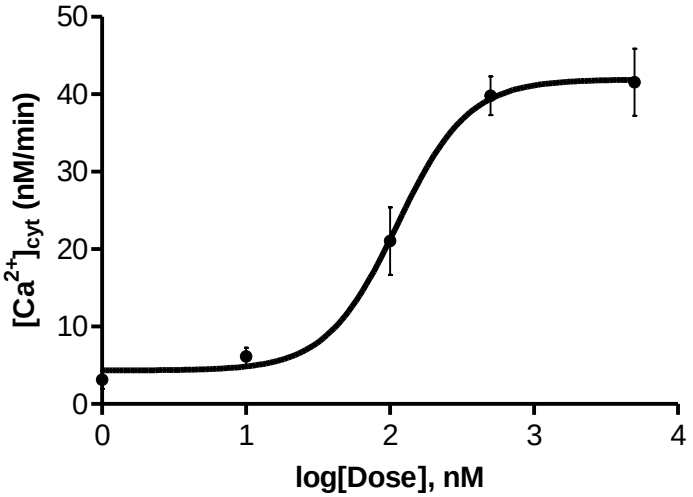

Fig. 5.4. Dose-response curve of exendin-4 in lipid-loaded H4IIE liver cells. The effective dose of exendin-4 that caused half-maximal reversal of the inhibited SOCE in lipid-loaded cells is ~ 100 nM. Maximal dose used here antilog of 4 = 10,000 nM = 10 μM. Effect of exendin-4 added to lipid-loaded H4IIE cells at the beginning of the measurement of Ca^{2+} imaging to lipid-loaded H4IIE cells. $[Ca^{2+}]_{cyt}$ was measured as a function of time in H4IIE cells loaded with fura-2, as described in the Methods section. The results shown are the mean values of 3 separate experiments for each concentration, in which each gave corresponding similar results. In each experiment, the fluorescence of 10-15 cells was measured. The curve was constructed with GraphPad Prism, 2014.

5.2.4. Exendin-4 does not affect Ca^{2+}_{cyt} or SOCE in hepatocytes isolated from lean Zucker rats

To determine further whether exendin-4 has any effect on normal non-steatotic cells, or on SOCE or ER Ca^{2+} release in hepatocytes isolated from lean Zucker rats, cells were loaded with fura-2, incubated in the absence of extracellular Ca^{2+} (Ca^{2+}_{ext}), exposed to exendin-4 to determine whether any Ca^{2+} release occurred from the ER, then Ca^{2+}_{ext} was added to permit Ca^{2+} entry. In hepatocytes isolated from lean Zucker rats, exendin-4 alone did not have any effect on $[Ca^{2+}]_{cyt}$ in the absence of DBHQ (Fig. 5.5). This result indicates that exendin-4 alone may not have a DBHQ-like effect in hepatocytes isolated from lean Zucker rats.

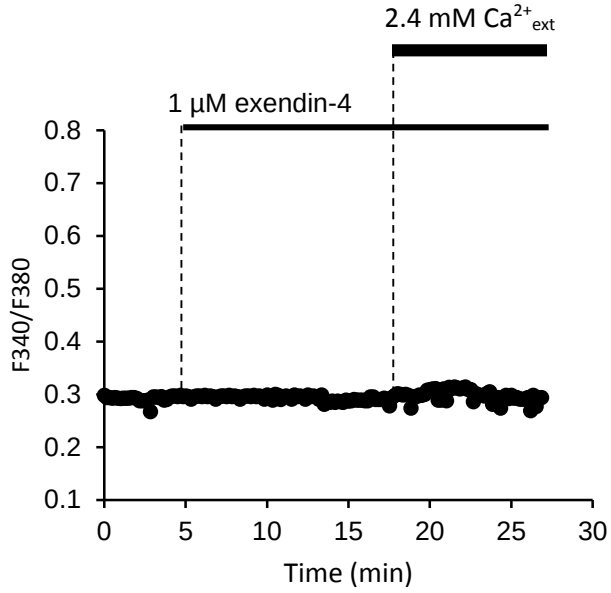

Fig. 5.5. Exendin-4 alone does not have any effect on $[Ca^{2+}]_{cyt}$ in the absence of DBHQ. (A) Hepatocytes isolated from lean Zucker rats were incubated in the presence of vehicle KRH (without Ca^{2+}). After 5 min, exendin-4 was added to cells initially in the absence of extracellular Ca^{2+}. Then extracellular 2.4 mM Ca^{2+} was added back to the incubation chamber. The results shown are representative traces of those obtained from 3 separate experiments (done on separate days) in which each gave similar results. In each experiment, the fluorescence of 10-15 cells was measured.

5.2.5. Exendin-4 reverses inhibited SOCE in hepatocytes isolated from obese Zucker rats

To test whether exendin-4 increases the rate of DBHQ-initiated Ca^{2+} entry in hepatocytes isolated from Zucker rats, the DBHQ-induced 'Ca^{2+} add back' protocol was followed. As in the case of vehicle control (non lipid-loaded) H4IIE cells (Fig. 5.2.), similar results were obtained in hepatocytes isolated from lean Zucker rats. Results showed that exendin-4 does not have any effect on DBHQ-induced Ca^{2+} entry but does inhibit DBHQ-induced ER Ca^{2+} release in hepatocytes isolated from lean Zucker rats (Fig. 5.6.). Hepatocytes isolated from obese Zucker rats showed a marked decrease in the rate of Ca^{2+} entry compared with hepatocytes isolated from lean Zucker rats (Fig 5.7.A *cf* Fig. 5.6.A). In hepatocytes isolated from Obese Zucker rats, exendin-4 substantially increased the rate of Ca^{2+} entry initiated by DBHQ and decreased the DBHQ-induced ER Ca^{2+} release as shown in the Fig 5.7.

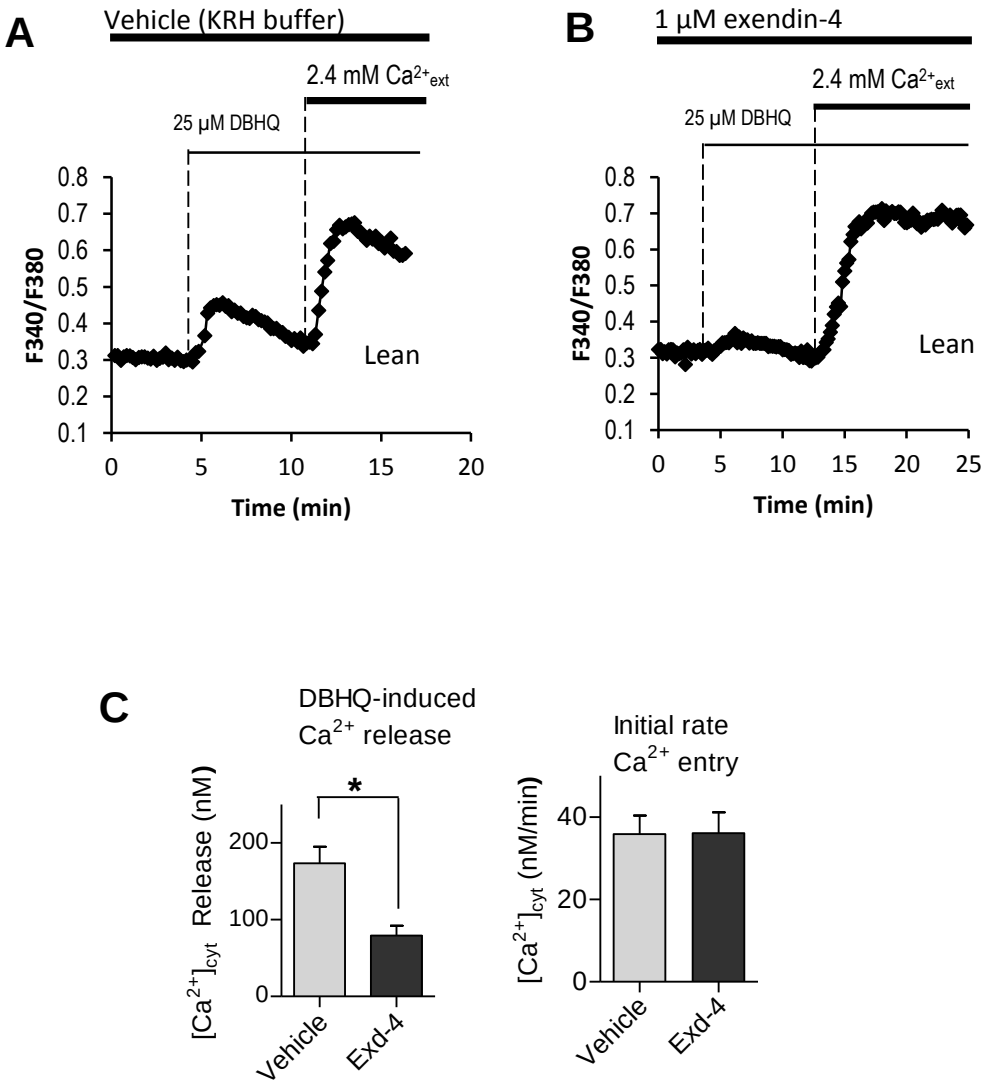

Fig. 5.6. Exendin-4 does not have any effect on DBHQ-induced Ca^{2+} entry in hepatocytes isolated from lean Zucker rats. Hepatocytes were incubated in the presence of vehicle (**A**) or exendin-4 (**B**). In each case DBHQ and Ca^{2+} were added to cells initially incubated in the absence of extracellular Ca^{2+}. The plots shown are each representative of those obtained in 3 similar experiments. In each experiment, the fluorescence of 10-15 cells was measured. (**C**) DBHQ induced ER Ca^{2+} release (left panel) and the initial rate of Ca^{2+} entry upon addition of extracellular Ca^{2+} (right panel). The values in **C** are the means ± SEM of 3 experiments of the type shown in A and B. * $P<0.05$.

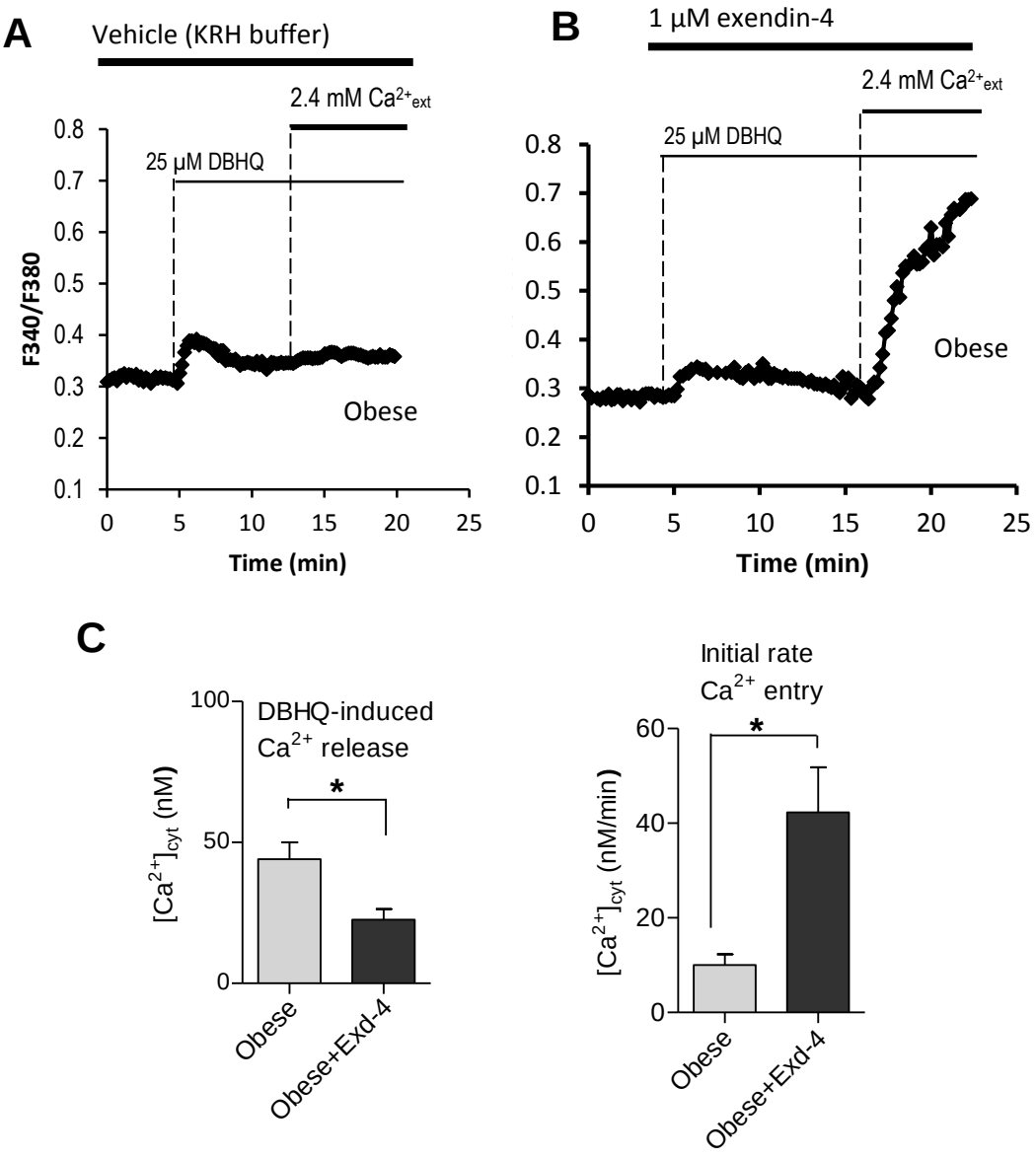

Fig. 5.7. Exendin-4 enhances the rate of DBHQ-induced Ca^{2+} entry in hepatocytes isolated from Obese Zucker rats. Hepatocytes were incubated in the presence of vehicle (**A**) or exendin-4 (**B**). In each case DBHQ and Ca^{2+} were added to cells initially incubated in the absence of extracellular Ca^{2+}. The plots shown are each representative of those obtained in 3 similar experiments. In each experiment, the fluorescence of 10-15 cells was measured. (**C**) DBHQ induced ER Ca^{2+} release (left panel) and the initial rate of Ca^{2+} entry upon addition of extracellular Ca^{2+} (right panel). The values in **C** are the means ± SEM of 3 experiments of the type shown in A and B. * $P<0.05$.

5.3 Discussion

The results of the study in this chapter have shown that an anti-diabetic agent, exendin-4, alone did not have any effect on $[Ca^{2+}]_{cyt}$ in the absence of DBHQ. There was no effect of this agent on SOCE, but it caused reduced ER Ca^{2+} release, in response to DBHQ, in normal non lipid-loaded H4IIE cells and hepatocytes isolated from lean Zucker rats. Exendin-4, however, has been shown to reverse impaired SOCE in lipid-loaded liver cells and steatotic hepatocytes isolated from Obese Zucker rats.

5.3.1. Exendin-4 reverses lipid-induced inhibition of store-operated Ca^{2+} entry

In the present experiments, exendin-4, a GLP-1 analogue, was employed to investigate the effect of that compound on SOCE in fatty liver cells, and interestingly, it was found that the lipid-induced inhibition of SOCE in H4IIE cells was substantially reversed by exendin-4. Using *in vivo* hepatocytes isolated from obese Zucker rats, exendin-4 exhibited similar results suggesting that exendin-4 may play a critical role in restoration of defective intracellular Ca^{2+} signalling in (patho) physiological environments. Moreover, the reversal of lipid-induced impaired SOCE by exendin-4 may point to a novel site of action for this anti-diabetic drug.

The effective dose (ED_{50}) of exendin-4 causing half-maximal reversal of the inhibited rate of SOCE in amiodarone-induced lipid-loaded H4IIE cells was found to be 100 nM. This experimental concentration of exendin-4 has been used by others to investigate various other effects of exendin-4 in hepatic lipid accumulation (Lee et al., 2012; Lee et al., 2014).

5.3.2. The possible mechanisms of action of exendin-4 to reverse impaired SOCE in steatotic liver cells

The likely mechanism(s) of reversal of inhibition of SOCE in lipid-loaded cells may involve exendin-4 activating store-operated Ca^{2+} entry in lipid-loaded liver cells by binding to glucagon-like peptide-1 receptors on the plasma membrane, enhancing movement of STIM1 to the plasma membrane and/or by dephosphorylation of Orai1. In lipid-loaded liver cells, the action of exendin-4 to reverse impaired SOCE was shown to be associated with a reduced ER Ca^{2+} content. The decrease in ER Ca^{2+} can be inferred from the figure 5.3 and 5.7. This reduction of ER Ca^{2+} may be due to an inhibition by exendin-4 of Ca^{2+} uptake by ER (through SERCA) – for which further investigation is needed.

It has been known for many years that upon binding to its receptor, GLP-1 increases cAMP levels via G-protein-coupled activation of adenylate cyclase, causing the activation of protein kinase A (PKA) (MacDonald et al., 2002). In islets cells, the movement of STIM1 to the junctions between ER and the plasma membrane and thereby binding of STIM1 to Orai1 is stimulated by PKA (Tian et al, 2012). While Tian et al., (2012) showed that STIM1 activity was shown to be considerably regulated by PKA in the islet cells, this phenomenon might be present in hepatocytes. Since Exendin-4 binds to GLP-1 receptors located on the plasma membrane of hepatocytes (Ding et al., 2006), it is possible that exendin-4-induced PKA may play a role in the up-regulation of STIM1 activity in the steatotic hepatocytes and subsequently may take part in the reversal of impaired SOCE in steatotic liver cells.

GLP-1 or exendin-4 has been shown to promote a continual increase in hepatocyte cAMP production which, in turn, can be associated with the induction of mRNA for both PPAR and AOX - that ultimately leads to reduction of lipid contents through the enhanced β-oxidation of fatty acids (Ding et al., 2006). The resultant reduced lipid content may decrease the production of DAG which, in turn, leads to reduced number of active PKC. Consequently the PKC-induced phosphorylation of Orai1 can be suppressed, thereby, leading to enhanced activity of SOCE (Kawasaki et al., 2010). In addition, since the activity of Orai1 or STIM1 can be regulated by phosphorylation (Lang et al., 2013; Pozo-Guisado et al. 2013), PKA-mediated phosphorylation of Orai1 or STIM1 can also account for the observed reversal of inhibited SOCE in steatotic liver cells. But no PKA-mediated phosphorylation of STIM1 or Orai1 has been reported yet. Further studies need to be done to provide the molecular mechanisms by which exendin-4 reverses lipid-induced SOCE inhibition in steatotic liver cells.

5.3.3. Future experiments employing exendin-4

Future study, as mentioned above, can be undertaken to determine the molecular mechanisms by which GLP-1 analogue exendin-4 improves impaired SOCE in fatty liver cells. Future experiments may investigate whether exendin-4 decreases the development of insulin resistance in liver cells by binding to GLP-1 receptors, inhibiting the PKC-mediated phosphorylation of Orai1, and triggering SOCE. It is also similarly important to investigate whether incubation with exendin-4 can re-store altered hormone-initiated intracellular Ca^{2+} signaling in lipid-loaded liver cells.

The results obtained in this chapter showed that application of exendin-4 is associated with reversal of impaired SOCE in steatotic liver cells. In such liver cells, in the absence of intervention, the impaired SOCE may have different pathophysiological consequences, in terms of hormone-regulated intracellular signaling cascades, glucose and lipid metabolism. The pathophysiological consequences that might be associated with impaired SOCE are to be investigated in the next chapter.

CHAPTER VI: EFFECTS OF INHIBITION OF STORE-OPERATED Ca^{2+} ENTRY ON GLUCOSE AND LIPID METABOLISM

6.1 Introduction

In the previous chapters (chapter 3 and 4), it was demonstrated that excess lipid accumulation in liver cells causes a substantial decrease in store-operated Ca^{2+} entry, and protein kinase C (PKC) mediates a substantial proportion of lipid-induced inhibition of SOCE. SOCE is required for the maintenance of hormone-initiated intracellular Ca^{2+} signalling (Gaspers and Thomas, 2005). Therefore we investigated the effect of steatosis on hormone-initiated Ca^{2+} signalling in the cells. Since a sustained increase in Ca^{2+}_{cyt} and hence SOCE are required for the activation of glycogen hydrolysis by hormones, the effect of steatosis on hormone-stimulated glucose release was also investigated.

Inhibited SOCE likely will lead to reduction of endoplasmic reticulum (ER) Ca^{2+} entry through SERCA2b and lead to a reduced amount of Ca^{2+} in the ER. This is known to alter ER Ca^{2+} homeostasis and function, and lead to the development of ER stress response (Fu et al., 2011; Park et al., 2010) and this ER stress has indeed been shown to be important in the development of insulin resistance (Fu et al., 2011; Samuel et al., 2004). Therefore, in this chapter, we have investigated pathophysiological consequences of lipid-induced SOCE on liver cells in terms of metabolic activities and intracellular signalling cascades.

Considering the evidence above, the specific aims of the experiments described in this chapter were: i) to test whether inhibition of SOCE alters hormonal signalling via intracellular Ca^{2+} ii) to test whether inhibition of SOCE leads to an altered rate of lipid accumulation in steatotic hepatocytes.

To test the effects of hormones on cytoplasmic Ca^{2+} in lipid-loaded cells, H4IIE cells were differentiated by incubation with insulin and dexamethasone (100 nM final concentration) to induce expression of plasma membrane hormone receptors and ATP and phenylephrine were used as agonists of physiological receptors. Additionally, hepatocytes isolated from obese Zucker rats were used to evaluate the effects of hormones on intracellular Ca^{2+} signalling in steatotic liver cells. To investigate whether inhibition of SOCE leads to an altered rate of lipid accumulation, two approaches were employed, viz., i) pharmacological inhibition of SOCE and ii) siRNA knockdown of SOCs components (STIM1 and Orai1).

6.2 Results

6.2.1 Lipid-loaded differentiated liver cells exhibit a reduced response to hormone-initiated intracellular Ca^{2+} signalling

Several studies have demonstrated that agonists such as ATP or phenylephrine can activate store-operated Ca^{2+} channels in liver cells (Barritt and Whiting, 1983; Gardner et al., 1997; Luo et al., 2001). Investigation of physiological consequences was conducted using H4IIE cells differentiated by incubating with 100 nM insulin and 100 nM dexamethasone for 10 to 14 days. It has been previously suggested that this incubation for differentiation was essential to induce expression of plasma membrane hormone receptors in H4IIE cells (Aromataris et al., 2006). The responses in $[Ca^{2+}]_{cyt}$ induced by the agonists ATP (P2Y purinergic) and phenylephrine (α-adrenergic) were recorded by fura-2 calcium imaging. In the presence of extracellular Ca^{2+}, the calcium signals generated consist of a quick initial rise followed by plateau, as described previously by Chen and Jan (2000). In freshly isolated primary hepatocytes, these types of hormone-initiated responses were observed by Thomas et al. (1991). In our investigations, differentiated lipid-loaded H4IIE cells showed a considerable decrease in the magnitude of ATP-induced intracellular Ca^{2+} signaling when compared to differentiated control cells. The intracellular Ca^{2+} signal is reduced in both initial peak height and the subsequent prolonged elevation of $Ca^{2+}{}_{cyt}$ (Fig. 6.1A-D). In the presence of extracellular Ca^{2+}, similar responses (but with less amplitude) were observed when intracellular Ca^{2+} signals were generated by the treatment with phenylephrine (Fig. 6.2 A-D).

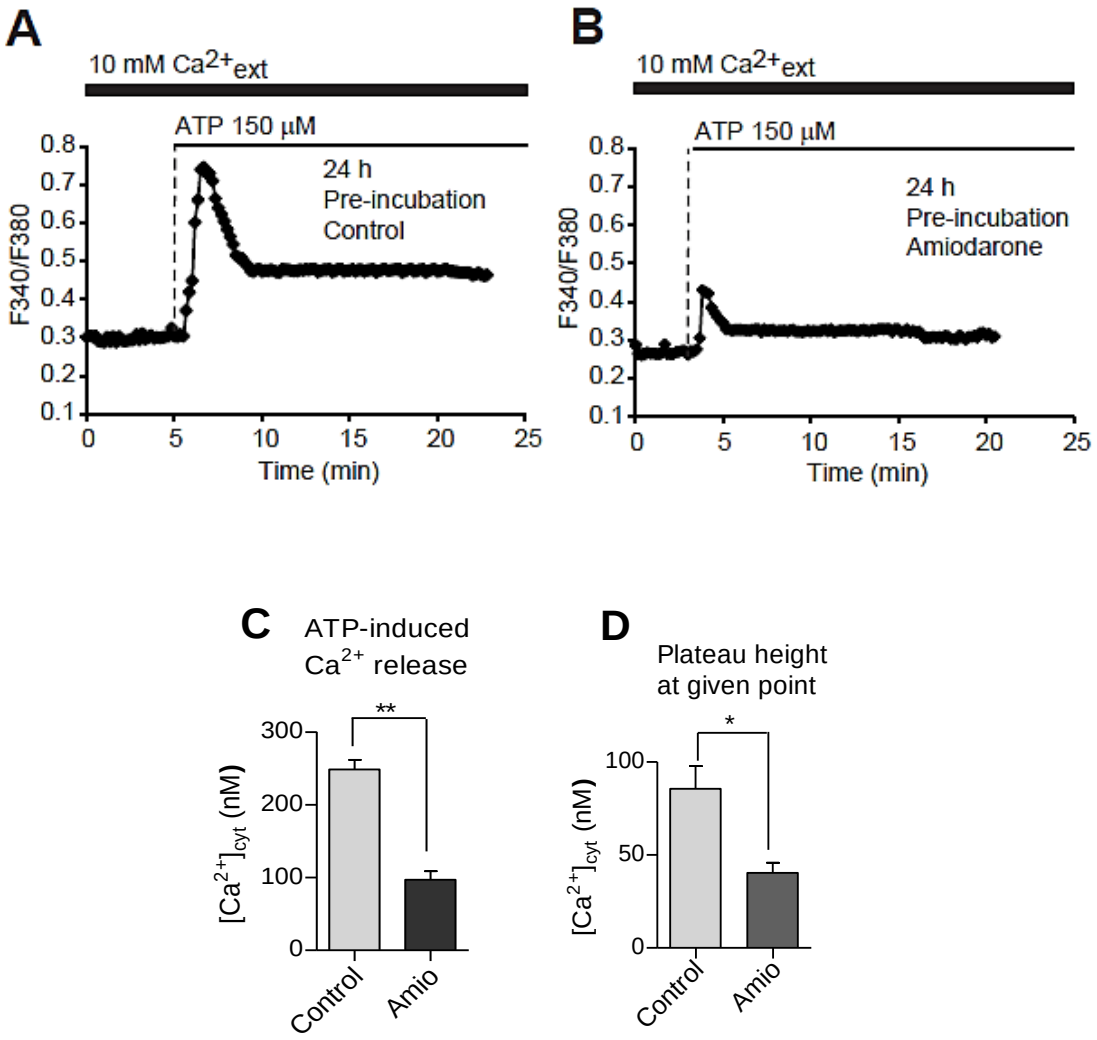

Fig. 6.1. Differentiated cells pre-treated with amiodarone show reduced ATP-initiated intracellular Ca^{2+} signaling. (A-B) Representative traces showing the effects of ATP (A, B) on $[Ca^{2+}]_{cyt}$ in the presence of $[Ca^{2+}]_{ext}$ in differentiated H4IIE cells pre-treated with vehicle (A) or amiodarone (B). $[Ca^{2+}]_{cyt}$ measurements as a function of time in cells loaded with fura-2, were performed as described in the Method section. The additions to the given bath are indicated by the horizontal bars. The results shown are representative traces of those obtained for 3 to 4 separate experiments (done on separate days) in which each gave similar results. In each experiment, the fluorescence of 10-15 cells was measured. (**C**) ATP induced ER Ca^{2+} release in lipid-loaded cells were significantly less than the ones obtained in control cells ($P<0.01$). (**D**) shows the plateau height at the 15^{th} min time point in differentiated control and amiodarone pre-treated cells ($P<0.05$). The values in **C** and **D** are the means ± SEM from 3 or 4 experiments of the type shown in **A** and **B**.

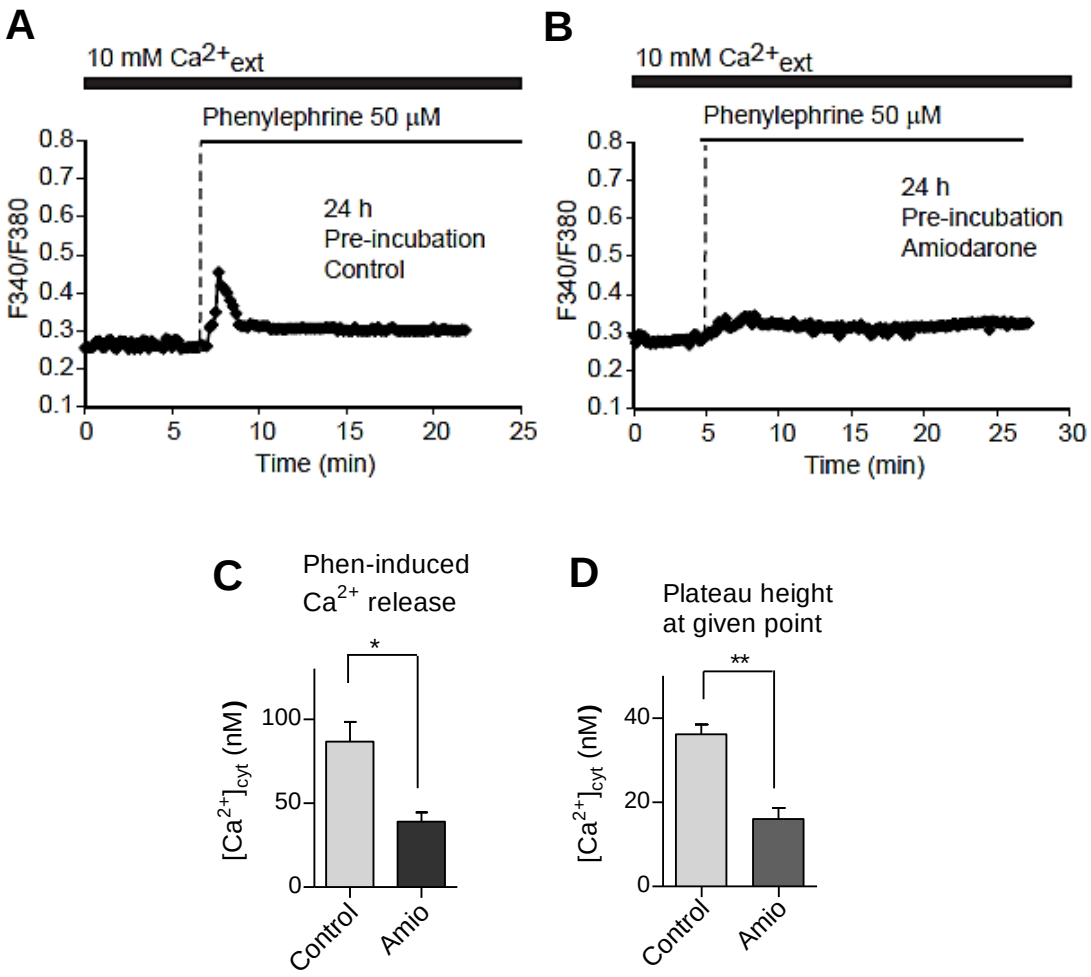

Fig. 6.2. Differentiated cells pre-treated with amiodarone show reduced phenylephrine-initiated intracellular Ca^{2+} signalling. (A-B) Representative traces showing the effects of phephyephrine (A,B) on $[Ca^{2+}]_{cyt}$ in the presence of $[Ca^{2+}]_{ext}$ in differentiated H4IIE cells pre-treated with vehicle (A) or amiodarone (B). $[Ca^{2+}]_{cyt}$ measurements as a function of time in cells loaded with fura-2, were performed as described in the Method section. The additions to the given bath are indicated by the horizontal bars. The results shown are representative traces of those obtained for 3 to 4 separate experiments (done on separate days) in which each gave similar results. (**C**) Phenylephrine induced ER Ca^{2+} release in lipid-loaded cells were significantly less than the ones obtained in control cells ($P<0.05$). (**D**) shows the plateau height at the 15^{th} min time point in differentiated control and amiodarone pre-treated cells ($P<0.01$). The values in **C** and **D** are the means ± SEM of 3 or 4 experiments of the type shown in A and B.

6.2.2 Hepatocytes isolated from obese Zucker rats exhibit decreased response to hormone-initiated intracellular Ca^{2+} signalling

After obtaining the cell line based *in vitro* results (mentioned above), the next step was to extend the investigation to a more *in vivo* physiological situation. As in the case of amiodarone pre-treated differentiated H4IIE cells, hepatocytes isolated from obese Zucker rats also showed reduced calcium signals in response to an agonist ATP or phenylephrine (Fig. 6.3 A-D). As mentioned before, for freshly isolated hepatocytes, these findings are consistent with the observations of Thomas et al. (1991). This result may indicate that altered SOCE is associated with decreased hormone-initiated intracellular Ca^{2+} signalling in obese Zucker rat hepatocytes.

These results provide additional evidence that intracellular Ca^{2+} signalling generated by physiological receptor agonists, is impaired in excess lipid loaded liver cells compared to normal liver cells.

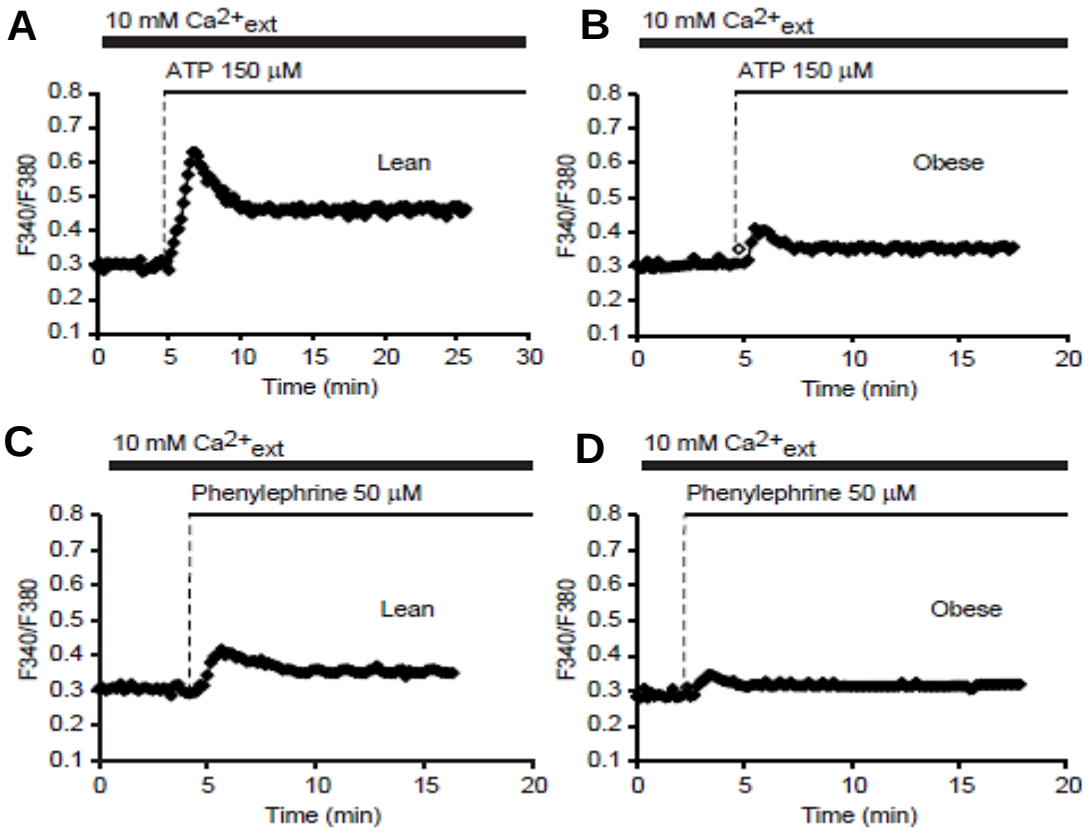

Fig. 6.3. Hepatocytes isolated from obese Zucker rats show an impaired Ca^{2+} signalling initiated by ATP or phenylephrine (A-D) Representative traces showing the effects of ATP (A,B) and phenylephrine (C,D) on $[Ca^{2+}]_{cyt}$ in the presence of $[Ca^{2+}]_{ext}$ in primary hepatocytes isolated from lean Zucker rats (A,C) or obese Zucker rats (B,D). The results shown are representative traces of those obtained for 3 separate experiments (done on separate days) in which each gave similar results. In each experiment, the fluorescence of 10-15 cells was measured.

6.2.3. Differentiated lipid-loaded cells shows reduced hormone-initiated glucose release into cell culture medium

Since there is an evidence to indicate that cytoplasmic free Ca^{2+} is the second messenger for the glycogenolytic effect of phenylephrine (Huhn et al., 1983), we tested the effect of phenylephrine on glycogen hydrolysis in lipid-loaded liver cells. To evaluate the effects of hormones on glycogenolysis, H4IIE cells were differentiated, as previously mentioned, by incubation with insulin and dexamethasone for 14 days. Glucose was added to the cells for the last 2 days (of two weeks) to maximise the glycogen reserves in cells, and during the hormone treatment, FBS- and glucose-free medium were used. Results from the glucose release assay showed that phenylephrine-initiated glucose release into cell culture medium is considerably reduced in differentiated lipid-loaded (pre-treated with amiodarone) cells compared to control (non lipid-loaded) cells (Fig. 6.4).

In addition to the investigations regarding the physiological consequence mentioned above, other experiments tested whether impaired SOCE in steatotic liver cells may cause any pathological burden on the cells (see subsection 6.2.4.).

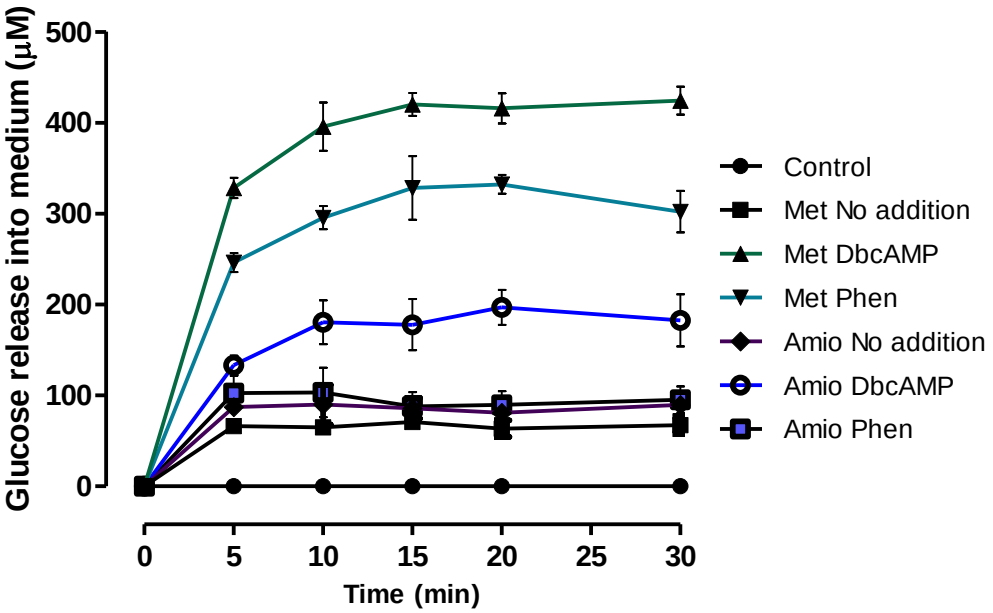

Fig. 6.4. Lipid accumulation in differentiated H4IIE liver cells contributes to altered hormone-initiated glycogen hydrolysis. During hormone treatment, DMEM medium contained 10 mM Ca^{2+}. The traces are the means of 3 different experiments in which each gave similar results. Dibutyryl-cAMP (DbcAMP) was used as a positive control. FBS- and glucose-free DMEM medium was considered as 'control'. Experimental details are described in Methods section. Met, methanol; Phen, phenylephrine; Amio, amiodarone.

6.2.4. SOCE inhibitor 2-APB enhances the accumulation of intracellular lipids in amiodarone or palmitate pre-treated H4IIE cells

To test whether inhibition of SOCE leads to altered rate of lipid accumulation, two approaches were employed, i) pharmacological inhibition of SOCE and ii) siRNA knockdown (results are in subsection 6.2.6) of SOCs components (STIM1 and Orai1), as mentioned in the introduction to this chapter. Incubation of H4IIE liver cells with the SOCE inhibitor 2-aminoethyl diphenylborate (2-APB) for 24h or 48h (48h not shown) caused an almost 2-fold enhancement of lipid accumulation compared with that caused by amiodarone alone (Fig. 6.5 A, 2-APB plus Amio cf Amio alone). As amiodarone may have some toxicity towards cells as suggested by others (McCarthy et al., 2004; Rao and Agarwal, 2012), a further evaluation was made by using palmitate (Nakamura et al., 2009). Fig 6.5 B shows that inhibition of Ca^{2+} entry through SOC channels by incubation of H4IIE rat liver cells with 2-APB (75 μM for 24h) increases the accumulation of lipid induced by incubation with palmitate (500 μM for 24h). Similar results were also obtained using insulin and dexamethasone incubated differentiated H4IIE cells (Fig. 6.5 C).

Several studies suggested that 2-APB may have some non-specific actions, and thus, careful titration of its concentration is needed for its specific target (Bootman et al., 2002; Diver et al., 2001). So to confirm the above (2-APB) results, a more selective SOCE inhibitor, BTP2 (Ishikawa et al., 2003), and knockdown strategy of SOC components were used next.

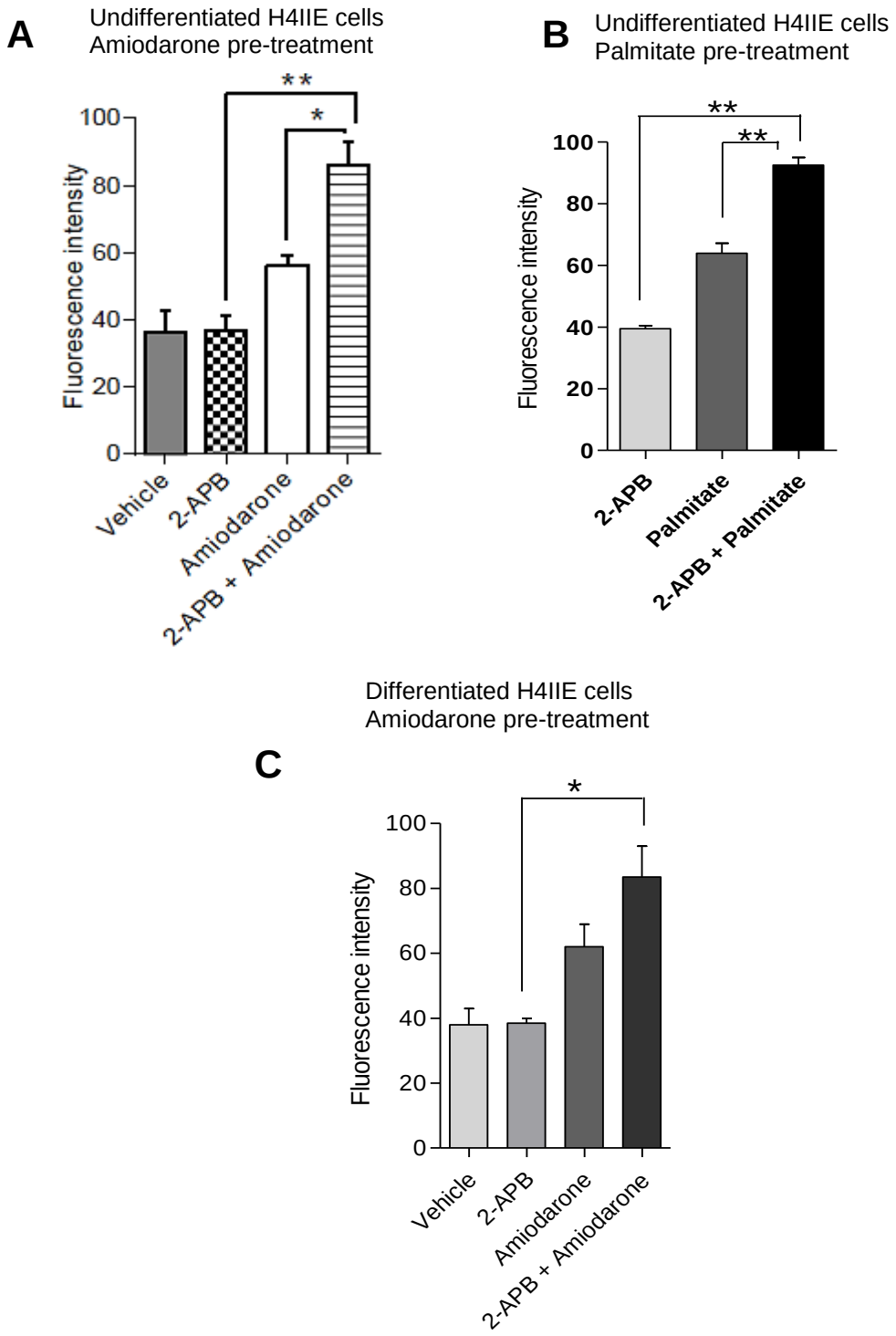

Fig. 6.5. Co-addition of 2-APB enhances the accumulation of intracellular lipids in amiodarone or palmitate pre-treated H4IIE cells. (A, B) Inhibition of Ca^{2+} entry through SOCs by incubation of H4IIE rat liver cells with 2-APB (75 μM co-added for 24h) increases the accumulation of lipid induced by incubation with amiodarone (Amio) (20 μM for 24h) or Palmitate (500 uM for 24h). Values (fluorescence intensity, arbitrary units) are means ± SEM n=4, *P<0.05, **P<0.01. (**C**) Results obtained using insulin- and dexamethasone-incubated differentiated H4IIE cells, n=3; *P<0.05. Intracellular lipid was measured by Nile red fluorescence as described in Methods section.

6.2.5. Pharmacological inhibition of SOCE by BTP-2 increases the accumulation of intracellular lipids in amiodarone or palmitate pre-treated H4IIE cells

In comparison with 2-APB as an inhibitor of SOCE, the pyrazole derivative, BTP2 (YM-58483) (Ishikawa et al., 2003) can act as a more specific inhibitor than other SOCE inhibitors (including 2-APB) because BTP-2 may not block K^+ channels (Ishikawa et al., 2003; Putney, 2010; Zitt et al., 2004). In order to test further whether the inhibition of SOCE will lead to increased lipid accumulation, BTP-2 was used next instead of 2-APB.

To test the effect of BTP-2 on lipid accumulation in amiodarone or palmitate pre-incubated H4IIE liver cells, cells were pre-incubated with BTP-2 and amiodarone (or palmitate) for 24h. Intracellular lipid measurement using Nile red fluorescence microscopy showed that cells, pre-incubated with amiodarone and BTP-2 (Fig. 6.6 A) or palmitate and BTP-2 (Fig. 6.6. B), displayed an enhanced accumulation of intracellular lipids. The findings using another SOCE blocker, BTP-2, further supported the idea that impaired SOCE in lipid-loaded cells may further aggravate intracellular lipid metabolism.

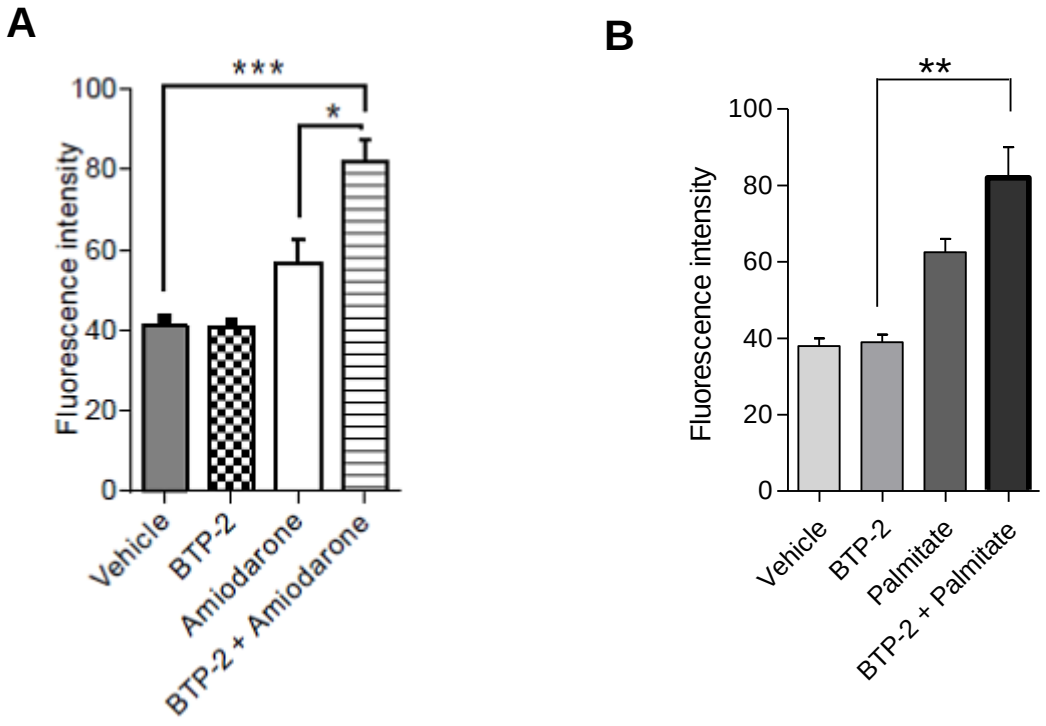

Fig. 6.6. BTP-2 (SOCE inhibitor) enhances the accumulation of intracellular lipids in amiodarone or palmitate pre-treated H4IIE cells. Inhibition of Ca^{2+} entry through SOCs by incubation of H4IIE rat liver cells with BTP-2 (10 μM for 24h) increases the accumulation of lipid induced by incubation with amiodarone (20 μM for 24h), shown in panel **A** or with palmitate (500 μM for 24h), shown in panel **B**. Intracellular lipid was measured using Nile red and fluorescence microscopy, and quantitated using MetaFluor software. Values (fluorescence intensity, arbitrary units) are means ± SEM, n=3, *P<0.01, **P<0.01, ***P<0.001.

6.2.6. Knockdown of SOCs components (Orai1 and STIM1) in liver cells enhances lipid accumulation

In order to investigate further whether the inhibition of SOCE in liver cells enhances lipid accumulation, a siRNA transfection strategy was next employed to knock down STIM1 and Orai1.

H4IIE liver cells were transfected with siRNA against STIM1 and Orai1, and incubated for 48 h. After the extraction of total RNA from transfected cells, STIM1 and Orai1 mRNA expression was measured by qPCR. Since highly abundant protein (e.g., SOCs components in liver cells) usually may have a highly expressed mRNA (Vogel et al, 2013), qPCR was performed to measure mRNA of STIM1 and Orai1 in siRNA transfected H4IIE cells. However, for the additional evidence of the knockdown efficiency, western blot should be done in future to measure the STIM1 and Orai1 protein levels in transfected cells. In our experiment, a knockdown efficiency of 22-50% was obtained for both STIM1 and Orai1 as determined by qPCR (Fig. 6.7. A, B).

Given the successful knockdown of STIM1 and Orai1, further tests were done to determine whether incubation with amiodarone could enhance the rate of lipid accumulation. For measurement of lipid accumulation, cells were treated with amiodarone 24h post-transfection. Results from these studies showed that when the expression of STIM1 and Orai1 in H4IIE cells was knocked down using siRNA, an enhancement of lipid accumulation was observed, as is shown in Fig 6.8. In Figure 6.8, the phrase ‘cells only’ represents H4IIE cells with no addition and no transfection reagent. Amiodarone was dissolved in vehicle methanol.

This result provides additional evidence about the effect of reduced SOCE on intracellular lipid accumulation in lipid-loaded liver cells.

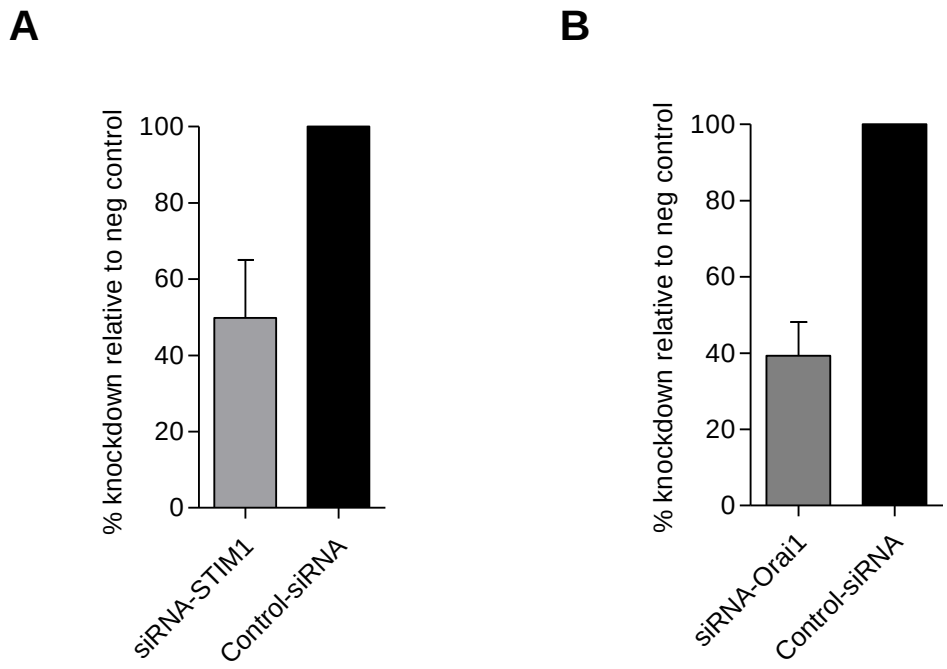

Fig. 6.7. Efficiency of siRNA knockdown of STIM1 and Orai1. The effect of STIM1-specific siRNA (**A**), and Orai1-specific siRNA (**B**) on STIM1 and Orai1 mRNA levels in H4IIE rat liver cells is shown. Cell transfections and mRNA extraction were performed as described in Materials and Methods (Sub-section: 2.6. and 2.7.). Average data from three separate transfections are shown.

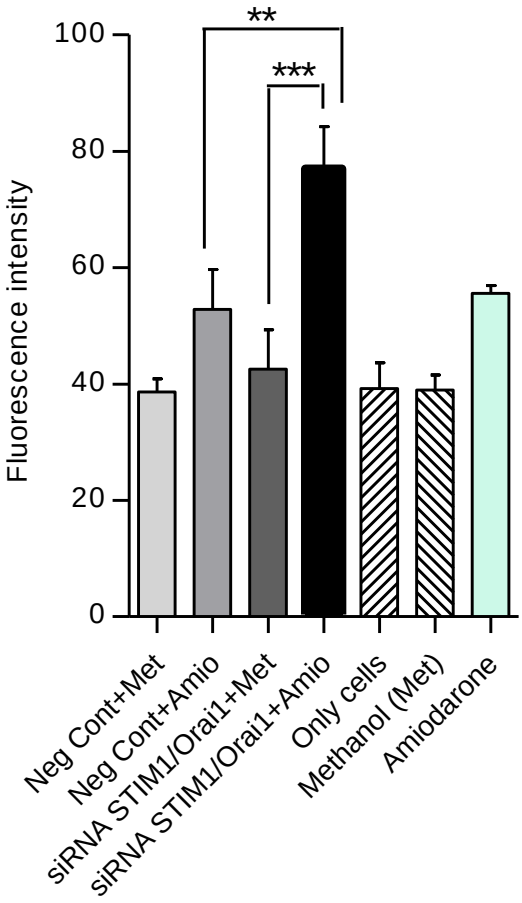

Fig. 6.8. Effects of combined STIM1/Orai1 siRNA knockdown on lipid-accumulation in liver cells induced by pre-treatment with amiodarone. Column graph displaying average intensity of yellow fluorescence from Nile Red-stained H4IIE cells co-transfected with siRNA targeting STIM1 and Orai1 or transfected with negative control siRNA and pre-treated with either amiodarone (20 μM for 24 h) or methanol (control). 'Only cells' represents H4IIE cells with no addition and no transfection reagent. Amiodarone was dissolved in vehicle methanol. Means ± SEM (n= 3). Degree of significance: ** $P<0.01$, and *** $P<0.001$.

6.3 Discussion

The results of the study in this chapter have shown that lipid-loaded cells exhibit an impaired hormone-initiated intracellular Ca^{2+} signalling which, in turn, contributes to altered hormone-initiated glycogen hydrolysis, and inhibition of SOCE was observed to be associated with enhanced lipid accumulation.

6.3.1. Hormone initiated Ca^{2+} signalling is decreased in steatotic liver cells

In the present study, it was shown that steatotic liver cells show reduced ATP- or phenylephrine-initiated Ca^{2+} release from intracellular stores and plateau height. The observed decrease in hormone-initiated plateau in lipid-loaded liver cells is most likely due to the inhibition of store-operated Ca^{2+} entry by excess intracellular lipid. The reduction of intracellular Ca^{2+} stores in lipid-loaded liver cells may be the result of lipid-initiated reduced SOCE and lipid-induced inhibition of SERCA2b as shown by others (Fu et al., 2011; Park et al., 2010). The intracellular Ca^{2+} mobilization (quite a transient response) induced by extracellular ATP or phenylephrine is consistent with the evidence shown previously by Leite et al. 2009. Similar responses were obtained using fresh primary hepatocytes isolated from Zucker rats.

The concentrations of the agonists ATP or phenylephrine which were employed are in the range used by others for the activation of liver cell metabolism (DeWitt and Putney, 1983; Dionisio et al., 2009; Horstman et al., 1986; Kitamura et al., 1995). In addition, the receptor density in differentiated H4IIE cells is likely to be lower than that in freshly-isolated hepatocytes, which is the reason why the concentration of phenylephrine, in particular, is at the higher limit of the concentration ranges employed by other research groups. Notwithstanding, altered reciprocal change in receptors or decreased receptor coupling efficiency may play a minor role in this

mechanism –which yet to be explored. There might be a reciprocal change (e.g., a decrease in the number of alpha-1 adrenergic receptors and an increase in beta-2 receptor density, without change in the affinity of agonists) in adrenergic receptors in isolated hepatocytes during primary cell culture as shown by Schwarz et al. (1985). In the case of lipid-loaded H4IIE cells, such evidence is not available yet.

In our experimental conditions, liver cells exposed to ATP or phenylephrine showed a typical hormone-initiated Ca^{2+} signals in the presence of 10 mM extracellular Ca^{2+}. Such a concentration of extracellular Ca^{2+} has previously been reported in the case of *Xenopus laevis* Oocytes (Bird et al., 1999). Initial trial experiments using from 2.4. mM, 5 mM and 10 mM extracellular Ca^{2+} showed that consistent agonist response was observed with 10 mM extracellular Ca^{2+}. This concentration was used in our experiments. This Ca^{2+}_{ext} concentration needed to be higher, may be, due to an altered selectivity of agonists for its receptors located on the plasma membrane or any alteration of ion permeability of plasma membrane – which needs to be investigated in future.

6.3.2. Implications of the decreased hormone-initiated Ca^{2+} signalling in steatotic liver cells

Evidence is also provided that lipid accumulation (induced by pre-treatment with amiodarone) in liver cells contributes to the altered hormone-initiated glycogen hydrolysis. The mechanism by which intracellular Ca^{2+} regulates hepatic glucose metabolism may be altered in lipid-loaded cells. Since in the steatotic or lipid-loaded liver cells, the activity of Ca^{2+} mobilizing agonists is likely to be reduced together with reduced SOCE, the interaction of Ca^{2+} ions with phosphorylase *b* kinase might be limited, thus reducing the stimulation of phosphorylase activity and thereby reducing both glycogen breakdown, and consequently glucose release, leading to

impaired glucose homeostasis. The speculation is, although indirectly, further supported by the observations that hepatocyte lipid accumulation causes ER stress and subsequently may alter glucose homeostasis (Amaya and Nathanson, 2013; Blackmore et al., 1986; Park et al., 2010; Wang and Kaufman, 2014). In lipid-loaded liver cells, both increased lipid droplets and reduced cytoplasmic Ca^{2+} can alter PKC function which may alter insulin receptor kinase function that potentially alter tyrosine phospohorylation of IRS-1 (Jornayvaz and Shulman, 2012). This in turn may lead to modification of the MEK pathway and gluconeogenesis (Anderson et al., 2012; Jornayvaz and Shulman, 2012; Racioppi and Means, 2012). As the regular function of SOCs channels is to sustain the agonist signal and refill the internal Ca^{2+} stores (Gaspers and Thomas, 2005), the lipid-induced inhibited SOCE may contribute to the exacerbation of the whole calcium signalling network in lipid-loaded liver cells.

6.3.3. Inhibition of SOCE in lipid-loaded liver cells enhances lipid accumulation

The results above have shown that lipid-induced inhibited SOCE may lead to reduced ER Ca^{2+} content, and pharmacological inhibition of SOCE or knock down of STIM1 and Orai1 can further enhance this lipid accumulation (induced by palmitate or amiodarone) which in turn supports the synthesis of TGs, DAGs or other lipids. The rate of intracellular lipid accumulation is likely to be dependent on the degree of knockdown of STIM1 and/or Orai1. In our experimental conditions, whether increased amiodarone–induced lipid accumulation resulted from knockdown of SOCs components is proportional to decreased Ca^{2+} entry - has not been tested directly. However, from the results of the studies mentioned in Chapter III (Effect of lipid accumulation in liver cells on SOCE), the observed increased lipid

accumulation (in knockdown followed by lipid-loading experiment) is likely to account for the reduction of SOCE.

Recently it has been well understood that altered Ca^{2+} homeostasis in the ER contributes to dysregulation of liver lipid metabolism and contributes to liver-associated metabolic diseases (Wang and Kaufman, 2014). There is also evidence that Ca^{2+} homeostasis of the ER is closely linked to the synthesis of triglycerides in hepatocytes (Park et al., 2010), and a low ER Ca^{2+} concentration may be further associated with increased triglyceride synthesis (Baumbach et al., 2014; Fu et al., 2012). Moreover, ER membranes are the site from which cytoplasmic lipid droplets may originate in response to an excess of palmitate and other fatty acids (Brasaemle and Wolins, 2012). It has been also suggested that expression of some genes involved in lipogenesis is considerably increased with a low ER Ca^{2+} concentration (Fu et al., 2012; Park et al., 2010). In our present observation, possibly, the reduced SOCE may act together with inhibition of SERCA2b to create a low ER Ca^{2+} concentration in lipid-loaded liver cells. This can be partly associated with an enhancement of the accumulation of cytoplasmic lipid droplets. Moreover, increased lipogenesis initiated by the ER stress response may incorporate more free fatty acids into the process of triglyceride synthesis in the ER membrane (Mekahli et al., 2011), which may provide another avenue for the formation of excess lipid droplets. The observation that inhibited SOCE increases lipid accumulation is consistent with the reported knock out of STIM1 in Drosophila leading to lipid accumulation in fat storage cells (Baumbach et al., 2014).

The combination of all the evidences supported in these four consecutive result chapters will be critically analysed and discussed collectively in the next chapter.

CHAPTER VII: GENERAL DISCUSSION

The primary aims of the studies undertaken in this thesis were to determine if store-operated Ca^{2+} entry (SOCE) is altered in steatotic liver cells and to investigate the role of protein kinase C (PKC) in impaired SOCE, if any, induced by steatosis. Further aims were to test whether the GLP-1 analogue exendin-4 reverses altered SOCE in lipid-loaded liver cells, and finally to evaluate the physiological and pathological consequences of lipid-induced altered SOCE in liver cells. The results of the study, using two different cultured cell models and *in vivo* hepatocytes isolated from obese Zucker rats, have shown that lipid accumulation in liver cells causes a significant decrease in store-operated Ca^{2+} entry and ER Ca^{2+} level, and protein kinase C (PKC) mediates a large proportion of the lipid-induced inhibition of SOCE. The observed reduction in ER Ca^{2+} has been inferred from the ER Ca^{2+} release or uptake experiments. The results also have shown that the GLP-1 analogue exendin-4 reverses the lipid-induced inhibition of SOCE, and that the inhibition of SOCE in lipid-loaded liver cells leads to an increase in the rate of lipid accumulation.

7.1 Limitations of models of liver cell steatosis

In our studies, we have employed three different models, as mentioned before. These are the amiodarone induced lipid-loaded cultured cell model (Puljak et al., 2005), the palmitate induced lipid-loaded cultured cell model (Nakamura et al., 2009) and primary hepatocytes isolated from obese Zucker rats (Buque et al., 2010; Domenech et al., 1993; Steenks et al., 2010).

Amiodarone induces intracellular lipid accumulation by inhibition of lipid oxidation within cells (Fromenty et al., 1990) and this amiodarone induced lipid-loaded cell model was previously used by Antherieu et al. (2011) in HepaRG cells. It has been reported by Antherieu et al. (2011) that in the case of HepaRG cells, transcript of thyroid hormone-inducible hepatic protein (THRSP) was significantly increased after 24-hour incubations with amiodarone. THRSP is associated with lipogenesis programme in liver cells. THRSP overexpression in human hepatocytes showed increased lipogenesis through activation of PXR (Moreau et al. 2009). Moreover, amiodarone itself is an iodine-rich compound. In Balb/C mice liver, excess iodine has been shown to alter thyroid hormone metabolism which in turn induces FAS mRNA that ultimately led to the accumulation of lipid in the liver (Xia et al. (2013). In our amiodarone-pre-treated experimental H4IIE cell model, further experiments need to be done to determine whether S14 gene (similar to *THRSP* gene in human hepatocytes) is involved in amiodarone-induced steatosis.

Amiodarone and its metabolite, desethylamiodarone, have a broad range of pharmacological actions and have been reported to affect multiple signaling pathways. This includes modulating activity of PKC (Vig and Desaiah, 1991), blocking calcium channels and perturbing cytosolic Ca^{2+} homeostasis (Lubic et al., 1994). This may raise the possibility that amiodarone could directly inhibit SOCE and/or deplete internal Ca^{2+} stores independent of cellular lipid levels. From this perspective, it was hypothesized that amiodarone may have a direct effect on the SOCs components in the plasma membrane. In experiments to test this possibility, H4IIE cells were incubated with amiodarone for 10 min, then washed off using the same protocol as for the 24 hour amiodarone treatment. The study showed no change in DBHQ-induced Ca^{2+} release or entry compared with control cells suggesting that

amiodarone does not directly inhibit store-operated Ca^{2+} entry or SOCs components in the plasma membrane.

As excess palmitate in the cells may cause growth arrest (Listenberger et al., 2001), generate ROS (Nakamura et al., 2009), and can be lipotoxic to cells of hepatic lineage *in vitro* (Mei et al., 2011), the results obtained from this palmitate model (also from the amiodarone induced lipid-loaded model) were verified by using steatotic fresh primary hepatocytes isolated from obese Zucker rats, and similar results were obtained. As the three different models showed a similar pattern of results, when the given results from the three models were compared for a particular experimental condition, it may essentially indicate that the results obtained from our studies are independent of the models used. Notwithstanding, with some limitations, use of the 3 different models in this study provides convincing evidence that inhibition of SOCE is one of the effects of liver cell steatosis. These cell models are valuable tools for studying Ca^{2+} signaling in hepatic steatosis, and may also be appropriate for the investigations of hepatic insulin resistance or further hepatic complications in type 2 diabetes and NAFLD.

7.2 The mechanism by which intracellular lipid inhibits store-operated Ca^{2+} entry via PKC activation

The second study (chapter four) employed the above-mentioned cell culture models, to investigate the underlying mechanisms linking the inhibition of SOCE and ER Ca^{2+} release in steatotic liver cells and involvement of PKC. Employing GFX and calphostin C, inhibitors of PKC, and PMA, an activator of PKC, the results have shown that PKC mediates the lipid-induced inhibition of store-operated Ca^{2+} entry. The observation in our experiments that treatment with PKC inhibitors reversed the

attenuated SOCE by 60 to 70% in steatotic liver cells led to the conclusion that PKC-mediated phosphorylation of SOCs components is not the only means by which inhibition of SOCE occurs in steatotic cells. However, the results obtained from the experiments where PKC was inhibited by 30 min incubation with GFX, or downregulated by 24h pre-treatment with PMA, suggest that activation of PKC accounts for the majority of the observed lipid-initiated inhibition of SOCE. The decreased ER Ca^{2+} content in steatotic liver cells is not likely to play a main role in the mechanisms by which lipid accumulation decreases SOCE. The observations, where GFX added after DBHQ (to initiate ER Ca^{2+} release) caused almost the same degree of reversal of SOCE inhibition as is shown when GFX is added before DBHQ may indicate that the step(s) involved in the inhibition of SOCE in steatotic liver cells will be the downstream events of ER Ca^{2+} release.

There is extensive evidence to suggest that hepatocyte steatosis is associated with the activation of PKCε, PKCδ, and PKCβ (Greene et al., 2010; Huang et al., 2009; Jornayvaz et al., 2011; Jornayvaz and Shulman, 2012; Puljak et al., 2005). It was shown in a recent study that PKC can suppress SOCE via phosphorylation of Orai1 in HEK293 cells (Kawasaki et al., 2010). Recent studies also show that the activity of STIM1 is regulated by phosphorylation (Pozo-Guisado et al., 2013; Pozo-Guisado and Martin-Romero, 2013; Smyth et al., 2009). Thus PKC-mediated phosphorylation of STIM1 may also play a role in the observed inhibition of SOCE in the experiments. While some extracellular-signal-regulated kinases (Pozo-Guisado et al. 2010) have been identified for the phosphorylation of STIM1 in various cell types, no PKC-mediated phosphorylation of STIM1 has been reported yet (Srikanth et al., 2013).

Several studies have reported that the activation of PKC inhibits SOCE in various cells types (Haverstick et al., 1997; Lee et al., 1997; Parekh and Penner, 1995) and employing PMA it was confirmed for hepatocyte SOCE in our experiments. The likely mechanism underlying inhibition of SOCE, therefore, involves the activation of one or more isoforms of PKC by DAG, the altered phosphorylation of Orai1 or STIM1 and inhibited Ca^{2+} entry through Orai1. However, the observation that GFX, when added after DBHQ-induced ER Ca^{2+} release, could reverse the lipid-initiated SOCE inhibition indicates that Orai1, rather than STIM1, may be the site of action of PKC.

As mentioned previously, in our experiments, it was found that use of GFX was associated with a decrease in the DBHQ-and ionomycin-releasable Ca^{2+} store in lipid-loaded liver cells. This is probably due to the inhibition of Ca^{2+} uptake into the ER by means of inhibited SOCE, as shown in this study, and lipid-initiated SERCA2b inhibition as documented by other groups (Fu et al., 2011; Park et al., 2010). In the present study, when liver cells were incubated with GFX for 5 or 30 min, a reduced amount of Ca^{2+} in the DBHQ-and ionomycin-releasable Ca^{2+} store was observed. This is probably due to a GFX induced-inhibition of Ca^{2+} uptake into ER, or independent of PKC activity (Sipma et al., 1996).

Recently it has been reported that during the meiosis, SOCE inactivation may result from the internalization of Orai1 into an intracellular vesicular compartment and from the failure of STIM1 to cluster in response to ER store depletion in *Xenopus laevis* oocytes (Yu et al., 2009) and mouse oocytes (Lee et al., 2013). Such evidence are still not available for hepatocytes or liver cell lines. However, we cannot rule out the possibility that steatosis itself might internalize some Orai1 and there might be a

little consequence of internalization on the PKC-induced degree of phosphorylation of Orai1 but further experiments are needed to determine that. In addition, it has been reported that little change was found in the expression of Orai1 and STIM1, the main isoforms of Orai and STIM, which constitute SOCs in liver cells (Barritt et al., 2008) suggesting that the lipid-induced inhibition of SOCE is unlikely to be due to decreased expression of Orai1 and STIM1 (Wilson et al., 2014).

The present study, therefore, demonstrates a major role for PKC in the mechanism contributing to inhibition of SOCE in lipid-loaded liver cells. It is proposed that DAG and/or lipid droplets can activate PKC, which, in turn, leads to PKC-mediated phosphorylation (inhibition) of Orai1, thereby causing inhibition of SOCE in steatotic liver cells (schematically shown in Figure 7.1).

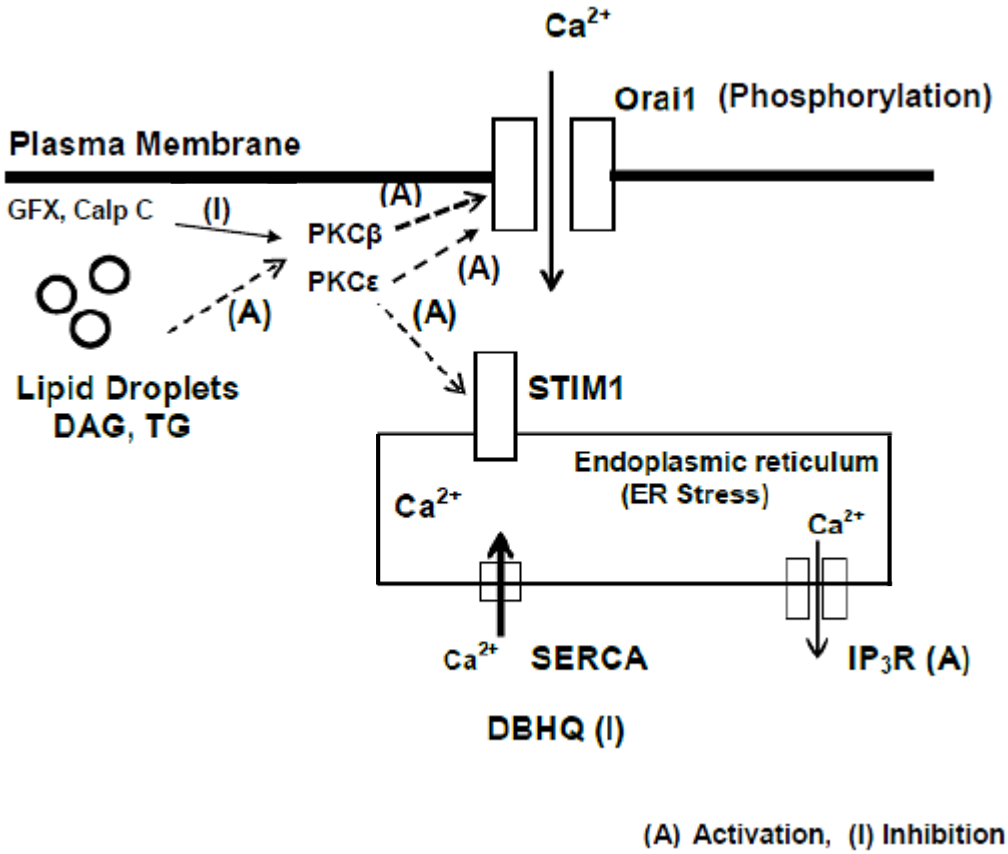

Fig. 7.1. A schematic representation of the proposed mechanism for inhibition of SOCE in steatotic liver cells. It is proposed that DAG and/or lipid droplets can activate PKC, which, in turn, leads to PKC-mediated phosphorylation (inhibition) of Orai1, causing inhibition of SOCE in steatotic liver cells. (A) denotes Activation and (I) denotes Inhibition. Adapted from (Kawasaki et al., 2010; Samuel et al., 2007).

7.3 Possible mechanism of exendin-4, a GLP1 agonist, to reverse impaired SOCE in steatotic hepatocytes

The results from the study (chapter five) demonstrated that the GLP-1 analogue exendin-4, reverses impaired SOCE almost completely in lipid-loaded immortalized and steatotic primary liver cells. While it has already been reported that exendin-4 can increase insulin sensitivity (Ahren and Pacini, 1999) and reverse hepatic steatosis by reducing lipid contents (Campbell and Drucker, 2013; Ding et al., 2006), one can possibly speculate that exendin-4 might defat the fatty liver cells first, and then may activate SOCE, conceivably via dephosphorylation of SOC components, in steatotic liver cells.

Likely mechanism(s) to reverse SOCE in lipid-loaded cells may involve exendin-4 activating store-operated Ca^{2+} entry in lipid-loaded liver cells by inhibiting one or more isoforms of PKC (pre-activated by DAG and/or lipid droplets), and/or by dephosphorylation of Orai1, and activation of Ca^{2+} entry through Orai1. In lipid-loaded liver cells, the action of exendin-4 to reverse impaired SOCE was shown to be associated with a reduced ER Ca^{2+} content. This reduction of ER Ca^{2+} may be due to an inhibition by exendin-4 of Ca^{2+} uptake by ER (through SERCA) – for which further investigation is needed. Moreover, since exendin-4 binds to GLP-1 receptors located on the plasma membrane of hepatocytes (Ding et al., 2006), it is possible that exendin-4-induced PKA may play a role in the up-regulation of STIM1 activity in the steatotic hepatocytes and subsequently may take part in the reversal of impaired SOCE in steatotic liver cells. Additionally, GLP-1 or exendin-4 has been shown to promote a continual increase in hepatocyte cAMP production which, in turn, can be associated with the induction of mRNA for both PPAR and AOX - that ultimately leads to reduction of lipid contents through the enhanced β-oxidation of fatty acids

(Ding et al., 2006). The resultant reduced lipid content may decrease the production of DAG which, in turn, leads to reduced number of active PKC. Consequently the PKC-induced phosphorylation of Orai1 can be suppressed, thereby, leading to enhanced activity of SOCE (Kawasaki et al., 2010). In addition, since the activity of Orai1 or STIM1 can be regulated by phosphorylation (Lang et al., 2013; Pozo-Guisado et al. 2013), PKA-mediated phosphorylation of Orai1 or STIM1 can also account for the observed reversal of inhibited SOCE in steatotic liver cells. As mentioned in subsection 7.6, further studies need to be done to provide the molecular mechanisms by which exendin-4 reverses lipid-induced SOCE inhibition in steatotic liver cells.

7.4 The mechanism by which inhibition (pharmacological or a siRNA strategy) of SOCE leads to further lipid accumulation

The given study (mentioned in chapter six) undertaken in this thesis was to investigate whether inhibition of SOCE has any effect on lipid accumulation in the cells. The results of this study provided, to our knowledge, the first evidence that impaired SOCE may induce further lipid accumulation in steatotic hepatocytes. The study by Park *et al.* suggested that in the liver of obese mice, SERCA2b expression and/or activity is considerably reduced (Park et al., 2010) which may, in turn, dysregulate ER Ca^{2+} homeostasis and subsequently lead to the ER stress response in steatotic hepatocytes. Disturbances to the re-filling of the ER may lead to a reduced ER Ca^{2+} content (Schroder, 2008) and this low ER Ca^{2+} content may have the propensity to increase triglyceride synthesis in the ER membrane (Fu et al. (2012). It has also been documented that reduced ER luminal Ca^{2+} is associated with saturated fatty acid-mediated ER stress (Wei et al., 2009). Additionally, an increased ER stress response may activate some lipogenesis programmes in the cytosol, which may in

turn supply free fatty acids for further DAG and TAG synthesis in the ER membrane (Antherieu et al., 2011; Fu et al., 2012; Mekahli et al., 2011). A low ER Ca^{2+}-initiated ER stress response stimulates the synthesis of DAG and TAG (Baumbach et al., 2014; Park et al., 2010) utilizing those excess fatty acids which ultimately causes enhanced lipid accumulation in the cytoplasmic space. The resultant increased DAGs, being translocated to the plasma membrane, may activate PKCs causing, therefore, subsequent inhibition of SOCE. These different inter-linked 'non-flexible' pathways could be cycled again to enhance the rate of lipid accumulation in the steatotic hepatocyte. As such, with an indication of a causative relationship between Ca^{2+} influx and lipid accumulation, these results also may suggest that SOCE may be a potential regulator of intracellular lipid synthesis in liver cells. Figure 7.2 schematically shows how DAGs and lipid droplets can be synthesized under the experimental conditions of liver cell culture in the presence of palmitate or amiodarone.

The present results have also shown that in the absence of amiodarone or palmitate to promote lipid accumulation, there is no additional lipid accumulation when SOCE is inhibited. However when there is a supply of lipids (increased endogenous synthesis or increased substrate) the inhibition of SOCE activates lipid accumulation. The situation is most likely associated with the conditions (addition of amiodarone or palmitate) which promote the synthesis of TAGs, DAGs and the accumulation of lipid droplets.

In addition, the mechanism by which inhibition of SOCE enhances lipid accumulation in liver cells in the presence of amiodarone or palmitate has been

proposed in figure 7.3. The detailed processes that might be involved in the mechanism of inhibition of SOCE and further lipid accumulation are summarised in the legend of figure 7.3.

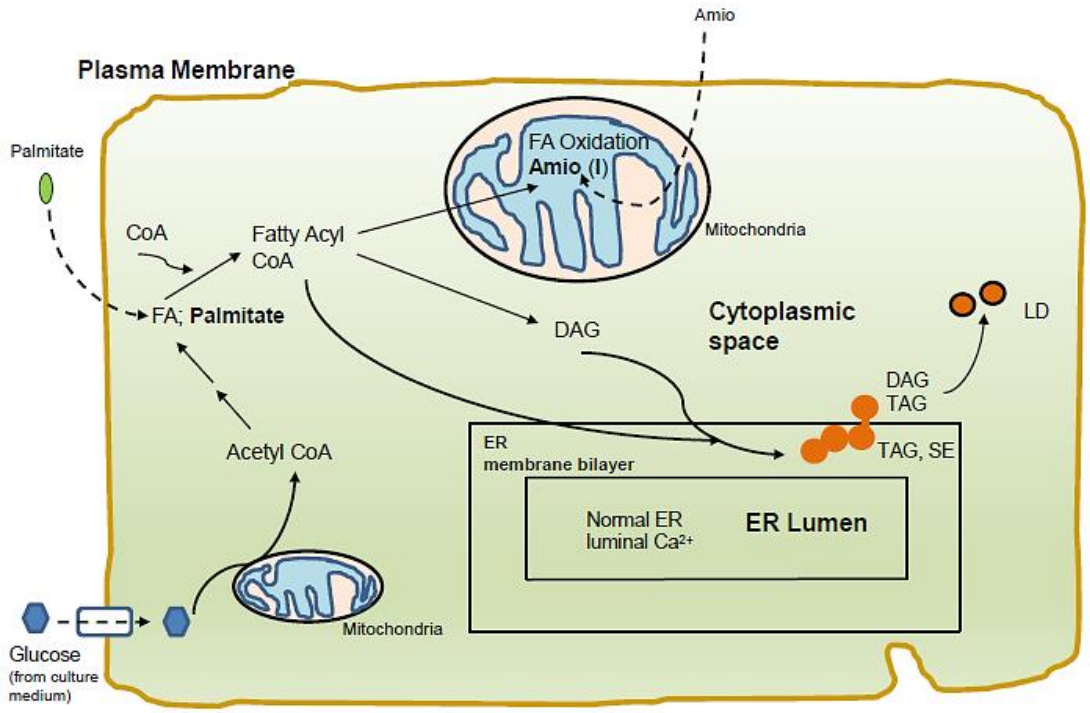

Fig. 7.2. A schematic representation of the formation of lipid droplets in normal hepatocytes when there is a driving force (e.g., acetyl CoA, amiodarone or palmitate) for lipid synthesis. It is proposed that amiodarone inhibits (indicated by (I) in figure) fatty acid oxidation in the mitochondria (Fromenty et al., 1990), which, in turn, results in increased availability of fatty acids in the cytoplasmic space. These resulting fatty acids and other fatty acids (derived from glucose in the culture medium) can be substrates for the synthesis of DAG, TAG or lipid droplets at the ER membrane (Fu et al., 2012; Jornayvaz and Shulman, 2012), and subsequently lipid droplets accumulate in the cytoplasmic space. When palmitate is used as an extracellular source of fatty acids for lipid synthesis, DAGs and/or cytoplasmic lipid droplets originate from ER membrane in response to an excess of palmitate and other fatty acids (e.g., derived from glucose) (Brasaemle and Wolins, 2012). (I) denotes Inhibition. SE, sterol esters; FA, fatty acid; LD, lipid droplets; DAG, diacylglycerol; TAG, triacylglycerol; Amio, amiodarone.

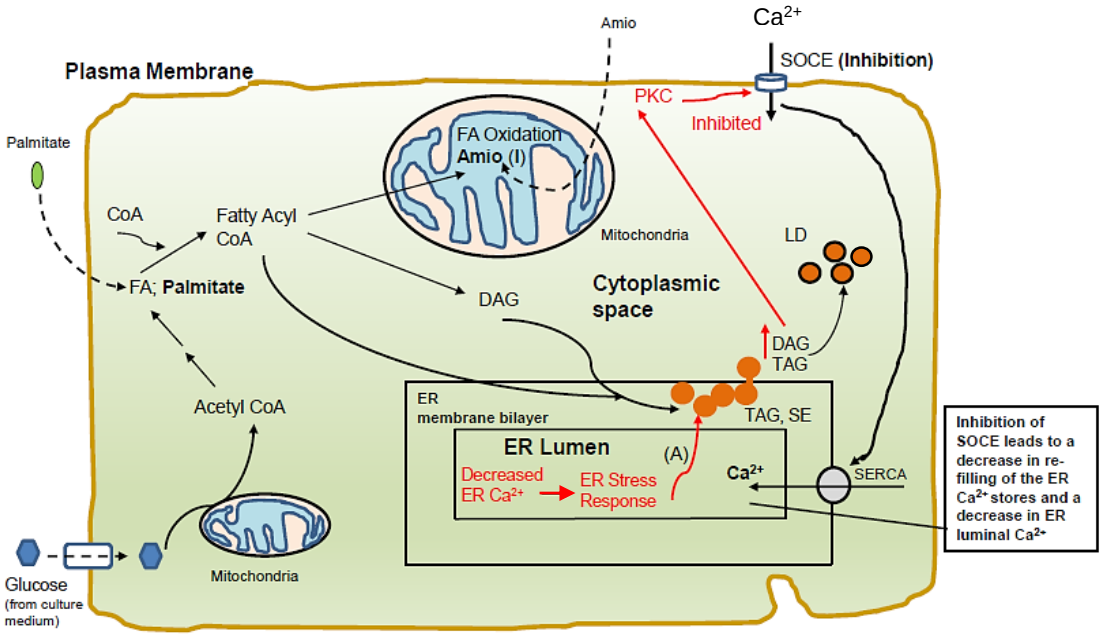

Fig. 7.3. A schematic representation of the proposed mechanism by which inhibition of SOCE leads to enhanced lipid accumulation in hepatocytes in the presence of amiodarone or palmitate. It is proposed that inhibition of SOCE leads to a decrease in re-filling of the ER Ca^{2+} stores and a decrease in ER luminal Ca^{2+}. Amiodarone inhibits fatty acid oxidation in mitochondria (Fromenty et al., 1990), which, in turn, increases fatty acid availability in the cytoplasmic space. These excess fatty acids can be utilized in the synthesis of DAG, TAG at the ER membrane (Fu et al., 2012; Jornayvaz and Shulman, 2012). Low ER Ca^{2+}-initiated ER stress response stimulates the synthesis DAG and TAG (Baumbach et al., 2014; Park et al., 2010) utilizing those excess fatty acids which ultimately causes enhanced lipid accumulation in the cytoplasmic space. When palmitate is used as an extracellular source of fatty acids for lipid synthesis, an excess of palmitate and other fatty acids (e.g., derived from glucose) is thought to be available in the ER membrane. As stated above, low ER Ca^{2+}-initiated ER stress response stimulates the synthesis of DAG and TAG (Brasaemle and Wolins, 2012; Mekahli et al., 2011) utilizing those excess fatty acids and palmitate, which ultimately causes enhanced lipid accumulation in the cytoplasmic space. Increased amount of DAG activates PKC (Jornayvaz and Shulman, 2012; Perry et al., 2014) which, in turn, inhibits SOCE through Orai1 phosphorylation (Kawasaki et al., 2010). Activation (A) and inhibition (I) indicated by the solid lines. SE, sterol esters; FA, fatty acid; LD, lipid droplets; DAG, diacylglycerol; TAG, triacylglycerol.

7.5 Pathological consequences for lipid accumulation, and insulin resistance of inhibition of SOCE

There is a substantial body of evidence to suggest that excessive lipid accumulation and endoplasmic reticulum stress response are the critical factors for the development of insulin resistance and type 2 diabetes (Jornayvaz and Shulman, 2012; Samuel et al., 2004; Schroder, 2008; Shulman, 2000). Alterations in hepatocyte intracellular Ca^{2+} signalling caused by lipid accumulation or abnormal lipid metabolism may be involved in the transition from NAFLD to hepatic insulin resistance (Fu et al., 2011). Optimal intracellular Ca^{2+} levels in hepatocytes regulate the synthesis and posttranslational modification of key intracellular signalling proteins involved in insulin pathways. Therefore, the homeostasis of intracellular Ca^{2+} is crucial to the proper function of insulin and other Ca^{2+} dependent pathways. Decreased store-operated Ca^{2+} entry to steatotic hepatocytes through SOCs may alter the intracellular Ca^{2+} dependent insulin signalling pathway, and ultimately develop hepatic insulin resistance. The following figure 7.4 shows how inhibited SOCE in steatotic hepatocyte may be a possible step in the development of hepatic insulin resistance.

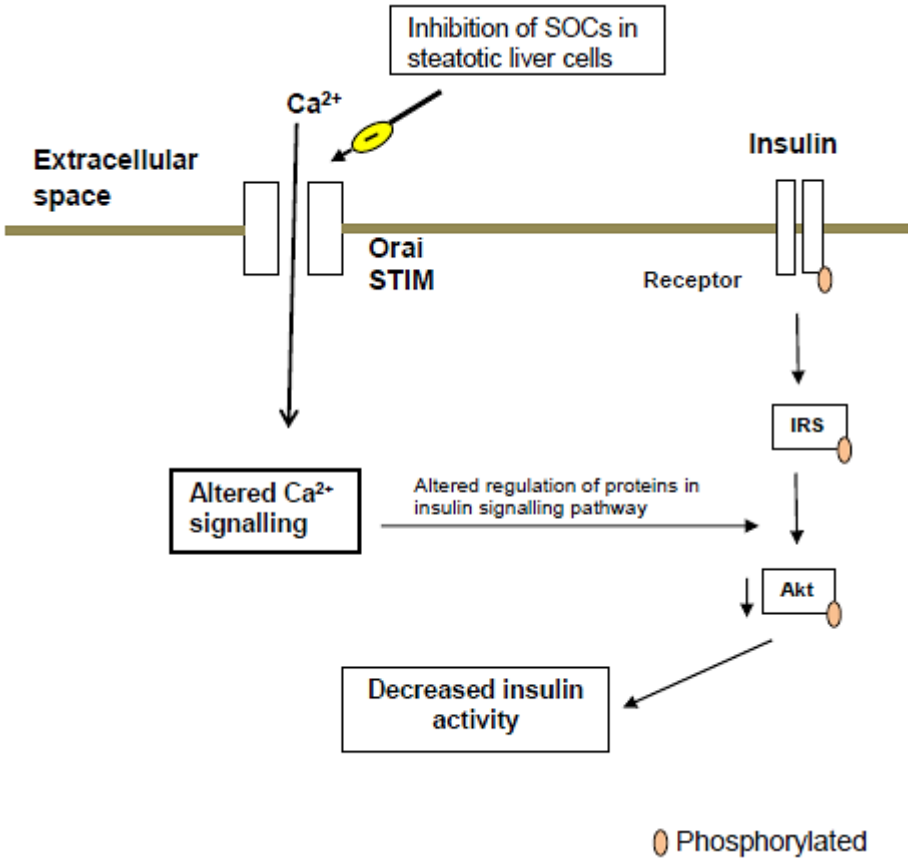

Fig. 7.4. Decreased Ca^{2+} entry to steatotic hepatocytes through SOCs: a possible step in the development of insulin resistance. It is proposed that the accumulation of diacylglycerol and lipid droplets in the liver leads to the activation of protein kinase Cε (PKCε), which subsequently inhibits the insulin receptor kinase (Jornayvaz and Shulman, 2012; Nakamura et al, 2009). In addition, altered intracellular Ca^{2+} signaling initiated by inhibition of SOCE in steatotic liver cells may alter the regulation of key proteins involved in insulin signaling pathways – and ultimately may decrease the insulin activity.

The effect of lipid accumulation in hepatocytes in response to different hormones may be a complex pathological event. The present results provided the evidence that lipid-induced impaired SOCE may be associated with a considerable decrease in the magnitude of hormone induced intracellular Ca^{2+} signaling. Cytoplasmic Ca^{2+} signalling initiated by hormones plays a critical role in hepatic glycogen hydrolysis or hepatic glucose release into the blood. The evidence from the present study shows that lipid accumulation in hepatocytes may contribute to the reduced hormone-initiated hepatic glucose release. Hormone-induced glucose release also can be impaired when intercellular communication via gap junctions is impaired in hepatocytes (Eugenin et al., 1998). While it seems to be a paradox in the case of hepatic type 2 diabetes, the answer to this puzzle might be that in amiodarone induced lipid loaded H4IIE cells, the phosphorylase *a* level and/or liver glycogen amount possibly has been decreased (Lavoie and van de Werve, 1991) or the steatotic H4IIE cell may have reduced Foxo-1 activity causing impaired regulation of hepatic glucose production (Matsumoto et al., 2007). As the hormone-induced glucose release in liver cells can be partly associated with intracellular communication via gap junctions (Nathanson et al., 1999), altered gap junctions in cultured lipid-loaded H4IIE cells may, in part, explain the paradox.

7.6 Future directions

In summary, the results from the studies of this thesis provide novel information regarding the regulatory properties of SOCE in liver lipid synthesis and the effects of a GLP-1 analogue on impaired SOCE in steatotic liver cells. Several important questions remain that can be addressed by future work.

7.6.1. Future experiments to investigate whether lipid-induced inhibition of SOCE in liver cells is dependent on the phosphorylation of Orai1 by PKC

The observation that impaired SOCE was reversed in steatotic liver cells by an inhibitor of PKC may raise the possibility that PKC acts as an important and potential target for the improvement of the altered SOCE in steatotic liver cells. To assess whether Orai1 is phosphorylated by PKC in lipid-loaded cells, extracts of lipid-loaded (incubated in the presence of palmitate) and control H4IIE liver cells, or of hepatocytes isolated from obese or lean Zucker rats can be prepared. Orai1 can be immunoprecipitated using an anti-Orai1 antibody. The total amount of phosphoserine phosphopeptide in each immunoprecipitate can be measured by immunoblotting with an anti-phosphoserine antibody. Phosphorylated Orai1 peptides can be identified and quantified by trypsin digestion and LC-MS/MS. The isoform(s) of PKC involved can be determined using siRNA targeted to a given PKC isoform to knock down that PKC isoform. The degree of knockdown efficiency of the PKC isoform being investigated can be assessed by qPCR. The effects of the PKC knockdown can be assessed by measuring SOCE (activated by DBHQ) and Orai1 phosphorylation.

7.6.2 Future experiments to investigate whether the inhibition of SOCE in liver cells enhances the development of insulin resistance

Since the inhibition of SOCE in liver cells may enhance lipid accumulation, a critical factor of insulin resistance, future experiments can be done to determine whether inhibited SOCE in liver cells enhances the development of insulin resistance. To evaluate whether the inhibition of SOCE in liver cells enhances the development of insulin resistance, *in vitro* cell models can be used. Primary cultures of hepatocytes isolated from lean rats or cultures of H4IIE rat liver cells can be incubated with an inhibitor of SOCE, or STIM1 and Orai1 can be knocked down with siRNA

(expression of knockdown mRNA encoding STIM1 and/or Orai1 can be measured by qPCR and subsequently knockdown protein level can be determined by western blotting), to mimic the inhibition of SOCE induced by lipid, and insulin resistance can be measured. Inhibitors of SOCE such as 2-APB and BTP2 can be tested. Insulin resistance can be assessed by measuring the ability of insulin to alter the degree of phosphorylation of downstream targets of insulin, IRS2 (tyrosine), Akt (serine).

7.6.3 Future experiments to investigate whether exendin-4 shows PKA-dependent regulation of STIM1 and reduces the rate of lipid accumulation and the development of insulin resistance in liver cells

Experiments can be done to investigate whether exendin-4 reverses impaired Ca^{2+} entry in steatotic liver cells via the PKA-dependent regulation of STIM1. The hepatocytes can be infected with adenovirus encoding STIM1-YFP. Using confocal and TIRF imaging, the translocation of STIM1-YFP (induced by cAMP) from the ER to the PM in hepatocytes can be detected and measured as described by Tian et al (2012). Using the specific PKA agonist e.g., N6-phenyladenosine-3′,5′-cyclic monophosphate or PKA activator (e.g., Sp-8-CPT-cAMPS), STIM1-YFP translocation towards the PM can be further induced in hepatocytes. PKA-induced-STIM1-translocation in hepatocytes pre-incubated with exendin-4 can be compared with PKA-induced-STIM1-translocation in non-treated control hepatocytes (Tian et al., 2012). Moreover, experiments can be designed to investigate whether exendin-4 reduces the rate of lipid accumulation and the development of insulin resistance in liver cells by inhibiting the PKC-mediated phosphorylation of Orai1, and activating SOCE. In lipid-loaded and control cells, the effects of exendin-4 on the phosphorylation of Orai1, SOCE, lipid accumulation, and insulin resistance can be assessed as described above. After incubation of lipid-loaded cells or hepatocytes

isolated from obese Zucker rats with exendin-4 for 24 hours, the effect of exendin-4 on insulin resistant liver cells can be determined.

Future studies to elucidate the intracellular mechanisms could include measurement of store-operated Ca^{2+} entry in H4IIE liver cells treated with siRNA against STIM1/Orai1 and subsequently loaded with palmitate- or amiodarone-induced intracellular lipid. In the future experiments, it is also worth exploring whether the GLP-1 analogue can reverse the impaired hormone generated intracellular Ca^{2+} signals in fatty liver cells. Such information will also provide evidence for the development of more effective, more specific anti-obesity or antidiabetic agents in future.

7.7 General conclusions

The results of this thesis provide evidence that steatosis leads to substantial inhibition of store-operated Ca^{2+} entry through a mechanism involving the activation of one or more isoforms of protein kinase C. The inhibition (pharmacological or siRNA) of store-operated Ca^{2+} entry enhances the rate of the accumulation of intracellular lipids suggesting that the inhibition of SOCE may contribute to the further accumulation of lipids and the development of non-alcoholic steatohepatitis and insulin resistance. In addition, the observation that the lipid-induced inhibition of SOCE is reversed by the antidiabetic drug exendin-4 may point to a new site of action for this drug.

APPENDICES

I. Publications arising from this thesis

Wilson, C. H.[*], Ali, E. S.[*], Scrimgour, N., Martin, A., Hua, J., Tallis, G. A., Rychkov, G. Y. and Barritt, G. J. (2014) Steatosis inhibits liver cell store-operated Ca^{2+} entry and reduces ER Ca^{2+} through a protein kinase C dependent mechanism., *Biochemical Journal* Immediate Publication, doi:10.1042/BJ20140881 [* Equal first-authors].

II. Presentations in scientific congresses as a result of PhD studies

Ali, E., Wilson, C., Tam, K. C., Rychkov, G. and Barritt, G. J. Protein kinase C mediates the inhibition of store-operated Ca^{2+} entry initiated by steatosis in hepatocytes. Oral presentation at the Australian Society for Medical Research Scientific Meeting, Adelaide, Oral-012, p. 58. (June 2013).

Ali, E., Wilson, C. H., Scrimgeour, N. R., Martin, A., Rychkov, G. Y. and Barritt, G. J. Evidence for a role for protein kinase C in impaired store operated Ca^{2+} entry in steatotic liver cells. poster presented at the ASBMB (Australia) organized ComBio2012 Conference, Adelaide, Australia. POS-MON-038, p. 108. (September 2012).

Wilson, C.H., Ali, E. S., Scrimgeour, N., Martin, A., Rychkov, G.Y. and Barritt, G.J. Impaired store-operated Ca^{2+} entry in lipid-loaded liver cells. poster presented at 4th International Congress on Cell Membrane and Oxidative Stress: Focus on Calcium Signaling and TRP channels, Isparta, Turkey (June 26-29, 2012).

Ali, E., Martin, A., Wilson, C., Rychkov, G. and Barritt, G.J. Lipid accumulation in liver cells causes a substantial decrease in store-operated Ca^{2+} entry, poster presented at the Australian Society for Medical Research, SA Scientific Meeting, Adelaide Convention Centre, Australia. POS-048, p.163 (June 2012).

III. Awards during PhD studies

International Postgraduate Research Scholarship (IPRS) (2010). Australian Government and Flinders University scholarship to support PhD studies at Flinders University, Adelaide, Australia.

REFERENCES

Abcam (2014). Counting cells using a heaemocytometer. http://www.abcam.com/index.html?pageconfig=resource&rid=11454, accessed on 10 June 2014.

Abdel-Misih, S.R., and Bloomston, M. (2010). Liver anatomy. The Surgical clinics of North America *90*, 643-653.

Abramian, A.M., Comenencia-Ortiz, E., Modgil, A., Vien, T.N., Nakamura, Y., Moore, Y.E., Maguire, J.L., Terunuma, M., Davies, P.A., and Moss, S.J. (2014). Neurosteroids promote phosphorylation and membrane insertion of extrasynaptic GABAA receptors. Proceedings of the National Academy of Sciences of the United States of America *111*, 7132-7137.

Ahren, B., and Pacini, G. (1999). Dose-related effects of GLP-1 on insulin secretion, insulin sensitivity, and glucose effectiveness in mice. The American journal of physiology *277*, E996-E1004.

Amaya, M.J., and Nathanson, M.H. (2013). Calcium signaling in the liver. Comprehensive Physiology *3*, 515-539.

Anderson, K.A., Lin, F., Ribar, T.J., Stevens, R.D., Muehlbauer, M.J., Newgard, C.B., and Means, A.R. (2012). Deletion of CaMKK2 from the liver lowers blood glucose and improves whole-body glucose tolerance in the mouse. Molecular endocrinology *26*, 281-291.

Anderson, N., and Borlak, J. (2006). Drug-induced phospholipidosis. FEBS letters *580*, 5533-5540.

Antherieu, S., Rogue, A., Fromenty, B., Guillouzo, A., and Robin, M.A. (2011). Induction of vesicular steatosis by amiodarone and tetracycline is associated with up-regulation of lipogenic genes in HepaRG cells. Hepatology *53*, 1895-1905.

Aromataris, E.C., Castro, J., Rychkov, G.Y., and Barritt, G.J. (2008). Store-operated Ca(2+) channels and Stromal Interaction Molecule 1 (STIM1) are targets for the actions of bile acids on liver cells. Biochimica et biophysica acta *1783*, 874-885.

Aromataris, E.C., Roberts, M.L., Barritt, G.J., and Rychkov, G.Y. (2006). Glucagon activates Ca2+ and Cl- channels in rat hepatocytes. The Journal of physiology *573*, 611-625.

Arsov, T., Silva, D.G., O'Bryan, M.K., Sainsbury, A., Lee, N.J., Kennedy, C., Manji, S.S., Nelms, K., Liu, C., Vinuesa, C.G., de Kretser, D.M., Goodnow, C.C., Petrovsky, N. (2006) Fat aussie--a new Alström syndrome mouse showing a critical

role for ALMS1 in obesity, diabetes, and spermatogenesis. Molecular Endocrinology. *20*:1610-22

Angulo, P. (2002). Nonalcoholic fatty liver disease. N Engl J Med *346*, 1221-1231.

Anstee, Q.M., Targher, G., and Day, C.P. (2013). Progression of NAFLD to diabetes mellitus, cardiovascular disease or cirrhosis. Nature reviews. Gastroenterology & hepatology *10*, 330-344.

Antherieu, S., Rogue, A., Fromenty, B., Guillouzo, A., and Robin, M.A. (2011). Induction of vesicular steatosis by amiodarone and tetracycline is associated with up-regulation of lipogenic genes in HepaRG cells. Hepatology *53*, 1895-1905.

Bailey, C.J. (2007). Treating insulin resistance: future prospects. Diabetes & vascular disease research : official journal of the International Society of Diabetes and Vascular Disease *4*, 20-31.

Barritt, G.J., Chen, J., and Rychkov, G.Y. (2008). Ca(2+) -permeable channels in the hepatocyte plasma membrane and their roles in hepatocyte physiology. Biochimica et biophysica acta *1783*, 651-672.

Barritt, G.J., and Whiting, J.A. (1983). Exogenous phospholipase enzymes mimic effects of phenylephrine on Ca2+ transport in hepatocytes. The Biochemical journal *210*, 115-119.

Basseri, S., and Austin, R.C. (2012). Endoplasmic reticulum stress and lipid metabolism: mechanisms and therapeutic potential. Biochemistry research international *2012*, 841362.

Baumbach, J., Hummel, P., Bickmeyer, I., Kowalczyk, K.M., Frank, M., Knorr, K., Hildebrandt, A., Riedel, D., Jackle, H., and Kuhnlein, R.P. (2014). A Drosophila in vivo screen identifies store-operated calcium entry as a key regulator of adiposity. Cell metabolism *19*, 331-343.

Bear, C.E. (1990). A nonselective cation channel in rat liver cells is activated by membrane stretch. The American journal of physiology *258*, C421-428.

Bear, C.E., and Li, C.H. (1991). Calcium-permeable channels in rat hepatoma cells are activated by extracellular nucleotides. The American journal of physiology *261*, C1018-1024.

Bechmann, L.P., Hannivoort, R.A., Gerken, G., Hotamisligil, G.S., Trauner, M., and Canbay, A. (2012). The interaction of hepatic lipid and glucose metabolism in liver diseases. Journal of hepatology *56*, 952-964.

Begriche, K., Igoudjil, A., Pessayre, D., and Fromenty, B. (2006). Mitochondrial dysfunction in NASH: causes, consequences and possible means to prevent it. Mitochondrion *6*, 1-28.

Berridge, M.J. (2002). The endoplasmic reticulum: a multifunctional signaling organelle. Cell calcium *32*, 235-249.

Berridge, M.J., Bootman, M.D., and Roderick, H.L. (2003). Calcium signalling: dynamics, homeostasis and remodelling. Nat Rev Mol Cell Biol *4*, 517-529.

Beuers, U., Irmelin, P., Soroka, C., Boyer, J., Kullak-Ublick, G. And Paumgartner, G. (1999) Modulation of protein kinase C by taurolithocholic acid in isolated rat hepatocytes. Hepatology, *29*:477-82.

Bhattacharya, S., Dey, D., and Roy, S.S. (2007). Molecular mechanism of insulin resistance. J Biosci *32*, 405-413.

Bird, G.S., DeHaven, W.I., Smyth, J.T., and Putney, J.W., Jr. (2008). Methods for studying store-operated calcium entry. Methods *46*, 204-212.

Bird, G.S., Takahashi, M., Tanzawa, K., and Putney, J.W., Jr. (1999). Adenophostin A induces spatially restricted calcium signaling in Xenopus laevis oocytes. The Journal of biological chemistry *274*, 20643-20649.

Blackmore, P.F., Strickland, W.G., Bocckino, S.B., and Exton, J.H. (1986). Mechanism of hepatic glycogen synthase inactivation induced by Ca2+-mobilizing hormones. Studies using phospholipase C and phorbol myristate acetate. The Biochemical journal *237*, 235-242.

Blouin, A., Bolender, R.P., and Weibel, E.R. (1977). Distribution of organelles and membranes between hepatocytes and nonhepatocytes in the rat liver parenchyma. A stereological study. The Journal of cell biology *72*, 441-455.

Boden, G., and Shulman, G.I. (2002). Free fatty acids in obesity and type 2 diabetes: defining their role in the development of insulin resistance and beta-cell dysfunction. European journal of clinical investigation *32 Suppl 3*, 14-23.

Bolt, M.W., Card, J.W., Racz, W.J., Brien, J.F., and Massey, T.E. (2001). Disruption of mitochondrial function and cellular ATP levels by amiodarone and N-desethylamiodarone in initiation of amiodarone-induced pulmonary cytotoxicity. The Journal of pharmacology and experimental therapeutics *298*, 1280-1289.

Bootman, M.D., Collins, T.J., Mackenzie, L., Roderick, H.L., Berridge, M.J., and Peppiatt, C.M. (2002). 2-aminoethoxydiphenyl borate (2-APB) is a reliable blocker of store-operated Ca2+ entry but an inconsistent inhibitor of InsP3-induced Ca2+ release. FASEB journal : official publication of the Federation of American Societies for Experimental Biology *16*, 1145-1150.

Bootman, M.D., Rietdorf, K., Collins, T., Walker, S., and Sanderson, M. (2013). Ca2+-sensitive fluorescent dyes and intracellular Ca2+ imaging. Cold Spring Harbor protocols *2013*, 83-99.

Brasaemle, D.L., and Wolins, N.E. (2012). Packaging of fat: an evolving model of lipid droplet assembly and expansion. The Journal of biological chemistry *287*, 2273-2279.

Brick-Ghannam, C., Huang,F., Temime, N., and Charron, D. (1991) Protein Kinase C (PKC) Activation via Human Leucocyte Antigen Class I1 Molecules, The Journal of Biological Chemistry, *266*: 24169-75.

Brookheart, R.T., Michel, C.I., and Schaffer, J.E. (2009). As a matter of fat. Cell metabolism *10*, 9-12.

Buque, X., Martinez, M.J., Cano, A., Miquilena-Colina, M.E., Garcia-Monzon, C., Aspichueta, P., and Ochoa, B. (2010). A subset of dysregulated metabolic and survival genes is associated with severity of hepatic steatosis in obese Zucker rats. Journal of lipid research *51*, 500-513.

Burcelin, R. (2014). The antidiabetic gutsy role of metformin uncovered? Gut *63*, 706-707.

Campbell, J.E., and Drucker, D.J. (2013). Pharmacology, physiology, and mechanisms of incretin hormone action. Cell metabolism *17*, 819-837.

Canbay, A., Bechmann, L., and Gerken, G. (2007). Lipid metabolism in the liver. Zeitschrift fur Gastroenterologie *45*, 35-41.

Capiod, T. (1998). ATP-activated cation currents in single guinea-pig hepatocytes. The Journal of physiology *507 (Pt 3)*, 795-805.

Cardoso, A.R., Kakimoto, P.A., and Kowaltowski, A.J. (2013). Diet-sensitive sources of reactive oxygen species in liver mitochondria: role of very long chain acyl-CoA dehydrogenases. PloS one *8*, e77088.

Castro, J. (2008). "Store operated Ca^{2+} channels in liver cells: regulation by bile acids and a sub-region of the endoplasmic reticulum." Ph.D. Thesis, Department of Medical Biochemistry, Flinders University.

Castro, J., Aromataris, E.C., Rychkov, G.Y., and Barritt, G.J. (2009). A small component of the endoplasmic reticulum is required for store-operated Ca2+ channel activation in liver cells: evidence from studies using TRPV1 and taurodeoxycholic acid. The Biochemical journal *418*, 553-566.

Chen, K., Yu, X., Murao, K., Imachi, H., Li, J., Muraoka, T., Masugata, H., Zhang, G.X., Kobayashi, R., Ishida, T., *et al.* (2011). Exendin-4 regulates GLUT2 expression via the CaMKK/CaMKIV pathway in a pancreatic beta-cell line. Metabolism: clinical and experimental *60*, 579-585.

Chen, L.W., and Jan, C.R. (2000). Mechanisms underlying ATP-induced Ca2+ mobilization in human neutrophils. Shock *14*, 509-513.

Christopher M. R. and Chen, X. (1998) The buffer barrier hypothesis, [Ca2+] homogeneity, and sarcoplasmic reticulum function in swine carotid artery. Journal of Physiology *513*, 477-492.

Conn, P.M. (2012). Imaging and spectroscopic analysis of living cells: live cell imaging of cellular elements and functions. (Elsevier Science).

Dardevet, D., Moore, M.C., Neal, D., DiCostanzo, C.A., Snead, W., and Cherrington, A.D. (2004). Insulin-independent effects of GLP-1 on canine liver

glucose metabolism: duration of infusion and involvement of hepatoportal region. American journal of physiology. Endocrinology and metabolism *287*, E75-81.

Darlington, G.J. (1987). Liver cell lines. Methods in Enzymology *151*, 19-38.

DeHaven, W.I., Smyth, J.T., Boyles, R.R., and Putney, J.W., Jr. (2007). Calcium inhibition and calcium potentiation of Orai1, Orai2, and Orai3 calcium release-activated calcium channels. The Journal of biological chemistry *282*, 17548-17556.

Desmet, V.J. (1994). Organizationl principles. In The liver biology and pathology, I.M.e.a. Arias, ed. (New York: Raven Press).

DeWitt, L.M., and Putney, J.W., Jr. (1983). Stimulation of glycogenolysis in hepatocytes by angiotensin II may involve both calcium release and calcium influx. FEBS letters *160*, 259-263.

Di Capite, J., Ng, S.W., and Parekh, A.B. (2009). Decoding of cytoplasmic Ca(2+) oscillations through the spatial signature drives gene expression. Current biology : CB *19*, 853-858.

Ding, X., Saxena, N.K., Lin, S., Gupta, N.A., and Anania, F.A. (2006). Exendin-4, a glucagon-like protein-1 (GLP-1) receptor agonist, reverses hepatic steatosis in ob/ob mice. Hepatology *43*, 173-181.

Dionisio, N., Garcia-Mediavilla, M.V., Sanchez-Campos, S., Majano, P.L., Benedicto, I., Rosado, J.A., Salido, G.M., and Gonzalez-Gallego, J. (2009). Hepatitis C virus NS5A and core proteins induce oxidative stress-mediated calcium signalling alterations in hepatocytes. Journal of hepatology *50*, 872-882.

Diver, J.M., Sage, S.O., and Rosado, J.A. (2001). The inositol trisphosphate receptor antagonist 2-aminoethoxydiphenylborate (2-APB) blocks Ca2+ entry channels in human platelets: cautions for its use in studying Ca2+ influx. Cell calcium *30*, 323-329.

Domenech, M., Lopez-Soriano, F.J., and Argiles, J.M. (1993). Alanine as a lipogenic precursor in isolated hepatocytes from obese Zucker rats. Cellular and molecular biology *39*, 693-699.

Dunn, J. S., H. L. Sheehan, et al. (1943). "Necrosis of islets of Langerhans." Lancet **1**:484–487

Enfissi, A., Prigent, S., Colosetti, P., and Capiod, T. (2004). The blocking of capacitative calcium entry by 2-aminoethyl diphenylborate (2-APB) and carboxyamidotriazole (CAI) inhibits proliferation in Hep G2 and Huh-7 human hepatoma cells. Cell calcium *36*, 459-467.

Eugenin, E.A., Gonzalez, H., Saez, C.G., and Saez, J.C. (1998). Gap junctional communication coordinates vasopressin-induced glycogenolysis in rat hepatocytes. The American journal of physiology *274*, G1109-1116.

Exton, J.H. (1987). Mechanisms of hormonal regulation of hepatic glucose metabolism. Diabetes/metabolism reviews *3*, 163-183.

Exton, J.H., Blackmore, P.F., El-Refai, M.F., Dehaye, J.P., Strickland, W.G., Cherrington, A.D., Chan, T.M., Assimacopoulos-Jeannet, F.D., and Chrisman, T.D. (1981). Mechanisms of hormonal regulation of liver metabolism. Advances in cyclic nucleotide research *14*, 491-505.

Flock, G., Laurie L. B., Christine, L. and Daniel J. D. (2007) The incretin receptors for GLP-1 and GIP are essential for the sustained metabolic actions of vildagliptin in mice. Diabetes *56*, 3006-13.

Fowler, S.D., and Greenspan, P. (1985). Application of Nile red, a fluorescent hydrophobic probe, for the detection of neutral lipid deposits in tissue sections: comparison with oil red O. The journal of histochemistry and cytochemistry : official journal of the Histochemistry Society *33*, 833-836.

Fromenty, B., Fisch, C., Labbe, G., Degott, C., Deschamps, D., Berson, A., Letteron, P., and Pessayre, D. (1990). Amiodarone inhibits the mitochondrial beta-oxidation of fatty acids and produces microvesicular steatosis of the liver in mice. The Journal of pharmacology and experimental therapeutics *255*, 1371-1376.

Fromenty, B., Fisch, C., Berson, A., Letteron, P., Larrey, D., and Pessayre, D. (1990). Dual effect of amiodarone on mitochondrial respiration. Initial protonophoric uncoupling effect followed by inhibition of the respiratory chain at the levels of complex I and complex II. The Journal of pharmacology and experimental therapeutics *255*, 1377-1384.

Fromenty, B., Robin, M.A., Igoudjil, A., Mansouri, A., and Pessayre, D. (2004). The ins and outs of mitochondrial dysfunction in NASH. Diabetes & metabolism *30*, 121-138.

Fu, S., Watkins, S.M., and Hotamisligil, G.S. (2012). The role of endoplasmic reticulum in hepatic lipid homeostasis and stress signaling. Cell metabolism *15*, 623-634.

Fu, S., Yang, L., Li, P., Hofmann, O., Dicker, L., Hide, W., Lin, X., Watkins, S.M., Ivanov, A.R., and Hotamisligil, G.S. (2011). Aberrant lipid metabolism disrupts calcium homeostasis causing liver endoplasmic reticulum stress in obesity. Nature *473*, 528-531.

Gallwitz, B. (2011). Glucagon-like peptide-1 analogues for Type 2 diabetes mellitus: current and emerging agents. Drugs *71*, 1675-1688.

Ganguly, J. (1960). Studies on the mechanism of fatty acid synthesis. VII. Biosynthesis of fatty acids from malonyl CoA. Biochim Biophys Acta *40*, 110-118.

Ganong, W.F. (1995). Regulation of gastrointestinal function., 17th edn (Connecticut: Appleton & Lange).

Gardner, J.P., Balasubramanyam, M., and Studzinski, G.P. (1997). Up-regulation of Ca2+ influx mediated by store-operated channels in HL60 cells induced to differentiate by 1 alpha,25-dihydroxyvitamin D3. Journal of cellular physiology *172*, 284-295.

Gaspers, L.D., and Thomas, A.P. (2005). Calcium signaling in liver. Cell calcium *38*, 329-342.

Gilbert, M., Magnan, C., Turban, S., Andre, J., and Guerre-Millo, M. (2003). Leptin receptor-deficient obese Zucker rats reduce their food intake in response to a systemic supply of calories from glucose. Diabetes *52*, 277-282.

GraphPad Prism (2014) What are Dose-response curves. http://www.graphpad.com/guides/prism/6/curve-fitting/index.htm?dose_response___special.htm. Accessed on: 23 Dec 2014.

Greenspan, P., Mayer, E.P., and Fowler, S.D. (1985). Nile red: a selective fluorescent stain for intracellular lipid droplets. The Journal of cell biology 100, 965-973.

Greene, M.W., Burrington, C.M., Ruhoff, M.S., Johnson, A.K., Chongkrairatanakul, T., and Kangwanpornsiri, A. (2010a). PKC{delta} is activated in a dietary model of steatohepatitis and regulates endoplasmic reticulum stress and cell death. Journal of Biological Chemistry *285*, 42115-42129.

Gregory, R.B., Hughes, R., and Barritt, G.J. (2004). Induction of cholestasis in the perfused rat liver by 2-aminoethyl diphenylborate, an inhibitor of the hepatocyte plasma membrane Ca2+ channels. Journal of gastroenterology and hepatology *19*, 1128-1134.

Grynkiewicz, G., Poenie, M., and Tsien, R.Y. (1985). A new generation of Ca2+ indicators with greatly improved fluorescence properties. Journal of Biological Chemistry *260*, 3440-3450.

Gu, C., and Cooper, D.M. (2000). Ca(2+), Sr(2+), and Ba(2+) identify distinct regulatory sites on adenylyl cyclase (AC) types VI and VIII and consolidate the apposition of capacitative cation entry channels and Ca(2+)-sensitive ACs. The Journal of biological chemistry *275*, 6980-6986.

Guo, J., Y. Lao, et al. eds. (2009) Calcium and Apoptosis. Springer US

Gupta, N.A., Kolachala, V.L., Jiang, R., Abramowsky, C., Romero, R., Fifadara, N., Anania, F., Knechtle, S., and Kirk, A. (2012). The glucagon-like peptide-1 receptor agonist Exendin 4 has a protective role in ischemic injury of lean and steatotic liver by inhibiting cell death and stimulating lipolysis. The American journal of pathology *181*, 1693-1701.

Gupta, N.A., Mells, J., Dunham, R.M., Grakoui, A., Handy, J., Saxena, N.K., and Anania, F.A. (2010). Glucagon-like peptide-1 receptor is present on human hepatocytes and has a direct role in decreasing hepatic steatosis in vitro by modulating elements of the insulin signaling pathway. Hepatology *51*, 1584-1592.

Halliwell, W.H. (1997). Cationic amphiphilic drug-induced phospholipidosis. Toxicologic pathology *25*, 53-60.

Hamada, Y., Karjalainen, A., and Bygrave, F.L. (1995). Hormone-induced bile flow and hepatobiliary calcium fluxes are attenuated in the perfused liver of rats made

cholestatic with ethynylestradiol in vivo and with phalloidin in vitro. Hepatology *21*, 1455-1464.

Haverstick, D.M., Dicus, M., Resnick, M.S., Sando, J.J., and Gray, L.S. (1997). A role for protein kinase CbetaI in the regulation of Ca2+ entry in Jurkat T cells. The Journal of biological chemistry *272*, 15426-15433.

He, L.P., Hewavitharana, T., Soboloff, J., Spassova, M.A., and Gill, D.L. (2005). A functional link between store-operated and TRPC channels revealed by the 3,5-bis(trifluoromethyl)pyrazole derivative, BTP2. The Journal of biological chemistry *280*, 10997-11006.

Hebbard, L., and George, J. (2011). Animal models of nonalcoholic fatty liver disease. Nature reviews. Gastroenterology & hepatology *8*, 35-44.

Holowka, D., Korzeniowski, M.K., Bryant, K.L., and Baird, B. (2014). Polyunsaturated fatty acids inhibit stimulated coupling between the ER Ca(2+) sensor STIM1 and the Ca(2+) channel protein Orai1 in a process that correlates with inhibition of stimulated STIM1 oligomerization. Biochimica et biophysica acta *1841*, 1210-1216.

Horstman, D.A., Tennes, K.A., and Putney, J.W., Jr. (1986). ATP-induced calcium mobilization and inositol 1,4,5-triphosphate formation in H-35 hepatoma cells. FEBS letters *204*, 189-192.

Hotamisligil, G.S. (2010). Endoplasmic reticulum stress and the inflammatory basis of metabolic disease. Cell *140*, 900-917.

Hoth, M., and Penner, R. (1992). Depletion of intracellular calcium stores activates a calcium current in mast cells. Nature *355*, 353-356.

Hoth, M., and Penner, R. (1993). Calcium release-activated calcium current in rat mast cells. The Journal of physiology *465*, 359-386.

Houstis, N., Rosen, E.D., and Lander, E.S. (2006). Reactive oxygen species have a causal role in multiple forms of insulin resistance. Nature *440*, 944-948.

Huang, W., Bansode, R., Mehta, M., and Mehta, K.D. (2009). Loss of protein kinase Cbeta function protects mice against diet-induced obesity and development of hepatic steatosis and insulin resistance. Hepatology *49*, 1525-1536.

Huhn, W., Schulze, H.P., and Dargel, R. (1983). Effect of glucagon, phenylephrine, and isoproterenol on glycogenolysis and glucose release from fetal rat hepatocytes in suspension. Biology of the neonate *44*, 153-157.

Hummel, K.P., Dickie, M.M., and Coleman, D.L. (1966). Diabetes, a new mutation in the mouse. Science *153*, 1127-1128.

Hundal, H.S., Ramlal, T., Reyes, R., Leiter, L.A., and Klip, A. (1992). Cellular mechanism of metformin action involves glucose transporter translocation from an intracellular pool to the plasma membrane in L6 muscle cells. Endocrinology *131*, 1165-1173.

Hwang, Y.P., and Jeong, H.G. (2010). Metformin blocks migration and invasion of tumour cells by inhibition of matrix metalloproteinase-9 activation through a calcium and protein kinase Calpha-dependent pathway: phorbol-12-myristate-13-acetate-induced/extracellular signal-regulated kinase/activator protein-1. British journal of pharmacology *160*, 1195-1211.

Ingalls, A.M., Dickie, M.M., and Snell, G.D. (1950). Obese, a new mutation in the house mouse. The Journal of heredity *41*, 317-318.

Ishibashi, H., Nakamura, M., Komori, A., Migita, K., and Shimoda, S. (2009). Liver architecture, cell function, and disease. Seminars in immunopathology *31*, 399-409.

Ishikawa, J., Ohga, K., Yoshino, T., Takezawa, R., Ichikawa, A., Kubota, H., and Yamada, T. (2003). A pyrazole derivative, YM-58483, potently inhibits store-operated sustained Ca2+ influx and IL-2 production in T lymphocytes. Journal of immunology *170*, 4441-4449.

Ivannikov, M.V., and Macleod, G.T. (2013). Mitochondrial free Ca(2)(+) levels and their effects on energy metabolism in Drosophila motor nerve terminals. Biophysical journal *104*, 2353-2361.

Jacobson, P.B., Kuchera, S.L., Metz, A., Schachtele, C., Imre, K., and Schrier, D.J. (1995). Anti-inflammatory properties of Go 6850: a selective inhibitor of protein kinase C. The Journal of pharmacology and experimental therapeutics *275*, 995-1002.

Jornayvaz, F.R., Birkenfeld, A.L., Jurczak, M.J., Kanda, S., Guigni, B.A., Jiang, D.C., Zhang, D., Lee, H.Y., Samuel, V.T., and Shulman, G.I. (2011). Hepatic insulin resistance in mice with hepatic overexpression of diacylglycerol acyltransferase 2. Proceedings of the National Academy of Sciences of the United States of America *108*, 5748-5752.

Jornayvaz, F.R., and Shulman, G.I. (2012). Diacylglycerol activation of protein kinase Cepsilon and hepatic insulin resistance. Cell metabolism *15*, 574-584.

Kahn, B.B., and Flier, J.S. (2000). Obesity and insulin resistance. The Journal of clinical investigation *106*, 473-481.

Kawasaki, T., Ueyama, T., Lange, I., Feske, S., and Saito, N. (2010). Protein kinase C-induced phosphorylation of Orai1 regulates the intracellular Ca2+ level via the store-operated Ca2+ channel. The Journal of biological chemistry *285*, 25720-25730.

Ketterer, C., Mussig, K., Heni, M., Dudziak, K., Randrianarisoa, E., Wagner, R., Machicao, F., Stefan, N., Holst, J.J., Fritsche, A., *et al.* (2011). Genetic variation within the TRPM5 locus associates with prediabetic phenotypes in subjects at increased risk for type 2 diabetes. Metabolism: clinical and experimental *60*, 1325-1333.

Kirpichnikov, D., McFarlane, S.I., and Sowers, J.R. (2002). Metformin: an update. Annals of internal medicine *137*, 25-33.

Kitamura, T., Watanabe, S., Ikejima, K., Hirose, M., Miyazaki, A., Yumoto, A., Suzuki, S., Yamada, T., Kitami, N., and Sato, N. (1995). Different features of Ca2+ oscillations in differentiated and undifferentiated hepatocyte doublets. Hepatology *21*, 1395-1404.

Kleineke, J., and Soling, H.D. (1987). The Ca2+-dependent actions of the alpha-adrenergic agonist phenylephrine on hepatic glycogenolysis differ from those of vasopressin and angiotensin. European journal of biochemistry / FEBS *162*, 143-150.

Kobayashi, E., Nakano, H., Morimoto, M., and Tamaoki, T. (1989). Calphostin C (UCN-1028C), a novel microbial compound, is a highly potent and specific inhibitor of protein kinase C. Biochemical and biophysical research communications *159*, 548-553.

Kotronen, A., Juurinen, L., Hakkarainen, A., Westerbacka, J., Corner, A., Bergholm, R., and Yki-Jarvinen, H. (2008a). Liver fat is increased in type 2 diabetic patients and underestimated by serum alanine aminotransferase compared with equally obese nondiabetic subjects. Diabetes care *31*, 165-169.

Kotronen, A., Juurinen, L., Tiikkainen, M., Vehkavaara, S., and Yki-Jarvinen, H. (2008b). Increased liver fat, impaired insulin clearance, and hepatic and adipose tissue insulin resistance in type 2 diabetes. Gastroenterology *135*, 122-130.

Kuc, R. E. Janet, J. M., Keith, S. Sheena, P. David R. D., Margaret, J., O'Shaughnessey, K. and Anthony P. D. (2014) Characterization of [125I]GLP-1(9-36), a novel radiolabeled analog of the major metabolite of glucagon-like peptide 1 to a receptor distinct from GLP1-R and function of the peptide in murine aorta. Life Sciences *102*, 134–138.

Lablanche, S., Cottet-Rousselle, C., Lamarche, F., Benhamou, P.Y., Halimi, S., Leverve, X., and Fontaine, E. (2011). Protection of pancreatic INS-1 beta-cells from glucose- and fructose-induced cell death by inhibiting mitochondrial permeability transition with cyclosporin A or metformin. Cell death & disease *2*, e134.

Lang, F., Münzer, P., Gawaz, M. and Borst, O. (2013) Regulation of STIM1/Orai1-dependent Ca2+ signalling in platelets. Thromb Haemost. *110*, 925-30.

Larroque-Cardoso, P., Swiader, A., Ingueneau, C., Negre-Salvayre, A., Elbaz, M., Reyland, M.E., Salvayre, R., and Vindis, C. (2013). Role of protein kinase C delta in ER stress and apoptosis induced by oxidized LDL in human vascular smooth muscle cells. Cell death & disease *4*, e520.

Lavoie, L., and van de Werve, G. (1991). Hormone-stimulated glucose production from glycogen in hepatocytes from streptozotocin diabetic rats. Metabolism: clinical and experimental *40*, 1031-1036.

Lee, A.G. (2002). Ca2+ -ATPase structure in the E1 and E2 conformations: mechanism, helix-helix and helix-lipid interactions. Biochimica et biophysica acta *1565*, 246-266.

Lee, B., Palermo, G. and Machaca, K. (2013) Downregulation of store-operated Ca2+ entry during mammalian meiosis is required for the egg-to-embryo transition. Journal of Cell Science *126*, 1672–1681.

Lee, H., Suh, B.C., and Kim, K.T. (1997). Feedback regulation of ATP-induced Ca2+ signaling in HL-60 cells is mediated by protein kinase A- and C-mediated changes in capacitative Ca2+ entry. The Journal of biological chemistry *272*, 21831-21838.

Lee, J., Hong, S.W., Chae, S.W., Kim, D.H., Choi, J.H., Bae, J.C., Park, S.E., Rhee, E.J., Park, C.Y., Oh, K.W., *et al.* (2012). Exendin-4 improves steatohepatitis by increasing Sirt1 expression in high-fat diet-induced obese C57BL/6J mice. PloS one *7*, e31394.

Lee, J., Hong, S.W., Park, S.E., Rhee, E.J., Park, C.Y., Oh, K.W., Park, S.W., and Lee, W.Y. (2014). Exendin-4 regulates lipid metabolism and fibroblast growth factor 21 in hepatic steatosis. Metabolism: clinical and experimental *63*, 1041-1048.

Leite, M. F., and Nathanson, M. H. (2001) The Liver Biology and Pathobiology. Lippincott, Williams & Wilkins: Philadelphia.

Lewis, R.S. (1999). Store-operated calcium channels. Advances in second messenger and phosphoprotein research *33*, 279-307.

Lewis, R.S. (2007). The molecular choreography of a store-operated calcium channel. Nature *446*, 284-287.

Lopez, E., Jardin, I., Berna-Erro, A., Bermejo, N., Salido, G.M., Sage, S.O., Rosado, J.A., and Redondo, P.C. (2012). STIM1 tyrosine-phosphorylation is required for STIM1-Orai1 association in human platelets. Cellular signalling *24*, 1315-1322.

Li, Y., Ge, M., Ciani, L., Kuriakose, G., Westover, E.J., Dura, M., Covey, D.F., Freed, J.H., Maxfield, F.R., Lytton, J., *et al.* (2004). Enrichment of endoplasmic reticulum with cholesterol inhibits sarcoplasmic-endoplasmic reticulum calcium ATPase-2b activity in parallel with increased order of membrane lipids: implications for depletion of endoplasmic reticulum calcium stores and apoptosis in cholesterol-loaded macrophages. The Journal of biological chemistry *279*, 37030-37039.

Liou, J., Fivaz, M., Inoue, T., and Meyer, T. (2007). Live-cell imaging reveals sequential oligomerization and local plasma membrane targeting of stromal interaction molecule 1 after Ca2+ store depletion. Proceedings of the National Academy of Sciences of the United States of America *104*, 9301-9306.

Listenberger, L.L., Ory, D.S., and Schaffer, J.E. (2001). Palmitate-induced apoptosis can occur through a ceramide-independent pathway. The Journal of biological chemistry *276*, 14890-14895.

Listenberger et al. (2003) Triglyceride accumulation protects against fatty acid-induced lipotoxicity. Proc. Natl. Acad. Sci. USA. 100, 3077–3082

Litjens, T., Nguyen, T., Castro, J., Aromataris, E.C., Jones, L., Barritt, G.J., and Rychkov, G.Y. (2007a). Phospholipase C-gamma1 is required for the activation of store-operated Ca2+ channels in liver cells. The Biochemical journal *405*, 269-276.

Litjens, T., Nguyen, T., Castro, J., Aromataris, E.C., Jones, L., Barritt, G.J., and Rychkov, G.Y. (2007b). Phospholipase C-gamma1 is required for the activation of store-operated Ca2+ channels in liver cells. Biochemical Journal *405*, 269-276.

Liu, W., Fang, Y., Wang, X.T., Liu, J., Dan, X., and Sun, L.L. (2014). Overcoming 5-Fu resistance of colon cells through inhibition of Glut1 by the specific inhibitor WZB117. Asian Pacific journal of cancer prevention : APJCP *15*, 7037-7041

Livak, K.J., and Schmittgen, T.D. (2001). Analysis of relative gene expression data using real-time quantitative PCR and the 2(-Delta Delta C(T)) Method. Methods *25*, 402-408.

Lu, Z., Liu, D., Hornia, A., Devonish, W., Pagano, M., and Foster, D.A. (1998). Activation of protein kinase C triggers its ubiquitination and degradation. Molecular and cellular biology *18*, 839-845.

Lubic, S.P., Nguyen, K.P., Dave, B., and Giacomini, J.C. (1994). Antiarrhythmic agent amiodarone possesses calcium channel blocker properties. Journal of cardiovascular pharmacology *24*, 707-714.

Luo, D., Broad, L.M., Bird, G.S., and Putney, J.W., Jr. (2001). Signaling pathways underlying muscarinic receptor-induced [Ca2+]i oscillations in HEK293 cells. The Journal of biological chemistry *276*, 5613-5621.

Ma, H.T., Patterson, R.L., van Rossum, D.B., Birnbaumer, L., Mikoshiba, K., and Gill, D.L. (2000). Requirement of the inositol trisphosphate receptor for activation of store-operated Ca2+ channels. Science *287*, 1647-1651.

MacDonald, P. E., El-kholy, W., Riedel, M. J., Salapatek, A. M. F., Light, P. E. and Wheeler, M. B. (2002) The multiple actions of GLP-1 on the process of glucose-stimulated insulin secretion. Diabetes *51*, S434–S442.

Madiraju, A.K., Erion, D.M., Rahimi, Y., Zhang, X.M., Braddock, D.T., Albright, R.A., Prigaro, B.J., Wood, J.L., Bhanot, S., MacDonald, M.J., *et al.* (2014). Metformin suppresses gluconeogenesis by inhibiting mitochondrial glycerophosphate dehydrogenase. Nature *510*, 542-546.

Majeed, Y., Bahnasi, Y., Seymour, V.A., Wilson, L.A., Milligan, C.J., Agarwal, A.K., Sukumar, P., Naylor, J., and Beech, D.J. (2011). Rapid and contrasting effects of rosiglitazone on transient receptor potential TRPM3 and TRPC5 channels. Molecular pharmacology *79*, 1023-1030.

Mak, D.O., Vais, H., Cheung, K.H., and Foskett, J.K. (2013). Isolating nuclei from cultured cells for patch-clamp electrophysiology of intracellular Ca(2+) channels. Cold Spring Harbor protocols *2013*, 880-884.

Malhi et al. (2000). KATP Channels Regulate Mitogenically Induced Proliferation in Primary Rat Hepatocytes and Human Liver Cell Lines. Journal of Biological Chemistry, 2753:26050–57.

Manna, P.R., Jo, Y., and Stocco, D.M. (2007). Regulation of Leydig cell steroidogenesis by extracellular signal-regulated kinase 1/2: role of protein kinase A and protein kinase C signaling. The Journal of endocrinology *193*, 53-63.

Matsumoto, M., Pocai, A., Rossetti, L., Depinho, R.A., and Accili, D. (2007). Impaired regulation of hepatic glucose production in mice lacking the forkhead transcription factor Foxo1 in liver. Cell metabolism *6*, 208-216.

McCarthy, T.C., Pollak, P.T., Hanniman, E.A., and Sinal, C.J. (2004). Disruption of hepatic lipid homeostasis in mice after amiodarone treatment is associated with peroxisome proliferator-activated receptor-alpha target gene activation. The Journal of pharmacology and experimental therapeutics *311*, 864-873.

Mei, S., Ni, H.M., Manley, S., Bockus, A., Kassel, K.M., Luyendyk, J.P., Copple, B.L., and Ding, W.X. (2011). Differential roles of unsaturated and saturated fatty acids on autophagy and apoptosis in hepatocytes. The Journal of pharmacology and experimental therapeutics *339*, 487-498.

Mekahli, D., Bultynck, G., Parys, J.B., De Smedt, H., and Missiaen, L. (2011). Endoplasmic-reticulum calcium depletion and disease. Cold Spring Harbor perspectives in biology *3*.

Meloni, A.R., DeYoung, M.B., Lowe, C., and Parkes, D.G. (2013). GLP-1 receptor activated insulin secretion from pancreatic beta-cells: mechanism and glucose dependence. Diabetes, obesity & metabolism *15*, 15-27.

Michelotti, G.A., Machado, M.V., and Diehl, A.M. (2013). NAFLD, NASH and liver cancer. Nature reviews. Gastroenterology & hepatology *10*, 656-665.

Mohammed, F.F., and Khokha, R. (2005). Thinking outside the cell: proteases regulate hepatocyte division. Trends in cell biology *15*, 555-563.

Moreau et al. (2009) A Novel Pregnane X Receptor and S14-Mediated Lipogenic Pathway in Human Hepatocyte. Hepatology *49*, 2068-2079.

Morgan, A.J., and Jacob, R. (1994). Ionomycin enhances Ca2+ influx by stimulating store-regulated cation entry and not by a direct action at the plasma membrane. The Biochemical journal *300 (Pt 3)*, 665-672.

Musso, G., Gambino, R., and Cassader, M. (2010). Non-alcoholic fatty liver disease from pathogenesis to management: an update. Obesity reviews : an official journal of the International Association for the Study of Obesity *11*, 430-445.

Nakamura, S., Takamura, T., Matsuzawa-Nagata, N., Takayama, H., Misu, H., Noda, H., Nabemoto, S., Kurita, S., Ota, T., Ando, H., *et al.* (2009). Palmitate induces insulin resistance in H4IIEC3 hepatocytes through reactive oxygen species produced by mitochondria. The Journal of biological chemistry *284*, 14809-14818.

Nathanson, M.H., Rios-Velez, L., Burgstahler, A.D., and Mennone, A. (1999). Communication via gap junctions modulates bile secretion in the isolated perfused rat liver. Gastroenterology *116*, 1176-1183.

Nelson, D. L.; Cox, M. M. (2008). Lehninger principles of biochemistry, 5th edn (W. H. Freeman & Company, USA).

Nyenwe, E. (2012). Intensive insulin therapy in hospitalised patients increases the risk of hypoglycaemia and has no effect on mortality, infection risk or length of stay. Evidence-based medicine *17*, 8-9.

Nyenwe, E.A., Jerkins, T.W., Umpierrez, G.E., and Kitabchi, A.E. (2011). Management of type 2 diabetes: evolving strategies for the treatment of patients with type 2 diabetes. Metabolism: clinical and experimental *60*, 1-23.

Ozcan, L., Wong, C.C., Li, G., Xu, T., Pajvani, U., Park, S.K., Wronska, A., Chen, B.X., Marks, A.R., Fukamizu, A., *et al.* (2012). Calcium signaling through CaMKII regulates hepatic glucose production in fasting and obesity. Cell Metab *15*, 739-751.

Ozcan, U., Cao, Q., Yilmaz, E., Lee, A.H., Iwakoshi, N.N., Ozdelen, E., Tuncman, G., Gorgun, C., Glimcher, L.H., and Hotamisligil, G.S. (2004). Endoplasmic reticulum stress links obesity, insulin action, and type 2 diabetes. Science *306*, 457-461.

Parekh, A.B., and Penner, R. (1995). Depletion-activated calcium current is inhibited by protein kinase in RBL-2H3 cells. Proceedings of the National Academy of Sciences of the United States of America *92*, 7907-7911.

Parekh, A.B., and Penner, R. (1997). Store depletion and calcium influx. Physiological reviews *77*, 901-930.

Parekh, A.B., Fleig, A., and Penner, R. (1997). The store-operated calcium current I(CRAC): nonlinear activation by InsP3 and dissociation from calcium release. Cell *89*, 973-980.

Parekh, A.B., and Putney, J.W., Jr. (2005). Store-operated calcium channels. Physiological reviews *85*, 757-810.

Park, C.Y., Hoover, P.J., Mullins, F.M., Bachhawat, P., Covington, E.D., Raunser, S., Walz, T., Garcia, K.C., Dolmetsch, R.E., and Lewis, R.S. (2009). STIM1 clusters and activates CRAC channels via direct binding of a cytosolic domain to Orai1. Cell *136*, 876-890.

Park, S.W., Zhou, Y., Lee, J., Lee, J., and Ozcan, U. (2010). Sarco(endo)plasmic reticulum Ca2+-ATPase 2b is a major regulator of endoplasmic reticulum stress and glucose homeostasis in obesity. Proceedings of the National Academy of Sciences of the United States of America *107*, 19320-19325.

Patti, M.E., and Kahn, C.R. (1998). The insulin receptor--a critical link in glucose homeostasis and insulin action. Journal of basic and clinical physiology and pharmacology *9*, 89-109.

Peirson, L., Douketis, J., Ciliska, D., Fitzpatrick-Lewis, D., Ali, M.U., and Raina, P. (2014). Treatment for overweight and obesity in adult populations: a systematic review and meta-analysis. CMAJ open *2*, E306-317.

Perry, R.J., Samuel, V.T., Petersen, K.F., and Shulman, G.I. (2014). The role of hepatic lipids in hepatic insulin resistance and type 2 diabetes. Nature *510*, 84-91.

Phillips, M.S., Liu, Q., Hammond, H.A., Dugan, V., Hey, P.J., Caskey, C.J., and Hess, J.F. (1996). Leptin receptor missense mutation in the fatty Zucker rat. Nature genetics *13*, 18-19.

Pilkis, S.J., and Granner, D.K. (1992). Molecular physiology of the regulation of hepatic gluconeogenesis and glycolysis. Annual review of physiology *54*, 885-909.

Pozo-Guisado, E., Casas-Rua, V., Tomas-Martin, P., Lopez-Guerrero, A.M., Alvarez-Barrientos, A., and Martin-Romero, F.J. (2013). Phosphorylation of STIM1 at ERK1/2 target sites regulates interaction with the microtubule plus-end binding protein EB1. Journal of cell science *126*, 3170-3180.

Pozo-Guisado, E., and Martin-Romero, F.J. (2013). The regulation of STIM1 by phosphorylation. Communicative & integrative biology *6*, e26283.

Puljak, L., Pagliassotti, M.J., Wei, Y., Qadri, I., Parameswara, V., Esser, V., Fitz, J.G., and Kilic, G. (2005). Inhibition of cellular responses to insulin in a rat liver cell line. A role for PKC in insulin resistance. The Journal of physiology *563*, 471-482.

Putney, J.W. (2010). Pharmacology of store-operated calcium channels. Molecular interventions *10*, 209-218.

Putney, J.W., Jr. (2005). Capacitative calcium entry: sensing the calcium stores. The Journal of cell biology *169*, 381-382.

Putney, J.W., Jr., Poggioli, J., and Weiss, S.J. (1981). Receptor regulation of calcium release and calcium permeability in parotid gland cells. Philosophical transactions of the Royal Society of London. Series B, Biological sciences *296*, 37-45.

Racioppi, L., and Means, A.R. (2012). Calcium/calmodulin-dependent protein kinase kinase 2: roles in signaling and pathophysiology. The Journal of biological chemistry *287*, 31658-31665.

Ramadori, G., Moriconi, F., Malik, I., and Dudas, J. (2008). Physiology and pathophysiology of liver inflammation, damage and repair. Journal of physiology and pharmacology : an official journal of the Polish Physiological Society *59 Suppl 1*, 107-117.

Rao, F., Deng, C.Y., Zhang, Q.H., Xue, Y.M., Xiao, D.Z., Kuang, S.J., Lin, Q.X., Shan, Z.X., Liu, X.Y., Zhu, J.N., *et al.* (2013). Involvement of Src tyrosine kinase and protein kinase C in the expression of macrophage migration inhibitory factor induced by H2O2 in HL-1 mouse cardiac muscle cells. Brazilian journal of medical and biological research *46*, 746-751.

Rao, U., and Agarwal, A. (2012). Amiodarone-induced acute hepatotoxicity. European journal of clinical pharmacology *68*, 449-450.

Rena, G., Pearson, E.R., and Sakamoto, K. (2013). Molecular mechanism of action of metformin: old or new insights? Diabetologia *56*, 1898-1906.

Ribeiro, C.M., McKay, R.R., Hosoki, E., Bird, G.S., and Putney, J.W., Jr. (2000). Effects of elevated cytoplasmic calcium and protein kinase C on endoplasmic reticulum structure and function in HEK293 cells. Cell calcium *27*, 175-185.

Rizzo, A., Spedicato, M., Cosola, C., Minoia, G., Roscino, M.T., Punzi, S., and Sciorsci, R.L. (2009). Effects of rosiglitazone, a PPAR-gamma agonist, on the contractility of bovine uterus in vitro. Journal of veterinary pharmacology and therapeutics *32*, 548-551.

Robb-Gaspers, L.D., Burnett, P., Rutter, G.A., Denton, R.M., Rizzuto, R., and Thomas, A.P. (1998). Integrating cytosolic calcium signals into mitochondrial metabolic responses. The EMBO journal *17*, 4987-5000.

Rolo, A.P., Teodoro, J.S., and Palmeira, C.M. (2012). Role of oxidative stress in the pathogenesis of nonalcoholic steatohepatitis. Free radical biology & medicine *52*, 59-69.

Rooney, T.A., Sass, E.J., and Thomas, A.P. (1989). Characterization of cytosolic calcium oscillations induced by phenylephrine and vasopressin in single fura-2-loaded hepatocytes. The Journal of biological chemistry *264*, 17131-17141.

Rotella, C.M., Pala, L., and Mannucci, E. (2005). Glucagon-like peptide 1 (GLP-1) and metabolic diseases. Journal of endocrinological investigation *28*, 746-758.

Rychkov, G., Brereton, H.M., Harland, M.L., and Barritt, G.J. (2001). Plasma membrane Ca2+ release-activated Ca2+ channels with a high selectivity for Ca2+ identified by patch-clamp recording in rat liver cells. Hepatology *33*, 938-947.

Samuel, V.T., Liu, Z.X., Qu, X., Elder, B.D., Bilz, S., Befroy, D., Romanelli, A.J., and Shulman, G.I. (2004). Mechanism of hepatic insulin resistance in non-alcoholic fatty liver disease. The Journal of biological chemistry *279*, 32345-32353.

Samuel, V.T., Liu, Z.X., Wang, A., Beddow, S.A., Geisler, J.G., Kahn, M., Zhang, X.M., Monia, B.P., Bhanot, S., and Shulman, G.I. (2007). Inhibition of protein kinase Cepsilon prevents hepatic insulin resistance in nonalcoholic fatty liver disease. The Journal of clinical investigation *117*, 739-745.

Schofl, C., Ponczek, M., Mader, T., Waring, M., Benecke, H., von zur Muhlen, A., Mix, H., Cornberg, M., Boker, K.H., Manns, M.P., *et al.* (1999). Regulation of cytosolic free calcium concentration by extracellular nucleotides in human hepatocytes. The American journal of physiology *276*, G164-172.

Schroder, M. (2008). Endoplasmic reticulum stress responses. Cellular and molecular life sciences : CMLS *65*, 862-894.

Schwarz et al. (1985) Rapid reciprocal changes in adrenergic receptors in intact isolated hepatocytes during primary cell culture. Mol Pharmacol. *27*, 200-9.

Sciorra, V.A., Hammond, S.M., and Morris, A.J. (2001). Potent direct inhibition of mammalian phospholipase D isoenzymes by calphostin-c. Biochemistry *40*, 2640-2646.

Scrimgeour, N., Litjens, T., Ma, L., Barritt, G.J., and Rychkov, G.Y. (2009). Properties of Orai1 mediated store-operated current depend on the expression levels of STIM1 and Orai1 proteins. The Journal of physiology *587*, 2903-2918.

Shulman, G.I. (2000). Cellular mechanisms of insulin resistance. The Journal of clinical investigation *106*, 171-176.

Sipma, H., van der Zee, L., van den Akker, J., den Hertog, A., and Nelemans, A. (1996). The effect of the PKC inhibitor GF109203X on the release of Ca2+ from internal stores and Ca2+ entry in DDT1 MF-2 cells. British journal of pharmacology *119*, 730-736.

Smith, B.W., and Adams, L.A. (2011). Non-alcoholic fatty liver disease. Critical reviews in clinical laboratory sciences *48*, 97-113.

Smith, K.E., Gu, C., Fagan, K.A., Hu, B., and Cooper, D.M. (2002). Residence of adenylyl cyclase type 8 in caveolae is necessary but not sufficient for regulation by capacitative Ca(2+) entry. The Journal of biological chemistry *277*, 6025-6031.

Smith, S.R., O'Neil, P.M., Astrup, A., Finer, N., Sanchez-Kam, M., Fraher, K., Fain, R., and Shanahan, W.R. (2014). Early weight loss while on lorcaserin, diet and exercise as a predictor of week 52 weight-loss outcomes. Obesity *22*, 2137-2146.

Smyth, J.T., Petranka, J.G., Boyles, R.R., DeHaven, W.I., Fukushima, M., Johnson, K.L., Williams, J.G., and Putney, J.W., Jr. (2009). Phosphorylation of STIM1 underlies suppression of store-operated calcium entry during mitosis. Nature cell biology *11*, 1465-1472.

Soboloff, J., Spassova, M.A., Tang, X.D., Hewavitharana, T., Xu, W., and Gill, D.L. (2006). Orai1 and STIM reconstitute store-operated calcium channel function. The Journal of biological chemistry *281*, 20661-20665.

Spassova, M.A., Soboloff, J., He, L.P., Hewavitharana, T., Xu, W., Venkatachalam, K., van Rossum, D.B., Patterson, R.L., and Gill, D.L. (2004). Calcium entry mediated by SOCs and TRP channels: variations and enigma. Biochim Biophys Acta *1742*, 9-20.

Srikanth, S., Ribalet, B., and Gwack, Y. (2013). Regulation of CRAC channels by protein interactions and post-translational modification. Channels *7*, 354-363.

Stathopulos, P.B., Li, G.Y., Plevin, M.J., Ames, J.B., and Ikura, M. (2006). Stored Ca2+ depletion-induced oligomerization of stromal interaction molecule 1 (STIM1) via the EF-SAM region: An initiation mechanism for capacitive Ca2+ entry. The Journal of biological chemistry *281*, 35855-35862.

Steenks, M., van Baal, M.C., Nieuwenhuijs, V.B., de Bruijn, M.T., Schiesser, M., Teo, M.H., Callahan, T., Padbury, R.T., and Barritt, G.J. (2010). Intermittent ischaemia maintains function after ischaemia reperfusion in steatotic livers. HPB : the official journal of the International Hepato Pancreato Biliary Association *12*, 250-261.

Tara, P. (2007). Weighing the Pros and Cons Of New Fat-Blocking Drug Alli. The Wall Street Journal, D1.

Targos, B., Baranska, J., and Pomorski, P. (2005). Store-operated calcium entry in physiology and pathology of mammalian cells. Acta biochimica Polonica *52*, 397-409.

Thomas, A.P., Renard, D.C., and Rooney, T.A. (1991). Spatial and temporal organization of calcium signalling in hepatocytes. Cell calcium *12*, 111-126.

Tian, G., Tepikin, A. V., Tengholm, A. and Gylfe, E. (2012) cAMP induces stromal interaction molecule 1 (STIM1) puncta but neither Orai1 protein clustering nor store-operated Ca2+ entry (SOCE) in islet cells. Journal of Biological Chemistry *287*, 9862-9872.

Toullec, D., Pianetti, P., Coste, H., Bellevergue, P., Grand-Perret, T., Ajakane, M., Baudet, V., Boissin, P., Boursier, E., Loriolle, F., *et al.* (1991). The bisindolylmaleimide GF 109203X is a potent and selective inhibitor of protein kinase C. The Journal of biological chemistry *266*, 15771-15781.

Toyoshima, C. (2009) Calcium, Proteins, Energy, and Life, retrieved from: http://www.uctv.tv/gradcouncil/ (Accessed on 10/06/2014)

Ubl, J.J., Chen, S., and Stucki, J.W. (1994). Anti-diabetic biguanides inhibit hormone-induced intracellular Ca2+ concentration oscillations in rat hepatocytes. The Biochemical journal *304 (Pt 2)*, 561-567.

Vangheluwe, P., Raeymaekers, L., Dode, L., and Wuytack, F. (2005). Modulating sarco(endo)plasmic reticulum Ca2+ ATPase 2 (SERCA2) activity: cell biological implications. Cell calcium *38*, 291-302.

Vig, P.J., and Desaiah, D. (1991). Modulation of protein kinase C activity by amiodarone and desethylamiodarone. Neurotoxicology *12*, 595-601.

Vogel, C and Marcotte, E. M. (2013) Insights into the regulation of protein abundance from proteomic and transcriptomic analyses. Nat Rev Genet. *13*, 227–232.

Wang, S., and Kaufman, R.J. (2014). How does protein misfolding in the endoplasmic reticulum affect lipid metabolism in the liver? Current opinion in lipidology *25*, 125-132.

Wei, Y., Wang, D., Gentile, C.L., and Pagliassotti, M.J. (2009). Reduced endoplasmic reticulum luminal calcium links saturated fatty acid-mediated endoplasmic reticulum stress and cell death in liver cells. Molecular and cellular biochemistry *331*, 31-40.

Wilson, H.C., Eunus, S.A., Nathan, S., Alyce, M.M., Jin, H., George, A.T., Grigori, Y.R., and Greg, J.B. (2014). Steatosis inhibits liver cell store-operated Ca2 {+} entry and reduces ER Ca2 {+} through a protein kinase C dependent mechanism. Biochemical Journal.

Wilson, C., Rychkov, G.Y., and Barritt, G.J. (2010) Expression of STIM and Orai in liver disease, Proceedings of the Australian Physiological Society, 41/204P

Wilson, C.H., Zeile, S., Chataway, T., Nieuwenhuijs, V.B., Padbury, R.T., and Barritt, G.J. (2011). Increased expression of peroxiredoxin 1 and identification of a novel lipid-metabolizing enzyme in the early phase of liver ischemia reperfusion injury. Proteomics *11*, 4385-4396.

Xia et al. (2013) Iodine excess induces hepatic steatosis through disturbance of thyroid hormone metabolism involving oxidative stress in BALB/c mice. Biol Trace Elem Res *154*, 103–110.

Yasuda, S.U., Sausville, E.A., Hutchins, J.B., Kennedy, T., and Woosley, R.L. (1996). Amiodarone-induced lymphocyte toxicity and mitochondrial function. Journal of cardiovascular pharmacology *28*, 94-100.

Yazaki, I., Tsurugaya, T., Santella, L., Chun, J.T., Amore, G., Kusunoki, S., Asada, A., Togo, T., and Akasaka, K. (2014). Ca2+ influx-linked protein kinase C activity regulates the beta-catenin localization, micromere induction signalling and the oral-aboral axis formation in early sea urchin embryos. Zygote, 1-21.

Yu, F., Sun, L. and Machaca, K.(2012) Orai1 internalization and STIM1 clustering inhibition modulate SOCE inactivation during meiosis, PNAS, *106*:17401–17406

Yu, J., Chu, E.S., Wang, R., Wang, S., Wu, C.W., Wong, V.W., Chan, H.L., Farrell, G.C., and Sung, J.J. (2010). Heme oxygenase-1 protects against steatohepatitis in both cultured hepatocytes and mice. Gastroenterology *138*, 694-704, 704 e691.

Zhang, G., Kazanietz, M.G., Blumberg, P.M., and Hurley, J.H. (1995). Crystal structure of the cys2 activator-binding domain of protein kinase C delta in complex with phorbol ester. Cell *81*, 917-924.

Zhang, S.L., Yu, Y., Roos, J., Kozak, J.A., Deerinck, T.J., Ellisman, M.H., Stauderman, K.A., and Cahalan, M.D. (2005). STIM1 is a Ca2+ sensor that activates CRAC channels and migrates from the Ca2+ store to the plasma membrane. Nature *437*, 902-905.

Zhou, Y., Ramachandran, S., Oh-Hora, M., Rao, A., and Hogan, P.G. (2010). Pore architecture of the ORAI1 store-operated calcium channel. Proceedings of the National Academy of Sciences of the United States of America *107*, 4896-4901.

Zitt, C., Strauss, B., Schwarz, E.C., Spaeth, N., Rast, G., Hatzelmann, A., and Hoth, M. (2004). Potent inhibition of Ca2+ release-activated Ca2+ channels and T-lymphocyte activation by the pyrazole derivative BTP2. The Journal of biological chemistry *279*, 12427-12437.